NASA TECHNICAL NOTE

NASA TN D-7551

NASA TN D-7551

PRELIMINARY PERFORMANCE ESTIMATES OF A HIGHLY MANEUVERABLE REMOTELY PILOTED VEHICLE

by Walter P. Nelms, Jr., and John A. Axelson

Ames Research Center
Moffett Field, Calif. 94035

NATIONAL AERONAUTICS AND SPACE ADMINISTRATION • WASHINGTON, D. C. • FEBRUARY 1974

1. Report No.	2. Government Accession No.	3. Recipient's Catalog No.
D-7551		

4. Title and Subtitle	5. Report Date
PRELIMINARY PERFORMANCE ESTIMATES OF A HIGHLY MANEUVERABLE REMOTELY PILOTED VEHICLE	February 1974
	6. Performing Organization Code
7. Author(s)	8. Performing Organization Report No.
Walter P. Nelms, Jr., and John A. Axelson	A-5157
	10. Work Unit No.
9. Performing Organization Name and Address	791–94–0401
NASA Ames Research Center Moffett Field, Calif. 94035	11. Contract or Grant No.
	13. Type of Report and Period Covered
12. Sponsoring Agency Name and Address	Technical Note
National Aeronautics and Space Administration Washington, D. C., 20546	14. Sponsoring Agency Code

15. Supplementary Notes

16. Abstract

A computerized synthesis program has been used to assess the effects of various vehicle and mission parameters on the performance of a highly maneuverable remotely piloted vehicle (RPV) for the air-to-air combat role. The configuration used in the study is a trapezoidal-wing and body concept, with forward-mounted stabilizing and control surfaces. The study mission consists of an outbound cruise, an acceleration phase, a series of subsonic and supersonic turns, and a return cruise. Performance is evaluated in terms of both the required vehicle weight to accomplish this mission and combat effectiveness as measured by turning and acceleration capability. The report describes the synthesis program, the mission, the vehicle, and the results of sensitivity and trade studies.

An optimization process has been used to establish the nominal RPV configuration, which exhibits relatively high levels of combat maneuvering performance while being relatively light in weight as compared to advanced manned fighters. This nominal configuration is then used as a base point for sensitivity studies to determine the vehicle- and mission-oriented parameters that have the most significant effect on the RPV weight and combat performance. Variations were made in vehicle geometry, aerodynamics, component weights, and mission parameters such as cruise altitude and Mach number, combat altitude and Mach number, range, and number of combat maneuvers. The effects of some 30 vehicle and mission parameters are included. Areas in which further study is needed or where possible payoffs can result from advancement in technology are suggested.

17. Key Words (Suggested by Author(s))	18. Distribution Statement
Remotely Piloted Vehicles Highly Maneuverable Aircraft Aircraft Synthesis Aircraft Systems Analysis Aircraft Performance Air Combat Aircraft	Unclassified – Unlimited

19. Security Classif. (of this report)	20. Security Classif. (of this page)	21. No. of Pages	22. Price*
Unclassified	Unclassified	100	$3.75

*For sale by the National Technical Information Service, Springfield, Virginia 22151

TABLE OF CONTENTS

SYMBOLS

AR	aspect ratio
b	span, m (ft)
C_{D_L}	drag-due-to-lift coefficient, $\frac{\text{drag due to lift}}{qS}$
C_{D_o}	zero-lift drag coefficient, $\frac{\text{zero-lift drag}}{qS}$
$C_{D_{o_W}}$	weapons drag coefficient, $\frac{\text{weapons drag}}{qS}$
C_L	lift coefficient, $\frac{\text{lift}}{qS}$
d	fuselage diameter, m (ft)
D	drag
l	fuselage length, m (ft)
L	lift
M	free-stream Mach number
N_Z	load factor, $\frac{L + T \sin \alpha}{W}$
N_{Z_i}	maximum instantaneous load factor
N_{Z_S}	sustained load factor
$N_{Z_{ult}}$	ultimate load factor
P_S	specific power, $\left(\frac{T \cos \alpha - D}{W}\right) V$, m/sec (ft/sec)
$P_{S_{1g}}$	specific power at one g flight condition ($\dot{\theta} = 0$), m/sec (ft/sec)
P_{S_i}	specific power at maximum instantaneous turn rate, m/sec (ft/sec)
q	free-stream dynamic pressure
S	wing planform area, m^2 (ft^2)
S_C	canard planform area, m^2 (ft^2)

T	thrust
$\frac{t}{c}$	thickness-to-chord ratio
$\frac{T}{W}$	thrust-to-weight ratio (launch)
V	free-stream velocity, m/sec (ft/sec)
W	weight, kg (lb)
W_g,$WGTO$	gross weight (launch), kg (lb)
$\frac{W}{S}$	wing loading (launch), kN/m^2 (lb/ft^2)
α	angle of attack, deg
$\dot{\theta}$	turn rate, deg/sec
$\dot{\theta}_i$	maximum instantaneous turn rate, deg/sec
$\dot{\theta}_s$	sustained turn rate, deg/sec
Λ	leading-edge sweep, deg
λ	taper ratio

PRELIMINARY PERFORMANCE ESTIMATES OF A HIGHLY MANEUVERABLE REMOTELY PILOTED VEHICLE

Walter P. Nelms, Jr., and John A. Axelson

Ames Research Center

SUMMARY

A computerized synthesis program has been used to assess the effects of various vehicle and mission parameters on the performance of a highly maneuverable remotely piloted vehicle (RPV) for the air-to-air combat role. The configuration used in the study is a trapezoidal-wing and body concept, with forward mounted stabilizing and control surfaces. The study mission consists of an outbound cruise, an acceleration phase, a series of subsonic and supersonic turns, and a return cruise. Performance is evaluated in terms of both the required vehicle weight to accomplish this mission and combat effectiveness as measured by turning and acceleration capability. The report describes the synthesis program, the mission, the vehicle, and the results of sensitivity and trade studies.

An optimization process has been used to establish the nominal RPV configuration, which exhibits relatively high levels of combat maneuvering performance while being relatively light in weight as compared to advanced manned fighters. This nominal configuration is then used as a base point for sensitivity studies to determine the vehicle- and mission-oriented parameters that have the most significant effect on the RPV weight and combat performance. Tradeoffs were made in vehicle geometry, aerodynamics, component weights, and mission parameters such as cruise altitude and Mach number, combat altitude and Mach number, range, and number of combat maneuvers. The effects of some 30 vehicle and mission parameters are included. Areas in which further study is needed or where possible payoffs can result from advancements in technology are suggested.

INTRODUCTION

There has been an increased interest in the use of remotely piloted vehicles (RPV) to complement or replace manned aircraft for several military missions. Modified drone aircraft are presently being operated as RPVs for reconnaissance and electronic warfare missions, and these same types of vehicles are being tested in the air-to-ground strike role. Several new configurations are under development, particularly for the reconnaissance missions. In addition, preliminary studies are being conducted on more advanced configurations for both the reconnaissance mission and the air superiority role. This latter mission is somewhat more long term because of its greater technology requirements, and therefore is not receiving as much attention as the more near-term missions.

Realization of an operational RPV for the air combat role will require technology advancements and cost reductions in many areas such as sensors, avionics, data links, airframe and

propulsion systems, control stations, and operational procedures. Nevertheless, it may well be that the next generation of air-to-air combat aircraft, beyond the advanced manned fighters now under development, will employ remote piloting technology. Such aircraft offer many advantages over manned aircraft, including increased maneuverability due to the absence of an onboard pilot, possible cost benefits to accomplish a given mission, and, obviously, the saving of human lives.

To strengthen the technology base required for the development of an RPV, the NASA-Ames Research Center has undertaken a research program focusing on a highly maneuverable RPV for the air-to-air combat role. One phase of the program is a computerized systems study of several configurations to identify critical areas where significant performance improvement may result from additional research. A computerized aircraft synthesis program (ACSYNT) has been used to assess the effects of various vehicle and mission parameters on the performance of a highly maneuverable RPV for the air-to-air combat role. This report is confined to a relatively conventional wing-body-canard concept. The study mission consists of an outbound cruise, an acceleration phase, a series of subsonic and supersonic turns, and a return cruise. Performance is evaluated in terms of both the required vehicle weight to accomplish this mission and the combat maneuverability of the resulting configuration. The report describes the selected mission, vehicle, and synthesis program, together with results from sensitivity and trade studies.

MISSION DESCRIPTION

There are many combinations of range and maneuvers required by an air-to-air combat vehicle. For purposes of the present study, a typical offensive mission, shown schematically in figure 1, was chosen. This nominal mission consists of a climb phase, a cruise phase, and a combat phase. The RPV, carrying a payload of two infrared missiles of the Sidewinder class, is ground launched using either a zero-length rocket assist technique or a catapult system. (Another possibility would be launch from an aircraft.) Following launch, the RPV climbs and accelerates to a cruise altitude of 13,716 m (45,000 ft) and then cruises to a combat range of 370 km (200 n.mi.) at 0.9 Mach number and at a constant altitude of 13,716 m (45,000 ft).

On reaching the combat area, the RPV performs the following series of maneuvers at an altitude of 9,144 m (30,000 ft) using maximum power:

An acceleration from $M = 0.9$ to 1.6
Three 360° $P_S = 0$ turn at $M = 1.2$
Four 360° $P_S = 0$ turns at $M = 0.9$

The RPV then cruises 370 km (200 n.mi.) back to its base, descends, and is recovered on the ground using a net or arresting gear and pad. (Details of the launch and recovery systems are beyond the scope of this report.) As a conservative measure in evaluating vehicle weight, the two missiles are not launched but are brought back to the base, resulting in a heavier vehicle for the return trip and therefore greater fuel consumption than if the weapons had been expended. The fuel used for all the various phases of the mission is then summed and the required gross weight vehicle is determined from the synthesis program.

The sensitivity of the vehicle weight and combat performance to the cruise altitude, cruise speed, combat range, combat altitude, and combat speed is discussed in a later section of the report as are the effects of a reduction in the number of combat turns.

VEHICLE DESCRIPTION

The RPV configuration discussed here is a relatively conventional wing-body-canard concept. Figure 2 presents a schematic of the nominal configuration along with the vehicle geometry and weight statement.

The engine used in the RPV configuration is a study turbojet with afterburner (ref. 1). A fixed geometry normal shock air induction system is employed with the inlet located beneath the fuselage (fig. 2). Weights of the engine, afterburner, engine controls, fuel system, and inlet system are included under "propulsion" in the weight statement. A gross weight of 2460 kg (5425 lb) is required to accomplish the nominal mission.

The fuselage is of conventional aluminum structure, and is sized to contain the propulsion system, the total fuel supply, and the avionics and electrical equipment. An electro-optical sensor system located in the vehicle nose accounts for its rather blunt shape. The trapezoidal-planform wing consists of conventional aluminum structure and contains no fuel or equipment (except control actuators and payload attachments).

The study configuration employs control configured vehicle (CCV) and fly-by-wire concepts, and the forward-mounted canard and vertical stabilizing and control surfaces are intended to be representative of these advanced systems. The canard is sized (in conjunction with the fore and aft location of the wing) to give a zero static margin with a full fuel load. The vertical surface of the nominal configuration is sized at 10 percent of the wing reference area; the sensitivity of vehicle weight to changes in size of this surface is determined in a later section.

The exact weight of the fixed equipment required for this mission (e.g., avionics, electrical systems, sensors) is difficult to assess at this time; based on current technology a nominal weight allowance of 227 kg (500 lb) is used. The vehicle payload consists of two infrared seeking missiles of the Sidewinder class weighing 145 kg (320 lb) and mounted under the wings. Note that the weights of payload attachments and residual fuel and oil are included under "residual load" in the weight statement.

The effects on weight and performance of varying many of the vehicle characteristics about the nominal configuration are shown in a later section. These characteristics include wing loading, thrust-to-weight ratio, load factor, wing geometry, aerodynamic performance, fixed equipment weight, and weapon systems weight.

METHOD OF ANALYSIS

Synthesis Program

The computerized synthesis program used in the RPV study is the latest version of the NASA-Ames program for *air*craft *synt*hesis (ACSYNT). Figure 3 is a block diagram of this modularized program. Each module consists of one or more subroutines, which are described below as they apply to the RPV study. The ACSYNT program provides geometrical, mass, and performance information for a vehicle concept as well as sensitivity information.

Control program– The control, or executive, program controls the sequence and information transfer for all the other modules, and handles the input to and output from the entire synthesis program. Limits of the various program loops and number of passes through the program for any one configuration are also set by this subroutine.

Inputs include various vehicle definition parameters, mission specification, and several initial assumptions required to start the program. Outputs from the program include vehicle characteristics required to accomplish the input mission, such as component weights and geometry, fuel requirements for the various phases of the mission, aerodynamic and propulsion system characteristics of the configuration, and combat performance parameters. Both data listings and computer graphics presentations may be used to display the results.

Geometry module– Based on input configuration parameters, some fixed and some assumed, the geometry module defines and sizes a vehicle to be used in the remaining parts of the program. The fuselage, engine, wing, and canard surface are initially sized in this module. The characteristics of these components are updated at each pass through the program. The fuselage is sized to contain the propulsion system, the entire fuel supply, and the fixed equipment, while the wing is sized on the basis of an input wing loading and shape parameters. In addition, the geometry module contains a section that calculates vehicle weight and balance on the basis of a specified static margin and tail volume coefficient. These later two parameters are varied in the sensitivities studies.

Aerodynamics module– This module consists of a procedure to calculate the aerodynamic characteristics of a configuration for a given mission altitude and Mach number. The aerodynamic characteristics of the wing-mounted missiles are also estimated. The calculation procedures employ both theoretical methods and empirical information, and have been calibrated with existing wind-tunnel data for similar configurations to high angles of attack.

The friction drag estimates are based on Frankl and Voishel's extension of von Kármán's mixing-length hypothesis to compressible flow (ref. 2), and an empirical correction for thickness-induced pressure fields derived from a correlation in reference 3 of a large amount of data. At subsonic speeds, the zero-lift drag level is increased by an appropriate form factor. For transonic speeds, an estimate is made of the wing drag accounting for separation as a function of angle of attack and shock location.

The fuselage wave drag ($M > 0.9$) is based on a Sears-Haack equation (ref. 4), which is a function of body length and diameter. This value is corrected for the blunt nose associated with the

electro-optical sensor system. Wave drag on the wing and stabilizing surfaces near Mach 1 is calculated by a modified empirical procedure from reference 3 obtained by a correlation of a wide variety of wing data. At Mach numbers equal to or greater than the shock attachment Mach number, the wave drag is estimated by linear supersonic theory modified for detached shock waves on rounded leading edges. Both the body and wing wave drag estimates have been calibrated against results generated by the wave drag program of reference 5.

The lift and drag due to lift are calculated for angles of attack from zero to beyond maximum lift using a nonlinear theory currently under development at Ames. This theory is derived from momentum integrations for a flow model using a disturbance-velocity gradient from potential theory. Results from this procedure have been calibrated with wind tunnel data on configurations similar to the study RPV.

The drag of the weapons and attachments is calculated using an empirical relationship that is a function of Mach number and missile size. This method is based on a correlation of data obtained in the wind tunnel for similar missiles and methods of attachment.

Propulsion module– The propulsion section of the synthesis program uses an engine similar to the study engine of reference 1. The engine is a turbojet with afterburner and has a maximum turbine inlet temperature of 1900° F. A four-stage compressor is driven by a single-stage turbine, and the compressor pressure ratio at sea level static conditions is 5 to 1. On the basis of a specified vehicle thrust-to-weight ratio, the propulsion subroutine sizes an engine and afterburner, and calculates its sea-level static performance and weight. Then, the values of thrust, fuel consumption, and air flow are calculated for any altitude, Mach number, and power setting. The following power settings are available: maximum afterburning, intermediate (100 percent rpm), maximum continuous, and 90, 70, and 50 percent maximum continuous. The latter power settings are used for throttling during the cruise phase. The basic engine thrust and fuel consumption are corrected for installation losses associated with the inlet and nozzle. The propulsion system characteristics have been programmed to allow the use of a wide range of engine sizes, power settings, altitude, and Mach numbers.

The engine characteristics are state of the art, and no performance improvements have been used that might be considered advanced propulsion system technology. Since the propulsion system has a significant effect on the size, weight, and performance of the RPV, technology advancements in this area are certainly important, particularly in terms of system cost.

Trajectory module– This module computes a vehicle trajectory for the specified mission from information generated in the aerodynamic and propulsion modules. The trajectory consists of climb, cruise, acceleration, and combat maneuvering segments. The amount of fuel used for each phase of the mission is calculated, thus establishing the total fuel requirement. In addition, combat performance parameters for the vehicle are determined at both supersonic and subsonic Mach numbers. These parameters are specific power levels and/or turn rate capability for zero turn rate, sustained turning, and maximum instantaneous turning maneuvers. These performance parameters are explained in a later section.

Structures module– After vehicle sizing, the structural weight is calculated in this module. The procedures used are based on correlations of existing data resulting in empirical equations for the weights of the various vehicle components. The wing and canard weights are a function of load

factor, aspect ratio, leading-edge sweep, taper ratio, thickness-to-chord ratio, and structural material. Load factor, length, and diameter are the parameters used in calculation of the fuselage weight. Methods similar to those described in references 6 and 7 have been used as a guide in developing the structures module. Wherever possible, the results have been calibrated against the weights of actual aircraft components of similar configurations, or with results from more elaborate prediction methods.

Weights module— This module calculates the weights of the remaining components by empirical methods, and uses them with data generated in other modules to compile a total vehicle weight statement. The subroutine then determines if the resulting gross weight meets the input mission requirements. If the vehicle is either too light or too heavy, the entire synthesis program is recycled until an acceptable weight is reached.

Optimizer— Two types of tradeoff studies are used. Generally, the effect on vehicle performance of varying a single parameter individually (all others held constant) is assessed, and a weight or performance sensitivity factor for the parameters in question is determined. This procedure comprises the greater portion of the results. There are a few instances, however, when it is desirable to determine the optimum combination of several parameters to maximize or minimize a preselected measure of vehicle performance subject to prescribed bounds on the vehicle and mission parameters. For these cases, an optimizing module is coupled to the synthesis program. The optimization algorithm is based on Zoutendijk's method of feasible directions; the method and computer program are described in references 8 and 9.

Design Philosophy

There are varied opinions as to the philosophy of design for a superior aircraft in air-to-air combat. For example, the designer may choose to provide high acceleration or high Mach number capability as contrasted to a lower speed design with greater maneuverability. Consideration must also be given to other factors such as the weapon system capability and operational environment of a threat aircraft. Because of the differing philosophies a brief description of the approach used in the present study may be in order before proceeding to the results.

There are several, often conflicting, performance objectives for a low-cost RPV for air superiority. The design philosophy for the combat RPV in this preliminary study is to minimize gross weight while maintaining a turning performance advantage over future threats, and to accept the acceleration capability of the resulting designs. A level of maximum instantaneous turn rate or maximum load factor capability is provided such that the level of performance is considerably higher than that of any known or planned manned fighter but is low enough to keep the structural weight and therefore vehicle gross weight and cost to reasonable values.

Also, the sustained turn rate capability at $M = 0.9$ is selected to provide a reasonable increment over that of any advanced aircraft; experience has shown that high-maneuvering engagements tend to occur at high subsonic speeds due to the fact that both the sustained and maximum instantaneous turn rates usually are a maximum here (ref. 12). Sustained turn rate is an improtant factor because of its strong effect in determining the vehicle propulsion system size. A relatively modest level of sustained turn rate is chosen for the nominal configuration to keep the resulting

thrust-to-weight ratio and therefore the engine and vehicle cost relatively low. However, the acceleration capability of the vehicle is a function of the available thrust, and a lower thrust-to-weight ratio will results in lower acceleration capability. A reduced level of acceleration performance may be acceptable for the present vehicle, since defensive breaks followed by high speed dashes to escape an opponent (for pilot or aircraft safety) may be less critical for an RPV. Therefore, the defensive ability of the RPV under study is given little consideration, with superior offensive capability being the primary objective. Note that if an adversary with a superior acceleration capability is fortunate enough to use this advantage to make a successful escape, the mission of the combat RPV – that is, to gain control of the airspace – is still essentially accomplished.

RESULTS

Form of the Results

The majority of the sensitivity results are presented in three forms: the effects on vehicle weights of variations in specified parameters; effects of various parameters on vehicle combat performance; and sensitivity factors derived from the weight and performance characteristics.

Vehicle weight– The effect on vehicle weights of varying a specific vehicle or mission parameter is presented in the format of figure 4(a), where wing loading is the parameter illustrated. Structural weight, propulsion system weight, and fuel weight (all in kilograms (lb)) are given along with the vehicle gross weight. A sketch, on the same figure, indicates effects of changes in the parameter on vehicle size and shape. Generally a sketch is shown on each plot for configurations with the maximum, minimum, and nominal values of the parameter. These sketches are all to a common scale to allow a quick comparison of vehicle sizes and shapes as a result of changes in configuration and mission parameters. The nominal configuration is usually identified by either filled symbols or by tic marks.

Vehicle combat performance– Effects on vehicle combat performance of changes in a particular parameter are presented as in figure 4(b), where performance is measured, for a given Mach number and altitude, in terms of specific power (P_S) in meters per second (ft per sec) plotted versus turn rate ($\dot{\theta}$) in degrees per second. There are three important areas on these performance plots that should be described.

First, the P_S level at zero turn rate ($P_{S_{1g}}$) indicates the vehicle's acceleration or rate of climb capability. This is important in the prepositioning phase of the engagement before the adversaries are in close contact and a margin in P_S at 1 g can be used to gain a speed or altitude advantage over an opponent. Also, an acceleration advantage can be important (particularly for a manned aircraft) for defensive purposes or escape. Second, the $P_S = 0$ point is the maximum sustained turn rate capability of a vehicle and involves neither a loss nor a gain in vehicle energy. A given number of maneuvers to be performed at $P_S = 0$ are specified in the input mission.

The final important area on the performance plot is the maximum instantaneous turn rate capability of a vehicle which is usually accomplished at the expense of large losses in vehicle energy (negative specific power). For manned aircraft, the maximum instantaneous turn rate

often is limited by pilot tolerance. For the present study of RPVs, the vehicle is allowed to maneuver to its design load factor or lift limit (whichever occurs first) since there is no pilot onboard the aircraft. In several cases, the combat performance presentation includes a second figure (fig. 4(b) concluded), which supplements the plots of P_S versus turn rate. Such a figure usually is included when a parameter appears to have a large effect on both the vehicle weight and combat performance. References 10-12 provide a complete discussion of the implications of specific power and turn rate in air-to-air combat.

Sensitivity factors– Results of the trade studies are summarized in terms of sensitivity factors for both the weight and combat performance characteristics. A sensitivity factor is defined herein as the percentage change in gross weight or performance resulting from a percentage change in the design parameter divided by the percentage change in the design parameter. The sensitivity factors are calculated about the parameter values of the nominal configuration. Using a gross weight (W_g) trade as an example, the sensitivity factor would be defined as follows:

$$\text{sensitivity factor} = \frac{\text{change in } W_g/\text{nominal value of } W_g}{\text{change in parameter/nominal value of parameter}}$$

where the parameter may be W/S, T/W, etc. The sensitivity factor may be positive or negative (or 0); if positive, the vehicle gross weight or performance increases as the parameter value increases. The magnitude of the effect that a given design parameter has on the vehicle weight or performance is indicated by the magnitude of the sensitivity factor.

Nominal Configuration

A nominal configuration to be used in the sensitivity and trade studies is established in this section. In accord with the design philosophy outlined earlier, an ultimate load factor of 11 is selected as giving a reasonable structural weight while allowing sufficient combat performance over that of any planned manned fighter. For this value, with the optimizer coupled to the synthesis program, minimum gross weight (W_g) vehicles are obtained for a range of sustained turn rates at $M = 0.9$ for the nominal mission. This is accomplished at each value of $\dot{\theta}$ by allowing the optimizer to select the optimum combination of wing loading (W/S), thrust-to-weight ratio (T/W), wing thickness-to-chord ratio, wing sweep, and wing taper ratio, while holding all other values constant. These parameters had been expected to have significant effect of vehicle weight and combat performance.

The results of the optimization process are presented in figure 5. Figure 5(a) shows the minimum vehicle weights as a function of sustained turn rate (and the corresponding sustained load factor) at $M = 0.9$. The results show that in order to provide greater sustained turn rate capability for a given value of maximum load factor the gross weight of the vehicle increases. Figure 5(b) indicates the values of the vehicle parameters associated with the minimum gross weight configurations. Higher values of turn rate are accomplished when the vehicle wing loading decreases, thrust-to-weight ratio increases, and the wing sweep is lowered, while only minor changes occur in wing taper and thickness-to-chord ratios.

The combat performance at 9144 m (30,000 ft) is presented in figure 5(c) for the optimized vehicles with sustained turn rates corresponding to the circled numbers in figure 5(a). Increases in sustained turn rate are seen to result in increases in P_S levels for 1 g flight (zero turn rate) and less

negative values of P_S for maximum instantaneous turn rate. The values of maximum turn rate of 22.6° and 16.7° per sec at $M = 0.9$ and 1.2, respectively, are a result of the ultimate load factor of 11 selected for the nominal configuration. The combat results are presented in greater detail in figure 5(c) concluded, for $M = 0.9$ and 1.2. For the sustained turn rates considered, the optimized configurations have maximum angles of attack (limited by load factor) ranging up to about 21°. These relatively low angles primarily are a result of the low wing loadings and the combat altitude of 9,144 m (30,000 ft). The acceleration times from $M = 0.9$ to 1.6 are seen to vary between about 72 to about 78 sec for the various configurations.

The configuration selected as nominal is indicated in figure 5 by tic marks and the circled number 2. A schematic of the nominal configuration is shown in figure 2 along with geometry and weight characteristics of the vehicle. Table 1 lists values of combat performance and summarizes the fuel usage and times required for various legs of the mission. As indicated in figure 5(a), a considerable increase in vehicle gross weight is required to obtain the desired turn performance. The wing loading and thrust-to-weight ratio at launch for the nominal configuration are seen to be 2.11 kN/m^2 (44 lb/ft^2) and 1.11, respectively (fig. 5(b)), and, as a matter of interest, the values at the beginning of combat are 1.87 kN/m^2 (39 lb/ft^2) and 1.25, respectively. The primary factor leading to the relatively high levels of turn performance is the optimum wing loading value, which is considerably lower than that of any known advanced fighter. Also, the optimum T/W is modest compared to some advanced fighters, which is an important factor in keeping vehicle costs down. Figure 5(b) shows the optimum values of wing Λ, λ, and t/c for the nominal configuration to be 40°, 0.22, and 0.052, respectively.

For the nominal configuration, a maximum angle of attack of about 15° was reached at maximum instantaneous turn rate for $M = 0.9$ (fig. 5(c) concluded), while the angles of sustained turn rate are 7° and below (again because of the low value of W/S). As indicated in table 1, the greater consumption for the combat phase of the mission occurs during the three supersonic turn maneuvers. Note also that the total time at maximum power for combat is on the order of about 5.3 min for the nominal configuration. This may be a longer time than is actually required for this vehicle to engage two opponents and launch two missiles.

Vehicle Parameter Sensitivities

General– This section presents the sensitivity of the weight and combat effectiveness of the nominal configuration to changes in wing loading, thrust-to-weight ratio, and ultimate load factor. The effects of a variation in (W/S) on the vehicle weights and relative size were shown earlier in figure 4(a) as an example of data presentation. The gross weight decreases rapidly with increasing W/S up to a value of about 3.35 kN/m^2 (70 lb/ft^2) due to an improving wing weight fraction and a decreasing drag level associated with a smaller wing. The sketch shows the relative size of the various configurations considered. The nominal configuration (filled symbols) is not selected as that having least gross weight due to a compromise with combat performance (fig. 4(b)). The turn rate capability of the vehicle is degraded at higher wing loadings, particularly for the $M = 0.9$ combat conditions. However, acceleration is improved by increasing the wing loading (lower drag).

The angle of attack for maximum instantaneous turn rate increases rapidly with increasing wing loading, particularly for $M = 0.9$. Again, it should be pointed out that the nominal launch

wing loading of 2.11 kN/m^2 (44 lb/ft^2) is a result of a compromise between vehicle weight and combat performance and is considerably lower than that of existing or planned manned combat aircraft. This low wing loading results in significant improvements in combat turning performance for the RPV as compared to a manned aircraft.

The effects of variations in vehicle takeoff thrust-to-weight ratio, T/W, are shown in figure 6. It is apparent that the vehicle weight and size are very sensitive to this parameter. The configuration gross weight and size increase significantly with higher T/W due to the cascading effects of increases in propulsion system weight and size. As noted, the nominal value of T/W (filled symbols) for the combat RPV in this study is lower than that proposed for advanced manned fighters. As with wing loading, the vehicle T/W is determined on the basis of a compromise between weight and combat performance. Figure 6(b) indicates that T/W has a significant effect on the vehicle's combat performance. An increase in T/W results in higher values of sustained turn rate as well as less negative levels of P_S for maximum instantaneous turn rate. More significant, however, are the increases in specific power for 1 g flight ($\dot{\theta} = 0$) and reductions in acceleration time associated with higher thrust-to-weight ratios. However, these improvements in combat performance are accompanied by increases in vehicle gross weight as indicated before. It is concluded that engine weight, cost, and performance have a strong effect on vehicle performance; advanced technology will produce significant payoffs in this area.

Higher levels of maximum instantaneous turn rate than those associated with the nominal configuration can be achieved through an increase in ultimate load factor. The effect of changes in this parameter on vehicle weight and combat effectiveness is shown in figure 7. The vehicle gross weight increases with increasing $N_{Z_{ult}}$ due to higher structural weight fractions, and the vehicle size grows accordingly, as shown in figure 7(a). For this study, the RPV is allowed to maneuver to its structural limit. Thus, very high levels of maximum instantaneous turn rate can be reached at the higher values of ultimate load factor (fig. 7(b)). This results in reductions in specific power for maximum instantaneous turn rate, but only minor changes in the other combat performance parameters. The use of advanced materials can result in sizable payoffs for vehicles with high ultimate load factors. Reductions in wing weight through the use of composite materials are considered in a later section.

Geometry– Figure 8 shows the results of variations in wing thickness-to-chord ratio. Figure 8(a) indicates that increases in t/c of the wing beyond the nominal value (filled symbols) will result in increased gross weight primarily due to increased fuel fractions associated with the higher supersonic drag of the thicker wing. Values of t/c below the nominal appear to have minor but beneficial effects on vehicle weight. Since the wing on this vehicle contains neither fuel nor equipment, a thinner wing could be used, resulting in a reduction in acceleration time as well as improvements in several other combat performance parameters with only a minor loss in sustained turn rate at $M = 0.9$ (fig. 8(b)). The optimization process did not yield a thinner wing because the optimizer was instructed to search for gains in sustained turn rate at $M = 0.9$ with minimum penalties in weight.

The effects of wing leading-edge sweep (Λ) are shown in figure 9. Vehicle weight is seen to decrease with increasing Λ primarily due to a lower unit wing weight associated with a decreasing wing aspect ratio (fig. 9(b) concluded). (The aspect ratio decreases with increasing sweep when taper ratio is held constant for a wing with an unswept trailing edge.) A nominal value of sweep of 40°

resulted from a compromise with combat performance (fig. 9(b)). As Λ is increased, sustained turn rate at $M = 0.9$ decreases due to a loss in lift (fig. 9(b) concluded). However, the lower supersonic drag levels at the higher Λ result in an increased acceleration capability (increasing $P_{S_{1g}}$ at $M = 1.2$) and substantially reduced acceleration times. An increased wing sweep thus offers the possibility of reducing vehicle weight and improving acceleration performance over that of the nominal configuration, but at the expense of a degradation in subsonic sustained turn rate.

Figure 10 shows the results of a variation in wing taper ratio (λ) about the nominal configuration value. For an unswept trailing edge (as in the study RPV) the taper ratio is solely a function of aspect ratio when the leading-edge sweep is held constant. When the taper ratio is increased, the aspect ratio is reduced as indicated in figure 10(b) concluded, resulting in planforms (fig. 10(a)) ranging from the nominal trapezoidal shape to a pure delta wing at $\lambda = 0$. Figure 10(a) shows that as the taper ratio is reduced, the vehicle weight increases as a result of the increasing unit wing weights at the higher aspect ratios. There are only minor effects on combat performance as shown in figure 10(b). The loss in sustained turn rate with increasing λ at $M = 0.9$ is due to a loss in lift accompanying the lower aspect ratios.

Figure 11 shows the effects of increasing the body fineness ratio above that of the nominal configuration value of 8.9. There is a slight reduction in vehicle gross weight with increasing body fineness ratio principally due to a lower supersonic wave drag and therefore reduced fuel requirements. Changes in this geometrical parameter have minor effects on combat effectiveness (fig. 11(b)).

The influence of the canard volume coefficient (defined as the ratio of canard moment arm to wing mean aerodynamic chord multiplied times the ratio of canard to wing planform area) on vehicle weight and combat performance is shown in figure 12. A nominal value of 0.4 was derived from a survey of the data for several typical aircraft-type configurations. Figure 12 shows that the larger canard and wing sizes and the associated weight and drag increases result in increased vehicle gross weight. Advanced control technology may allow a volume coefficient lower than the nominal value used here, thus leading to reductions in gross weight as indicated in figure 12(a). Combat performance is only slightly affected by the canard-volume coefficient (fig. 12(b)).

Figures 13, 14, and 15 show the effects of canard thickness-to-chord ratio, leading-edge sweep, and taper ratio, respectively. Variations in these parameters have essentially no effect on combat performance. Similarly, there are only minor effects on vehicle gross weight, with a slight reduction in W_g accompanying increases in canard sweep and taper ratio (figs. 14(a) and 15(a)).

A zero static margin is assumed for the fully loaded vehicle, since controlled configured vehicle (CCV) concepts are to be employed. The effects of a variation in static margin from +5 percent to −10 percent are shown in figure 16. In this study, the selected static margin affects primarily the wing longitudinal location and the canard size. It appears, at least for the depth of analysis performed, that the chosen static margin has little effect on vehicle weight and combat performance. However, this parameter, together with tail volume coefficient, will probably have a more significant effect when advanced control technology is fully exploited in a more detailed design.

The final parameter investigated in the geometry section is the vertical surface size expressed in terms of percentage of wing area. The results of a variation in tail size from 5 to 20 percent of the

wing area are shown in figure 17, with a value of 10 percent being used for the nominal configuration. Vehicle gross weight increases with vertical size requirements and accompanying increased surface weight and drag, but combat performance remains essentially the same.

Aerodynamics– Figure 18 shows the effects of numerically imposing a ±10 percent change in lift coefficient about the nominal value over the entire mission. This increment in lift could be accomplished, for example, by using a variable incidence wing. An increase in the lifting efficiency of the vehicle (fig. 18(a))produces a significant reduction in gross weight, as well as substantial improvements in the sustained turn rate and specific power for maximum instantaneous turn rate (fig. 18(b)). There is a small but beneficial effect on vehicle acceleration capability due to increases in vehicle lift.

Figure 19 presents the effects of an assumed ±10 percent change in zero-lift drag coefficient about the nominal configuration. The vehicle gross weight appears to be very sensitive to changes in this parameter (fig. 19(a)), which has a strong effect on fuel usage during the mission. This parameter in turn affects the vehicle size as shown. Increased C_{D_o} significantly reduces the sustained turn rate at supersonic speeds as shown in figure 19(b). (The slight rise in some of the performance curves at $M = 0.9$ is a result of the order of performing the mission legs in the synthesis program.) From figure 19(b) concluded, it is apparent that there is a very large effect on the vehicle acceleration capability due to changes in zero-lift drag coefficient.

The effects of numerically imposing a ±10 percent change in drag due-to-lift coefficient about the nominal configuration throughout the mission is shown in figure 20. This parameter does not have as significant an effect on the vehicle gross weight as the previous two aerodynamic parameters. However, an increase in drag-due-to-lift does result in an increased gross weight (fig. 20(a)) and a significant reduction in P_S for maximum instantaneous turn rate (fig. 20(b)).

Figure 21 presents the effects of a ±30 percent change about the nominal value of the drag of the weapons, consisting of two missiles and their attachments. As previously indicated, this spread in the drag level is representative of that noted from wind-tunnel data on similar weapons and mounting methods. The results show an increase in the vehicle's gross weight with increasing weapons drag (fig. 21(a)), but only minor effects on combat effectiveness (fig. 21(b)).

Aerodynamic characteristics clearly have a very significant effect on the RPV weight and combat performance. Although the aerodynamic characteristics used here are hopefully conservative in nature, these large effects dictate the need for substantiating wind-tunnel data on this type of configuration before additional studies are undertaken.

Weights– Figure 22 shows the effects of a variation in the weight of fixed equipment (such as avionics, electro-optical sensor, and electrical systems) from 45 to 340 kg (100 to 750 lb). The nominal value of 227 kg (500 lb) was selected on the basis of a survey of the weights of various components anticipated for the RPV combat mission. This value is believed conservative in view of projections for miniaturization of this kind of equipment in the future. Vehicle gross weight and size increase with increased fixed equipment weight, but the vehicle combat performance is only slightly affected (fig. 22).

For the above variation in fixed equipment weight, the density of packaging the components into the fuselage was assumed constant at 481 kg/m^3 (30 lb/ft^3). The effects of varying the density

of the fixed equipment for a constant weight of 227 kg (500 lb) is shown in figure 23. Increasing the fixed equipment density results in a vehicle that is shorter but actually has a slightly higher gross weight. This apparent inconsistency is explained by the greater supersonic wave drag and increased fuel fraction that accompanies the lower fineness ratio body resulting from the higher values of equipment density. The higher drag level of the body also results in a slight reduction in supersonic combat effectiveness as shown in figure 23(b). Increasing fineness ratio while increasing equipment density would give the expected result of lower gross weight. The fixed equipment requirements for this mission should be defined in more detail, including assessment of the impact of technology advancements in weight and cost.

Figure 24 shows the effects of a change in wing weight from the value associated with the all-aluminum structure of the nominal configuration. Allowances of 20 percent above and 40 percent below the nominal wing weight were made to cover nearly every possible material or method of construction. The relatively high reduction of 40 percent is based on indications that a wing weight saving of as much as 35 percent may be realized through the use of composite materials and improved structural arrangements. As figure 24(a) shows, decreased wing weight significantly reduces gross weight but has only minor effects on combat performance (fig. 24(b)). Of course, there are other areas in the vehicle where the use of advanced materials would result in further weight reductions. However, it is of prime importance to keep the RPV cost down, and therefore a trade between structural material weight and cost must be considered. This would seem to be an area to address in more detail in any follow-on studies of combat RPVs.

Figure 25 presents the effects of variations in payload weight from 36 to 227 kg (80 to 500 lb). The payload consists of two missiles, one mounted under each wing; the above weight range therefore covers weapons weighing from 18 to 113 kg (40 to 250 lb) each. As previously indicated, the nominal configuration carries two infrared seeking missiles of 72.5 kg (160 lb) each, for a total of 145 kg (320 lb). As the weight of the weapons is varied, their size and, therefore, their drag are appropriately accounted for in this study. An empirical procedure based on available data is used to estimate the drag level of each missile size. Of course, each weapon system size and mounting scheme should be investigated in the wind tunnel to establish the exact aerodynamic penalty. The vehicle gross weight obviously increases with heavier weapons, but combat performance is only slightly affected (fig. 25).

Mission Parameter Sensitivities

Cruise altitude and Mach number— Figure 26 shows the effects of lowering the cruise Mach number (both out and back) below the nominal value of 0.9. As can be seen, there is no particular advantage of cruising at a lower speed; in fact, there is an increase in gross weight for Mach numbers below about 0.8. There is no effect on combat effectiveness due to changing cruise Mach number as indicated in figure 26(b). As shown in figure 27(a), variations in cruise *altitude* (both out and back) have a greater effect on vehicle gross weight, which continuously decreases as the cruise altitude is increased up to a value of 15,240 m (50,000 ft). Improved cruise performance is obtained at higher altitudes due to the very low wing loading. A 13,716 m (45,000 ft) cruise altitude is used for the nominal mission. Again, there is essentially no effect of cruise altitude on combat performance (fig. 27(b)).

Combat altitude and Mach number– The nominal combat altitude is 9,144 m (30,000 ft); effects on vehicle weight and combat performance of changes in this altitude are shown in figure 28. Figure 28(a) indicates that the minimum gross weights occur at altitudes between about 9,144 to 12,192 m (30,000 to 40,000 ft); outside this range, the vehicle weight increases rapidly. Combat altitude also has a very significant effect on RPV combat performance (fig. 28(b)). Reduced engine performance with increasing altitude results in a steady decrease in both specific power for 1 g flight ($\dot{\theta} = 0$) and sustained turn rate (and the corresponding sustained load factor) with increasing combat altitude for both the combat Mach numbers of 0.9 and 1.2. As a result of reduced engine thrust with increasing altitude (fig. 28(b) concluded), acceleration time greatly increases for combat altitudes above 10,668 to 12,192 m (35,000 to 40,000 ft).

For the Mach 1.2 combat condition, there is a small but continuous increase in maximum instantaneous turn rate with increasing altitude for a constant limiting load factor of 11. This is accompanied by a loss in P_S for maximum instantaneous turn rate and an increase in angle of attack required to maintain a load factor of 11 up to a value of 23° at 15,240 m (50,000 ft).

An increase in combat altitude for the Mach 0.9 combat phase of the mission produces a somewhat different result (fig. 28(b) concluded). For this Mach number, the RPV can maintain a limiting load factor of 11 with increasing combat altitude up to about 12,802 m (42,000 ft). At this point, the vehicle reaches its maximum lift condition at an angle of attack of about 34°. Above this altitude, the vehicle can no longer generate sufficient lift to reach its maximum load factor, and therefore the maximum instantaneous turn rate (and load factor) drops off. It should be pointed out again that the aerodynamic characteristics (as well as the air-induction system characteristics) need investigation at high angles of attack in the wind tunnel, since the prediction methods for these nonlinear conditions are not well developed.

Figure 29 shows the effects of increasing the supersonic combat Mach number above the nominal mission value of 1.2. It is apparent that a higher supersonic Mach number combat capability will necessitate significant increases in vehicle weight (fig. 29(a)). The combat performance for both the $M = 0.9$ and the supersonic legs of the mission is shown in figure 29(b), where the major changes are seen to occur for the supersonic combat Mach numbers. Figure 29(b) concluded thus presents only the variations in combat effectiveness for vehicles designed for different supersonic combat Mach numbers. As shown, there is an initial loss in sustained turn rate and an increase in acceleration time with increasing Mach number above 1.2, but at about $M = 1.4$ these curves tend to level off. The maximum instantaneous turn rate continuously decreases with increasing supersonic combat Mach number.

Figure 30 shows the effects of decreasing the subsonic combat Mach number below the nominal mission value of 0.9. The gross weight of the RPV is somewhat reduced for the lower Mach numbers (fig. 30(a)), and there are some significant changes in the combat effectiveness of the vehicle. Since figure 30(b) indicates that the major performance changes occur at the subsonic Mach number, figure 30(b) concluded presents only the subsonic combat performance results. As can be seen, there is a continuous decrease in specific power for 1 g flight ($\dot{\theta} = 0$) with a decrease in Mach number, but there is little effect on acceleration time. There is an initial rapid increase in sustained turn rate with decreasing Mach numbers below 0.9, but the curve levels off and begins to reverse direction at about Mach number 0.75.

The most interesting results associated with changes in subsonic combat Mach number occur for the maximum instantaneous turn rate condition. As speed is reduced, the angle of attack continuously increases to maintain a load factor of 11 until a Mach number of about 0.62 is reached. At speeds below this point, the configuration can no longer generate sufficient lift to reach its maximum load factor, and therefore the maximum instantaneous turn rate (and load factor) drops off. This finding once again demonstrates the importance of wind tunnel data on the aerodynamic, inlet, and propulsion system characteristics at high angles of attack so that a wide Mach number and altitude combat capability for the RPV can be achieved.

Combat range and maneuvers– Figure 31 shows the effects of variations in the combat radius from 185 to 741 km (100 to 400 n.mi.). As the range increases, the vehicle gross weight increases and the vehicle size goes up, since the total fuel supply is carried internally in the fuselage. The nominal vehicle weighs 2,460 kg (5,425 lb) for the 370 km (200 n.mi.) mission; to double this combat radius to 740 km (400 n.mi.); the RPV would weigh a little more than twice as much, or some 5,198 kg (11,460 lb). The use of external fuel tanks or air launch becomes more attractive for the longer range missions. The small changes in combat performance (fig. 31(b)) are associated with the relative weights of the vehicles on reaching the combat area; that is, for the same takeoff thrust-to-weight ratio, the vehicle flying the longer range mission uses up more fuel and therefore has a relatively higher T/W (and slightly higher performance) on reaching the combat zone.

Additional effect on gross weight of variations in the number of supersonic and subsonic combat turning maneuvers is shown in figure 32. The nominal curve (repeated from fig. 31) is for three supersonic ($M = 1.2$) and four subsonic ($M = 0.9$) turns of 360° at $P_S = 0$. For the nominal configuration (tic mark), this results in a total combat time at maximum power of about 5.3 min (including acceleration time from $M = 0.9$ to 1.6). As the number of turns is reduced, the vehicle becomes lighter for any given range (fig. 32). For example, taking curve D (one supersonic and one subsonic turn) for the 370 km (200 n.mi.) range case, the vehicle weight is down to about 1,678 kg (3,700 lb) and the total combat time is on the order of 2.5 min. Thus the range and turning maneuver requirements can have a significant effect on the gross weight of the RPV. Additional studies are needed to obtain a better assessment of the maneuvering time that may be required of an air-to-air combat RPV. This time will depend to a large extent on the weapons system of the RPV and the capabilities of its opponent.

Sensitivity Factors

The preceding sections have presented the effects of variations in both vehicle and mission parameters on the RPV weight and combat performance. The range of the individual parameters was large enough to exhibit the overall, nonlinear sensitivity characteristics. Another method of presenting the results is in terms of sensitivity factors, as defined earlier, which are based on local slopes about the nominal configuration. The sensitivity factors derived from the results discussed above are presented in table 2 for both vehicle and mission parameters. The arrows indicate the desired direction of the sensitivity factors: that is, a decline in gross weight and acceleration times and an increase in the three combat performance factors. If a sensitivity has a sign indicating movement in the desired direction (+ for an increase and − for a decrease), then an increase in the parameter is beneficial and conversely. The gross weight sensitivity factors are given for variations in most all vehicle and mission parameters, and for any significant changes in combat performance. The sensitivity factors for combat performance are given for $M = 0.9$ and 1.2.

The data in table 2 indicate that the following parameters have a significant effect (i.e., a sensitivity factor greater than one) on either weight on combat performance:

	Vehicle or mission parameter
gross weight, (W_g)	W/S, T/W $(t/c)_{\text{wing}}$, $(\Lambda)_{\text{wing}}$, C_L, C_{D_o}, combat M
acceleration time, (Acc)	W/S, T/W, $N_{Z_{ult}}$, $(t/c)_{\text{wing}}$, $(\Lambda)_{\text{wing}}$, C_{D_o}
sustained turn rate, $(\dot{\theta}_s)$	T/W, C_L, C_{D_o}, combat altitude, combat M
specific power at 1 g flight condition $(\dot{\theta} = 0)$, $(P_{S_{1g}})$	T/W, $(t/c)_{\text{wing}}$, $(\Lambda)_{\text{wing}}$, C_{D_o}, combat altitude, subsonic combat M
specific power for maximum instantaneous turn rate, (P_{S_i})	W/S, $N_{Z_{ult}}$, C_L, C_{D_L}, combat altitude, supersonic combat M

Based on the number of times a parameter appears above, the nominal configuration is the most sensitive to changes in vehicle thrust-to-weight ratio, zero-lift drag coefficient, and combat Mach number. Next come wing loading, wing thickness and sweep, lift coefficient, and combat altitude. Note that the sensitivity factors indicate only the local effects about the nominal configuration point, and that the parametric trade curves presented in the previous sections should be consulted for detailed effects.

CONCLUDING REMARKS

A computerized synthesis program has been used to assess the effects of various vehicle and mission parameters on the performance of a highly maneuverable remotely piloted vehicle (RPV) for the air-to-air combat role. Performance has been evaluated in terms of both the required vehicle weight to accomplish a specified mission and the combat effectiveness as measured by turning and acceleration capability.

Using an optimization process with minimum values specified for certain combat parameters, a nominal configuration has been established having a gross weight of 2460 kg (5425 lb), the minimum required to accomplish the study mission. This configuration has a relatively high level of combat maneuvering performance compared to advanced manned fighters, primarily due to its lower optimum wing loading of 2.1 kN/m^2 (44 psf) at launch. The optimum thrust-to-weight ratio of 1.11 (at launch), which is relatively modest compared to advanced manned fighters, tends to reduce the weight and therefore cost of the propulsion system, but it also causes some reduction in acceleration performance. Effects of this reduced acceleration capability on the overall RPV combat performance should be assessed from combat simulation studies. The strong influence of the propulsion system on the weight of this vehicle indicates that technology advancements leading to lighter and less costly engines can result in significant payoffs.

Principal results of sensitivity studies using the nominal vehicle as a base point are as follows:

1. The configuration characteristics that exhibit the greatest effects on vehicle weight and combat performance are thrust-to-weight ratio, wing loading, wing-thickness ratio, and wing sweep. The mission parameters having the most significant effects are combat Mach number and combat altitude. The combat range and number of turning maneuvers selected for the basic mission can also have a large effect on the RPV design weight. Additional studies are needed to obtain a better assessment of the amount of maneuvering time required of an air-to-air combat RPV. These studies should account for the characteristics of the weapons system and the capabilities of the opponent.

2. Of the aerodynamic characteristics considered in the sensitivity studies, zero-lift-drag coefficient and lift coefficient have the greatest effects; effects of variations in the former are particularly pronounced. Increasing combat altitude or decreasing combat Mach number results in excursions to maximum lift capability of the RPV. It is apparent that the methods of high angle-of-attack aerodynamic analysis need further experimental verification, particularly wind tunnel tests of the aerodynamic and inlet characteristics over a wide range of angles of attack and Mach number for this type of configuration.

3. Technology advancements leading to reduced structural weights and lower fixed equipment weights are shown to reduce the RPV gross weight, but trade-offs against cost should be considered in these areas.

4. The results indicate that increased combat performance can be designed into the RPV by any of several methods, such as increasing thrust-to-weight ratio, lowering wing loading, increasing limiting load factor, as well as changes in several other vehicle parameters, or through a combination of these. However, these improvements in performance generally come at the expense of significant increases in vehicle gross weight and therefore cost. Thus, studies should be pursued to assess the level of combat performance that will be required in a highly maneuverable RPV.

Ames Research Center
National Aeronautics and Space Administration
Moffett Field, Calif. 94035, October 5, 1973

REFERENCES

1. Staff of AiResearch Manufacturing Co.: Parametric Engine Performance Data for Remotely-Piloted Vehicle Application. Rept. PE-8215-R, Rev. 2, June 1971. (A division of Garrett Corp., Phoenix, Arizona.)

2. Shapiro, Ascher H.: The Dynamics and Thermodynamics of Compressible Fluid Flow. Ronald Press Company, New York, vol. II, 1954.

3. Koelle, Heinz Herman: Handbook of Astronautical Engineering. McGraw-Hill Book Company, Inc., New York, 1961.

4. Miele, Angelo: Theory of Optimum Aerodynamic Shapes. Academic Press, New York, 1965.

5. Harris, Roy V., Jr.: An Analysis and Correlation of Aircraft Wave Drag. NASA TM X-947, 1964.

6. Sanders, K. L.: Aircraft Predesign Weight Estimation Handbook, vol. I Gross, Empty and Structure Weight. Rept. no. 29244-2, Ryan Aeronautical Company, 1965.

7. Sanders, K. L.: Wing Weight Correlation and Preliminary Estimation Method, with Special Emphasis on Drones and Advanced Structural Materials. ASTM 71-49, Teledyne Ryan Aeronautical Company, Nov. 1967.

8. Vanderplaats, Garret N. and Moses, Fred: Structural Optimization by Methods of Feasible Directions. Presented at National Symposium on Computerized Analysis and Design, Washington, D. C., March 1972.

9. Vanderplaats, Garret N.: CONMIN – A Fortran Program for *Con*strained *Mini*mization. NASA TM X-62,282, Aug. 1973.

10. Rutowski, Edward S.: Energy Approach to the General Aircraft Performance Problem. Presented at Annual Summer Meeting, IAS, Los Angeles, July 1953. Douglas Aircraft Company, IAS Preprint 420.

11. Boyd, John R. and Christie, Thomas P.: Energy-Maneuverability Theory. Rept. no. APGC-TDR-64-35, May 1964 (Secret). A. F. Systems Command, Air Proving Ground Ctr., Eglin AFB, Fla.

12. Fellers, W. E. and Patierno, J.: Fighter Requirements and Design for Superiority Over Threat Aircraft at Low Cost. AIAA Paper no. 70-516, Northrop Corporation, March 1970.

TABLE 1.– MISSION PERFORMANCE SUMMARY OF THE NOMINAL CONFIGURATION

Fuel and time					
Mission leg	Power setting	Fuel used		Time, min	
		kg	lb		
Climb	Intermediate	131.5	(289.9)	4.51	
Cruise out	Cruise	142.2	(313.4)	20.38	
Acceleration (M=0.9 to 1.6)	Maximum afterburning	112.6	(248.3)	1.22	Total
Supersonic turns (M=1.2)	Maximum afterburning	175.9	(387.8)	2.16	Combat time = 5.29 min
Subsonic turns (M=0.9)	Maximum afterburning	120.3	(265.3)	1.91	
Cruise back	Cruise	151.0	(333.0)	23.25	
Descent and reserves	–	22.7	(50.0)	–	
		856.2	(1887.7)		

Combat performance

Supersonic turns (M=1.2)

$P_{S_{1g}}$ = 110 m/sec (362 ft/sec)
$\dot{\theta}_s$ = 8.32° per sec
N_{Z_S} = 5.5
Sustained turn radius = 2506 m (8221 ft)

P_{S_i} = -315 m/sec (-1034 ft/sec)
$\dot{\theta}_i$ = 16.93° per sec
N_{Z_i} = 11.0
Maximum instantaneous turn radius = 1231 m (4040 ft)

Subsonic turns (M=0.9)

$P_{S_{1g}}$ = 169 m/sec (556 ft/sec)
$\dot{\theta}_s$ = 12.55° per sec
N_{Z_S} = 6.2
Sustained turn radius = 1246 m (4087 ft)

P_{S_i} = -500 m/sec (-1640 ft/sec)
$\dot{\theta}_i$ = 22.57° per sec
N_{Z_i} = 11.0
Maximum instantaneous turn radius = 693 m (2273 ft)

TABLE 2.– SENSITIVITY FACTORS

Parameter varied (P)	Weight,(Wg) $\frac{\Delta W_g/W_g}{\Delta P/P}$ ↓	Acccleration time (Acc.) $\frac{\Delta Acc./Acc.}{\Delta P/P}$ ↓	Combat, M	$P_{S_{1g}}$ $\frac{\Delta P_{S_{1g}}/P_{S_{1g}}}{\Delta P/P}$ ↑	$\dot{\theta}_s$ ↑ $\frac{\Delta \dot{\theta}_s/\dot{\theta}_s}{\Delta P/P}$ ↑	P_{S_i} $\frac{\Delta P_{S_i}/P_{S_i}}{\Delta P/P}$ ↑
Vehicle parameters						
W/S	-1.224	-1.821	0.9 1.2	-0.119 .972	-0.738 .159	-1.502 -.850
T/W	1.461	-2.151	.9 1.2	1.358 2.330	.301 1.147	.311 .623
$N_{Z_{ult}}$	.792	1.029	.9 1.2	0 0	0 0	-2.566 -2.899
(t/c)wing	1.000	2.167	.9 1.2	.234 -1.149	.249 -.719	-.428 .314
(Λ)wing	-1.282	-1.803	.9 1.2	-.342 1.657	-.669 .553	-.768 -.580
(λ)wing	-.253	-.080	.9 1.2	-.132 .172	-.138 -.044	-.157 -.142
C_L	-1.037	-.410	.9 1.2	-.225 .552	.797 1.082	2.561 2.901
C_{D_o}	2.442	3.620	.9 1.2	.360 -2.417	.319 -1.142	.457 -.604
C_{D_L}	.461	.205	.9 1.2	0 0	-.119 -.601	-1.220 -1.378
l/d body	-.335	---	---	---	---	---
Canard volume coefficient	.295	---	---	---	---	---
(t/c) canard	0	---	---	---	---	---
(Λ) canard	-.295	---	---	---	---	---
(λ) canard	-.076	---	---	---	---	---
Vertical tail size	.074	---	---	---	---	---
C_{D_o} weapons	.330	---	---	---	---	---
Fixed equipment weight	.513	---	---	---	---	---
Fixed equipment density	.142	---	---	---	---	---
Wing weight	.691	---	---	---	---	---
Payload weight	.429	---	---	---	---	---
Mission parameters						
Combat altitude	-0.479	0	0.9 1.2	-1.349 -.939	-1.235 -.871	-2.180 -1.750
Combat Mach number						
· Supersonic	2.212	.738	---	0	-1.875	-2.901
· Subsonic	1.327	.266	---	1.619	-3.586	.091
Cruise Mach number	.270	---	---	---	---	---
Cruise altitude	-.622	---	---	---	---	---
Combat radius	.691	---	---	---	---	---

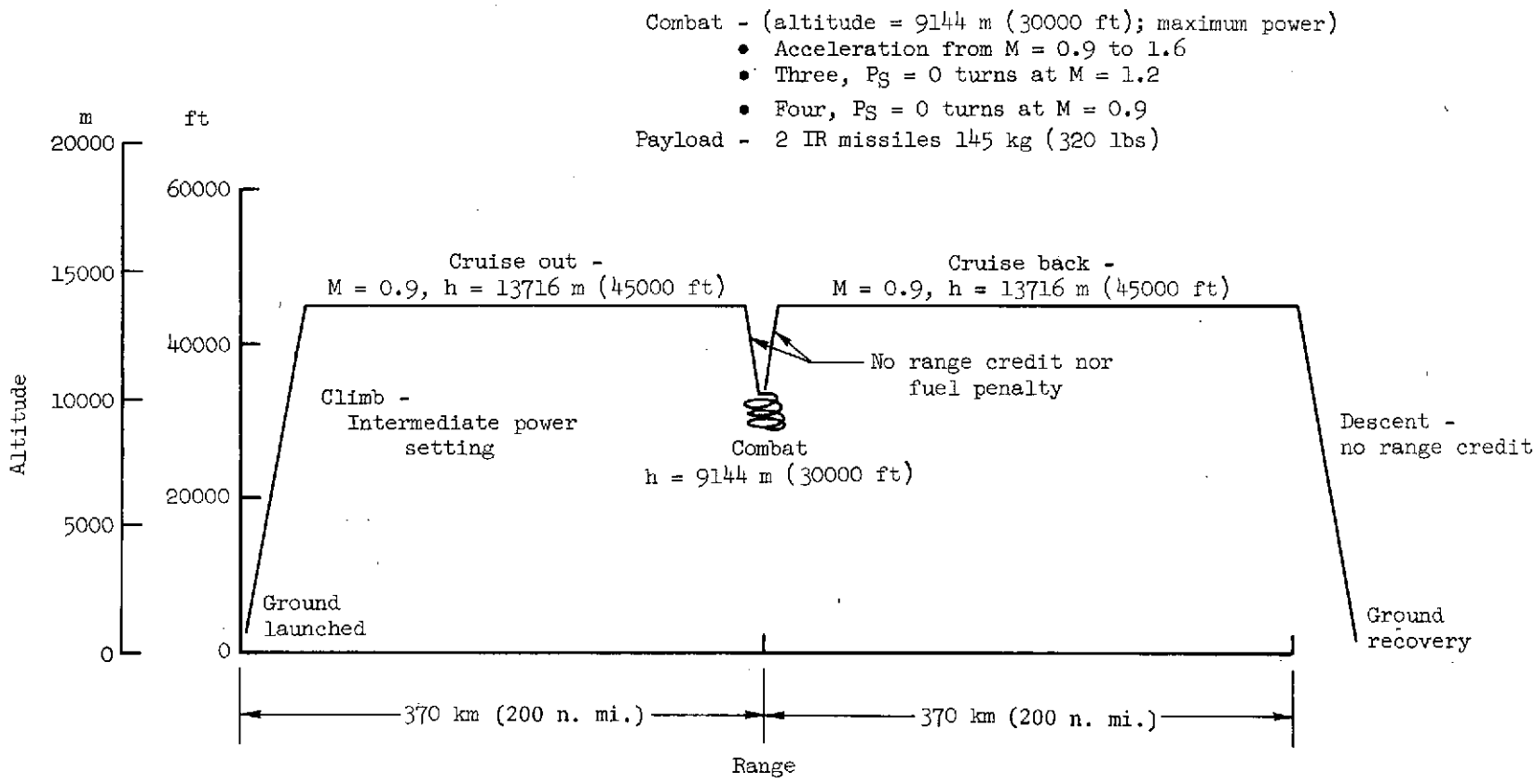

Figure 1.– Nominal mission.

$W/S = 2.1\ kN/m^2\ (44.0\ lb/ft^2)$ $T/W = 1.11$ $N_{Z_{ult}} = 11.0$

Geometry summary

Wing	Canard
$S = 11.47\ m^2 (123.50\ ft^2)$	$S = 2.77\ m^2\ (29.80\ ft^2)$
$b = 5.91\ m\ (19.40\ ft)$	$b = 2.90\ m\ (9.53\ ft)$
$AR = 3.05$	$AR = 3.05$
$\Lambda = 40.0$	$\Lambda = 40.0$
$t/c = 0.052$	$t/c = 0.050$

Body

$l = 8.00\ m\ (26.26\ ft)$
$d = 0.90\ m\ (2.95\ ft)$

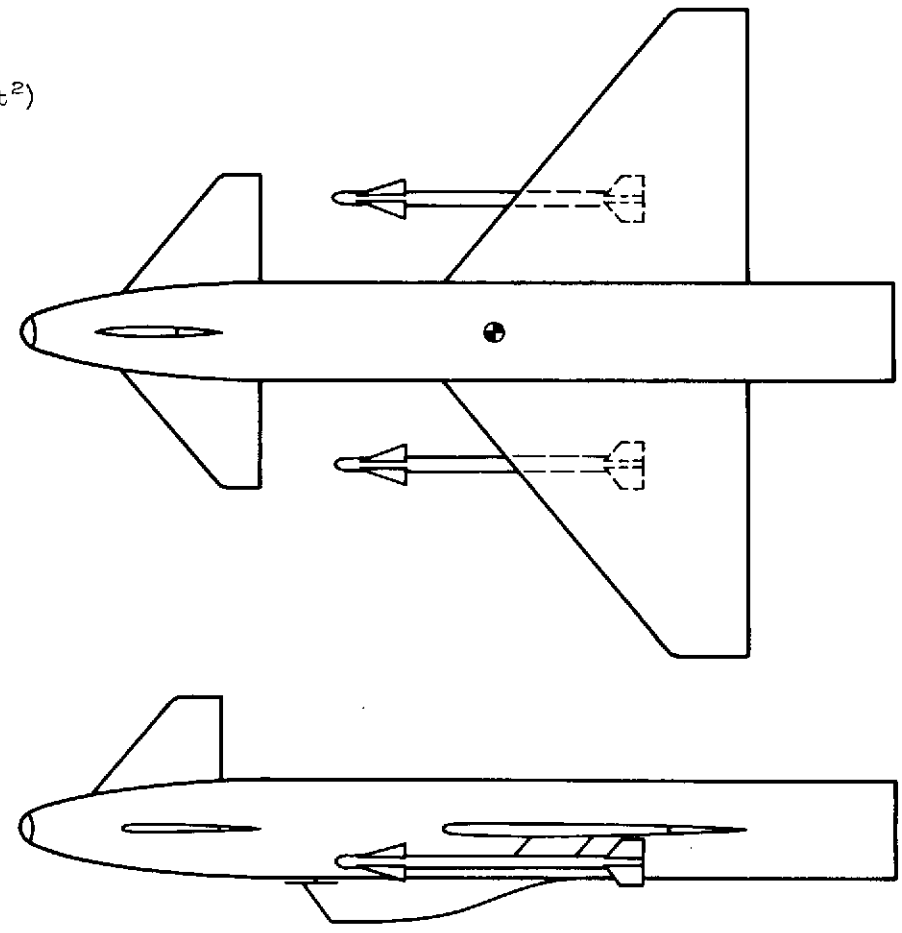

Weight statement

	Weight		%Wg
Structure	646	(1425)	26.2
Propulsion	524	(1156)	21.3
Fixed equipment	227	(500)	9.2
Residual load	62	(136)	2.5
Fuel	856	(1888)	34.8
Payload	145	(320)	5.9
Wg =	2460	(5425)	

Figure 2.– Nominal configuration; all dimensions are in meters (feet), areas in square meters (square feet), and weights in kilograms (pounds).

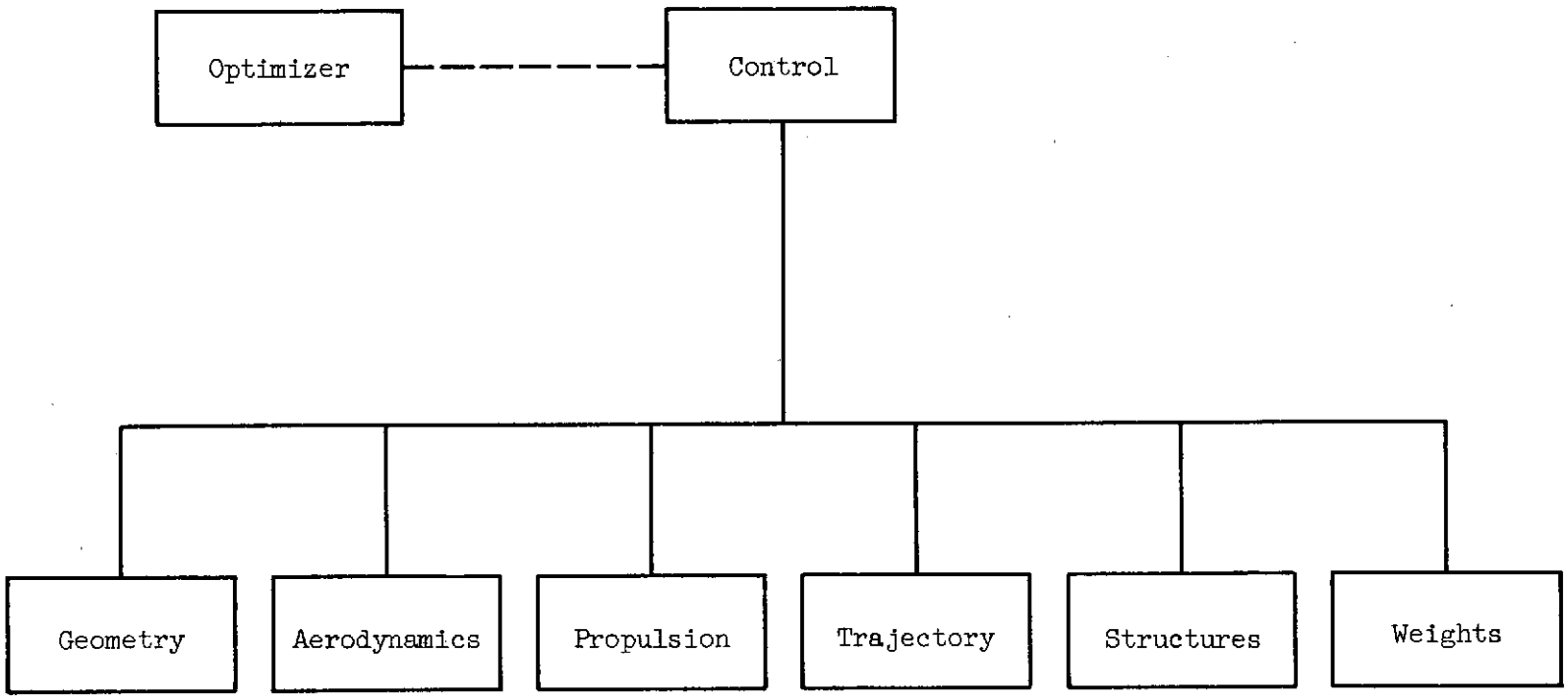

Figure 3.– Synthesis program block diagram.

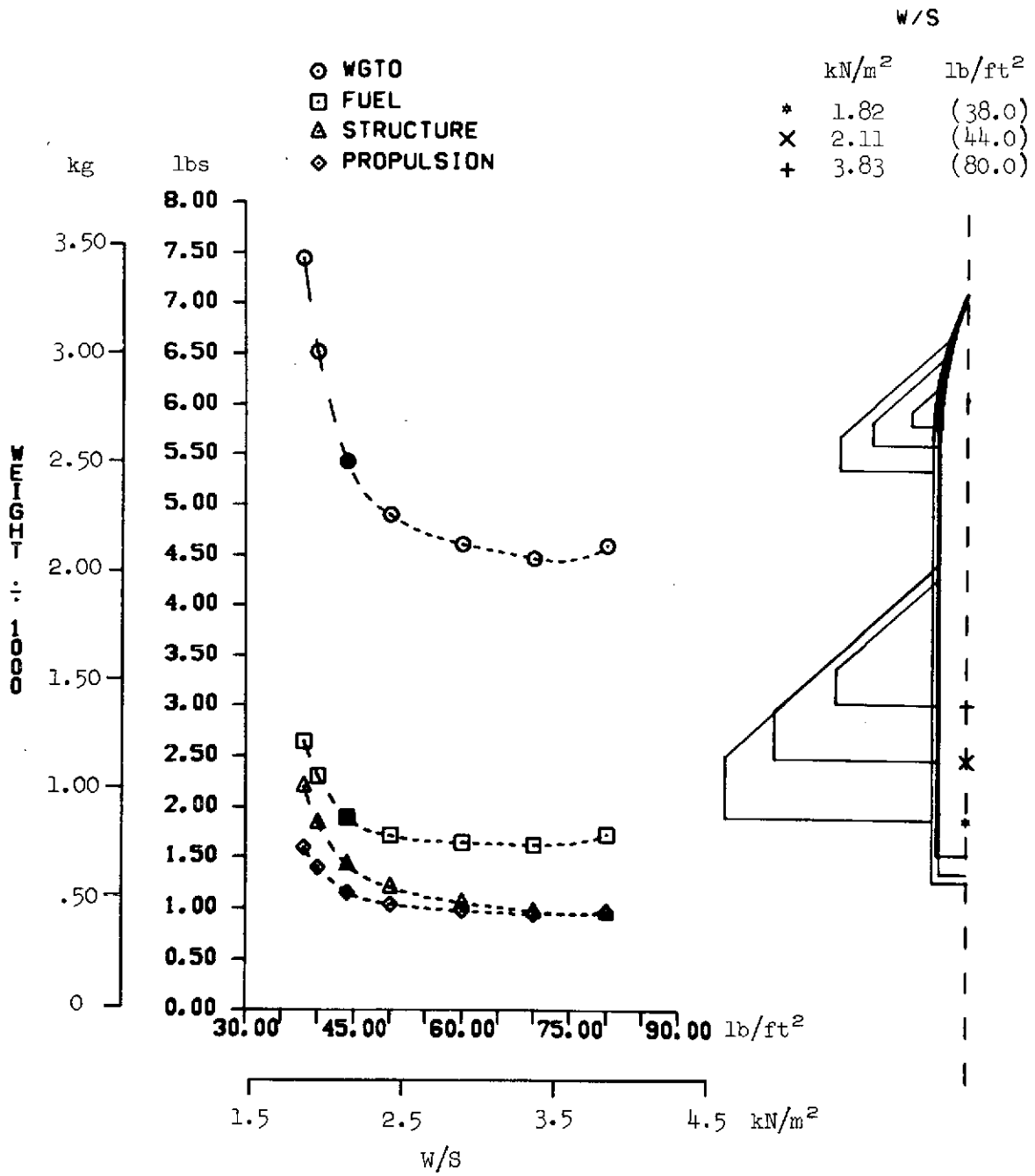

(a) Weights.

Figure 4.– Effect of wing loading.

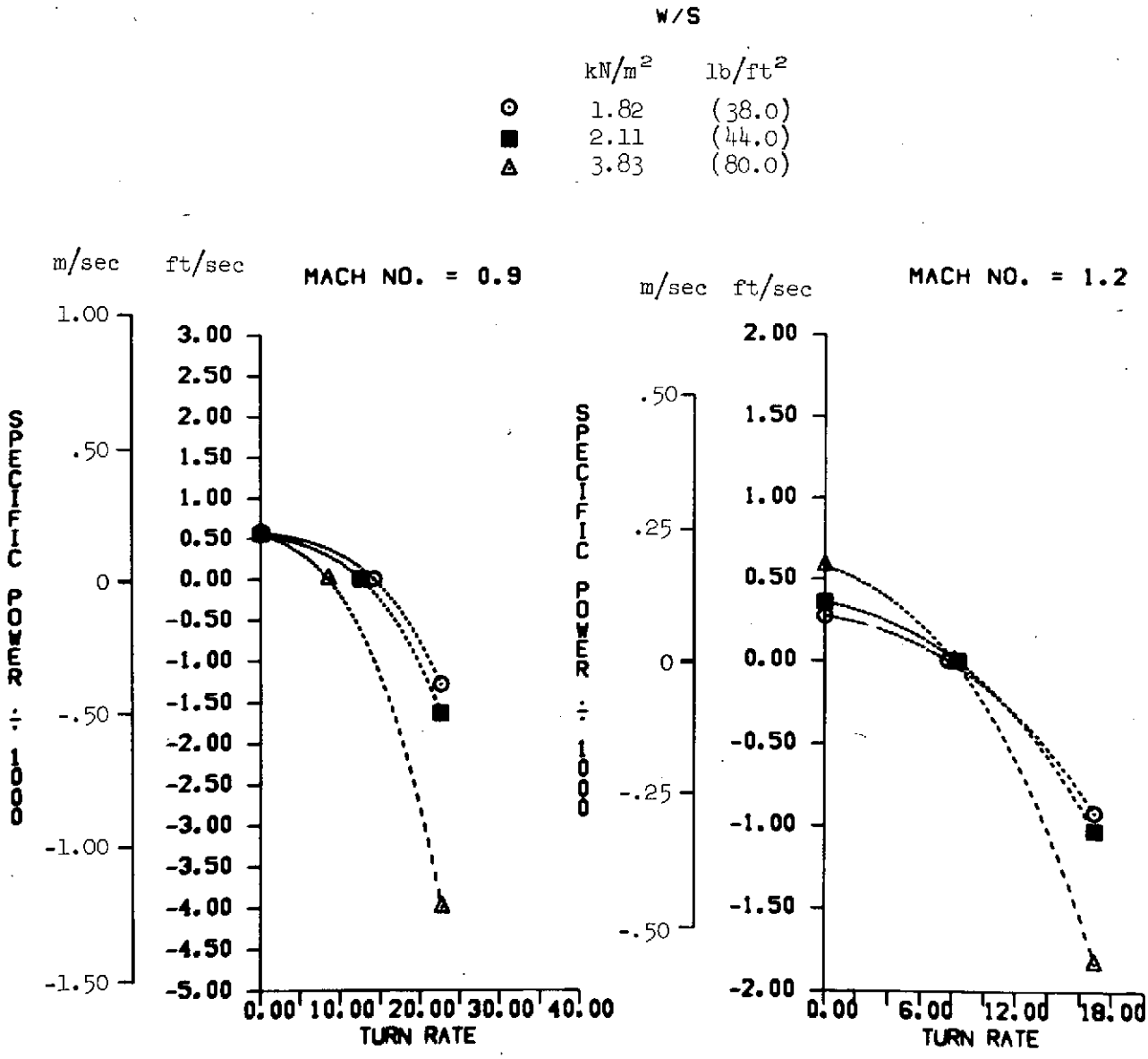

(b) Combat performance.

Figure 4.– Continued.

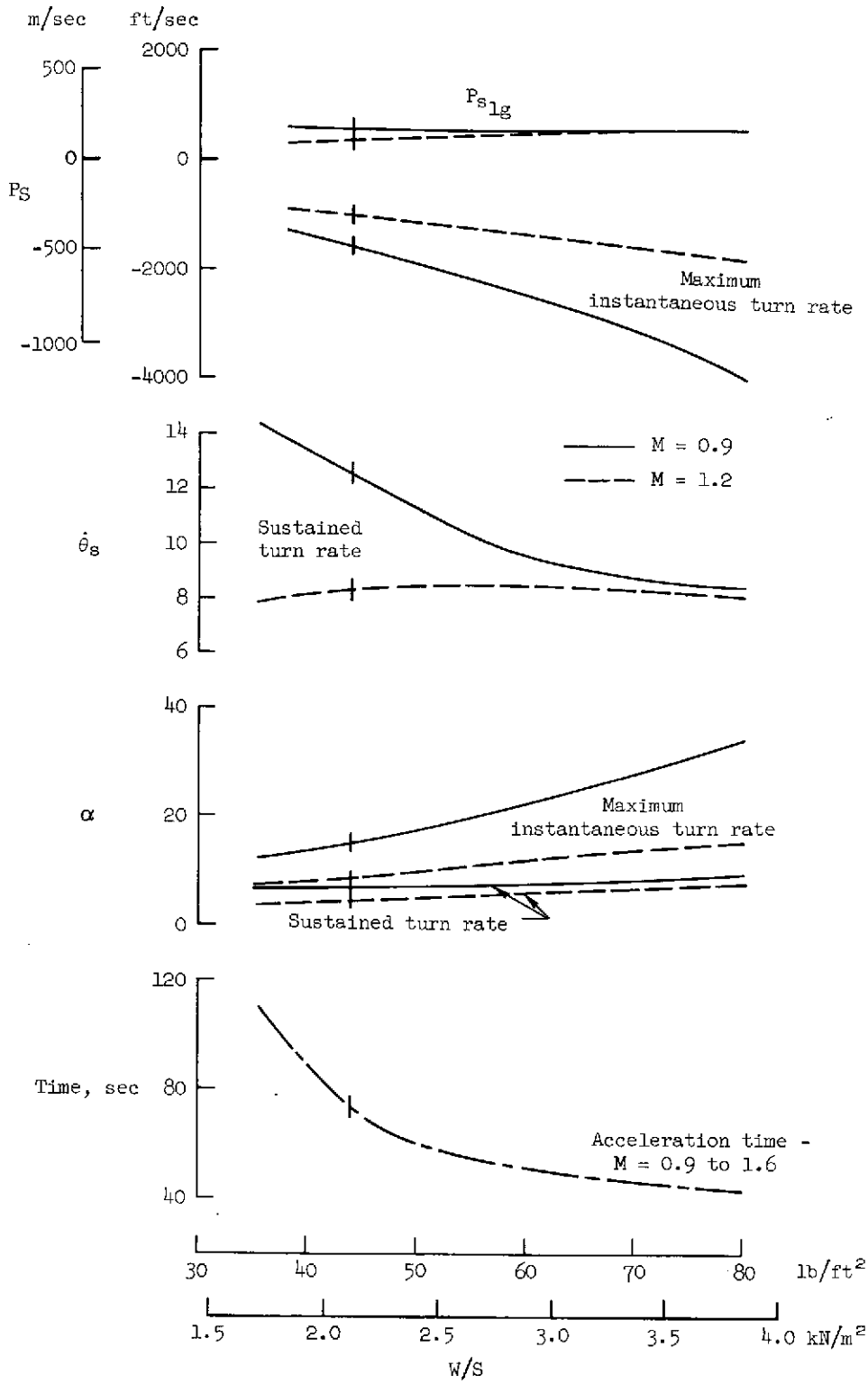

(b) Combat performance (concluded).

Figure 4.– Concluded.

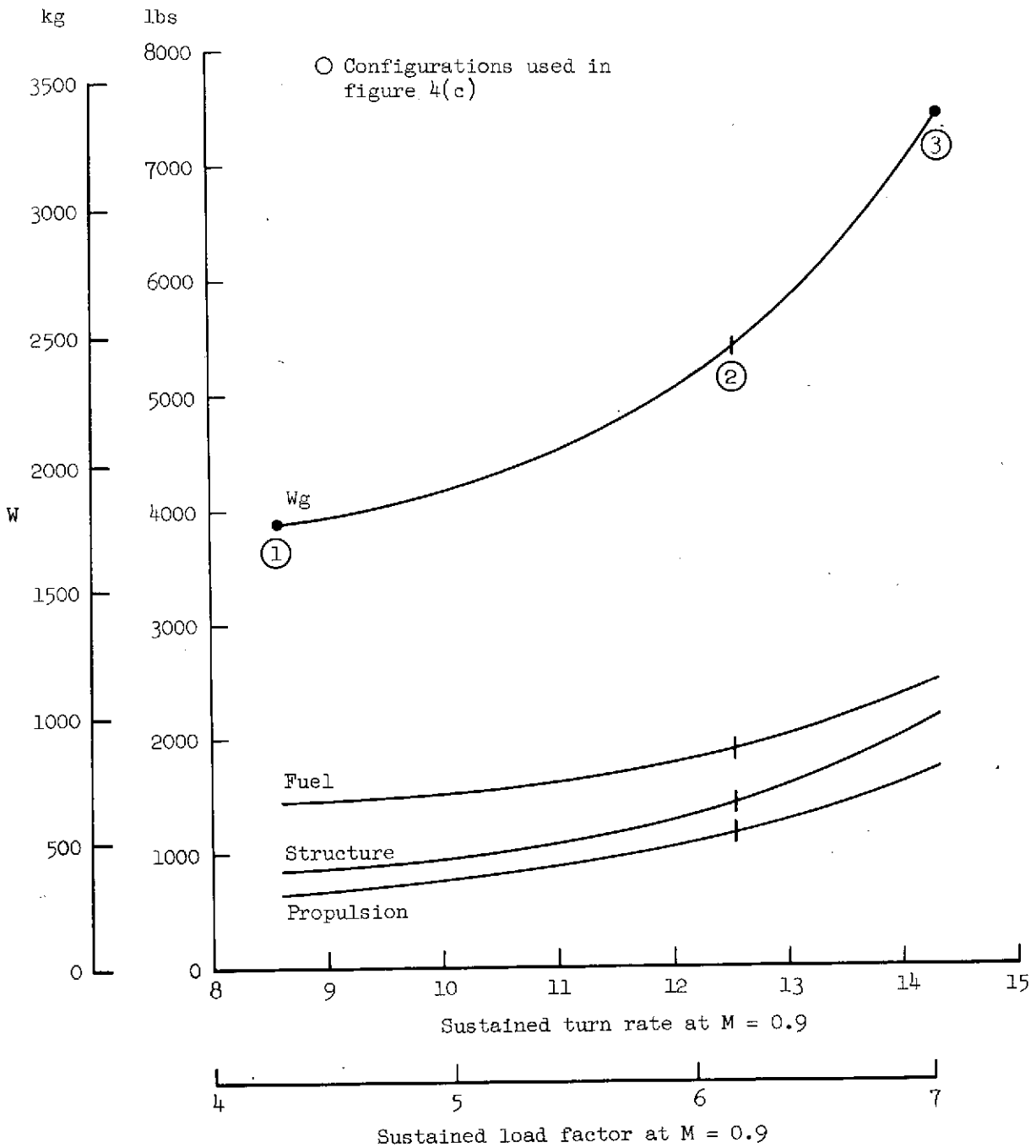

(a) Weights.

Figure 5.– Optimized configurations for various levels of combat performance; $N_{Z_{ult}} = 11$.

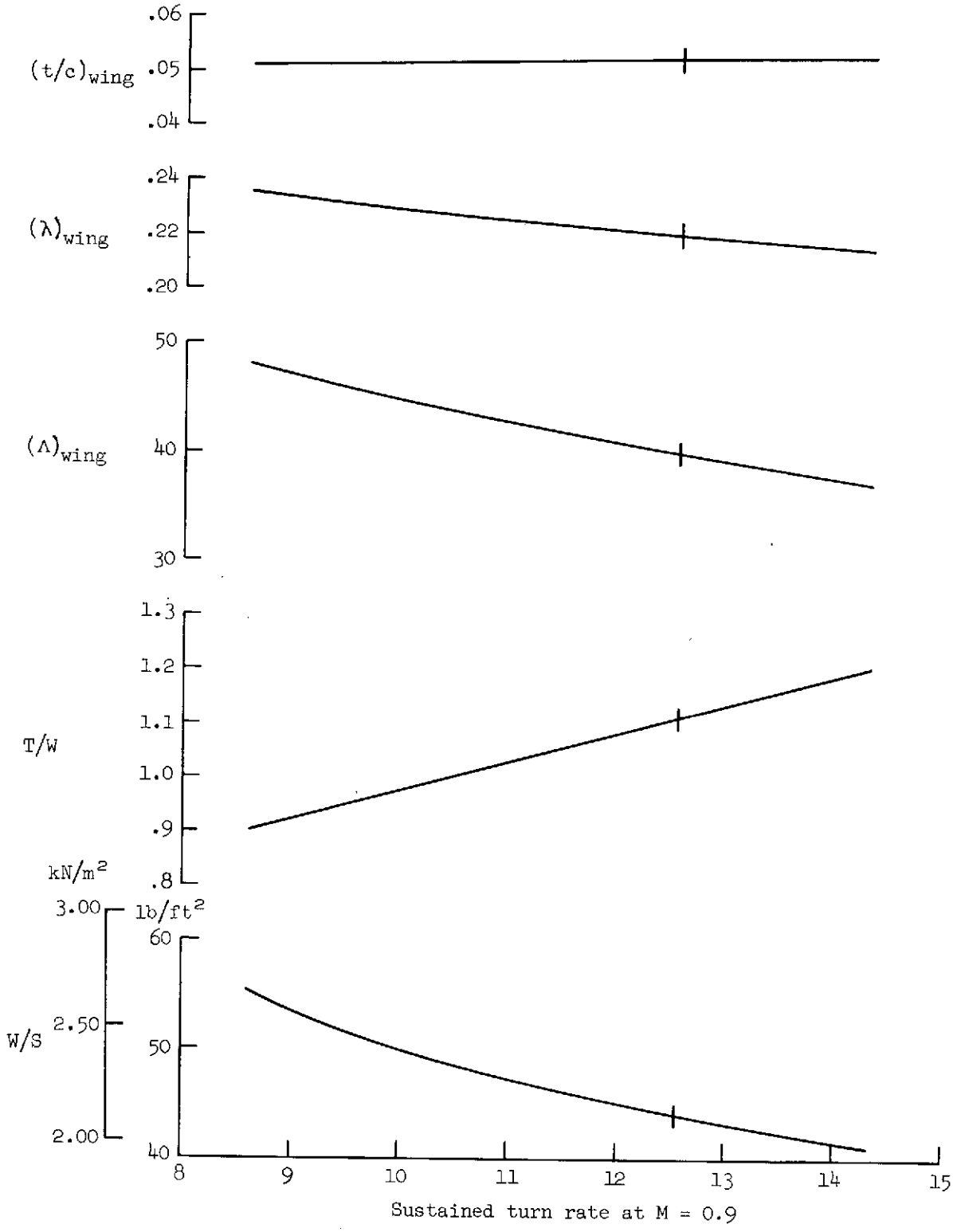

(b) Geometry.

Figure 5.– Continued.

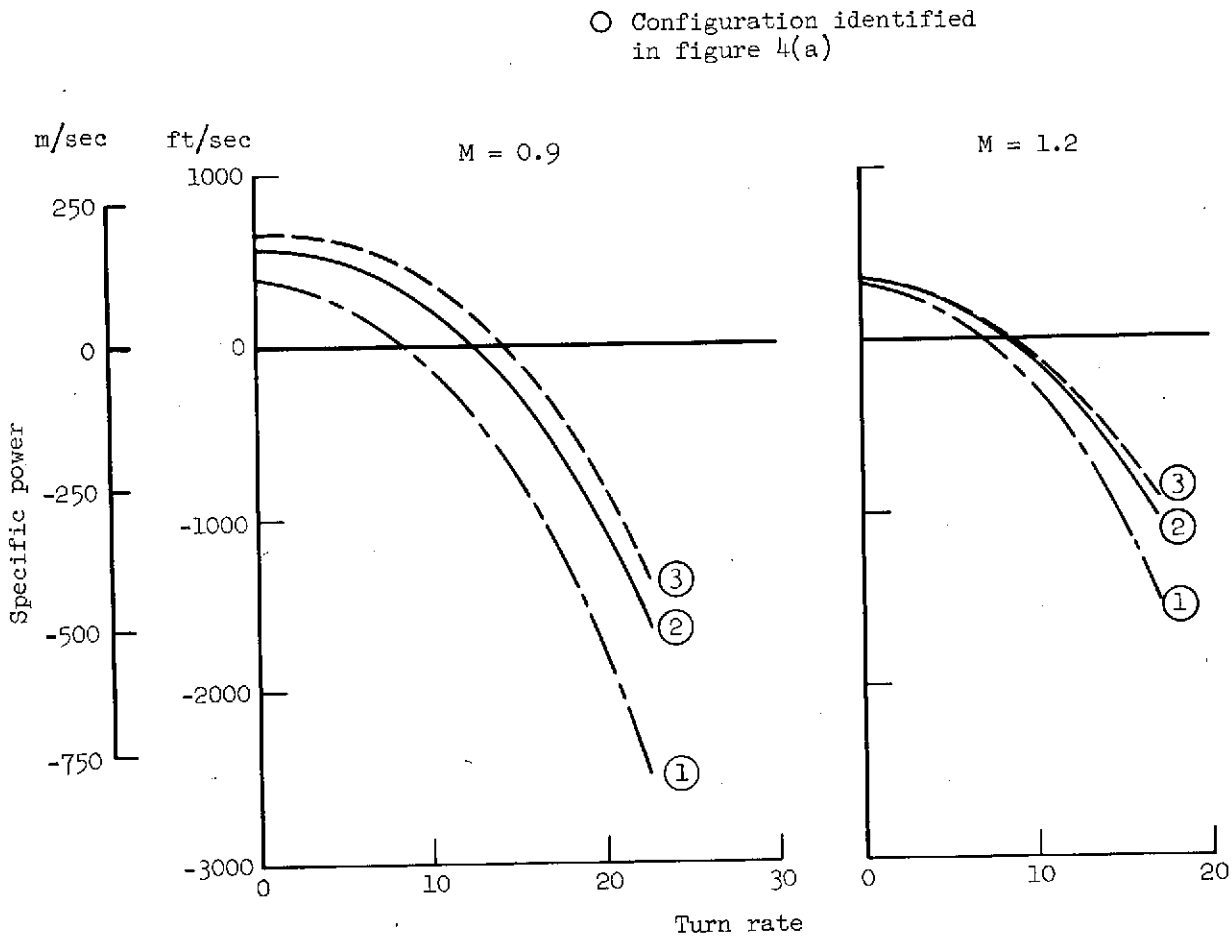

(c) Combat performance.

Figure 5.– Continued.

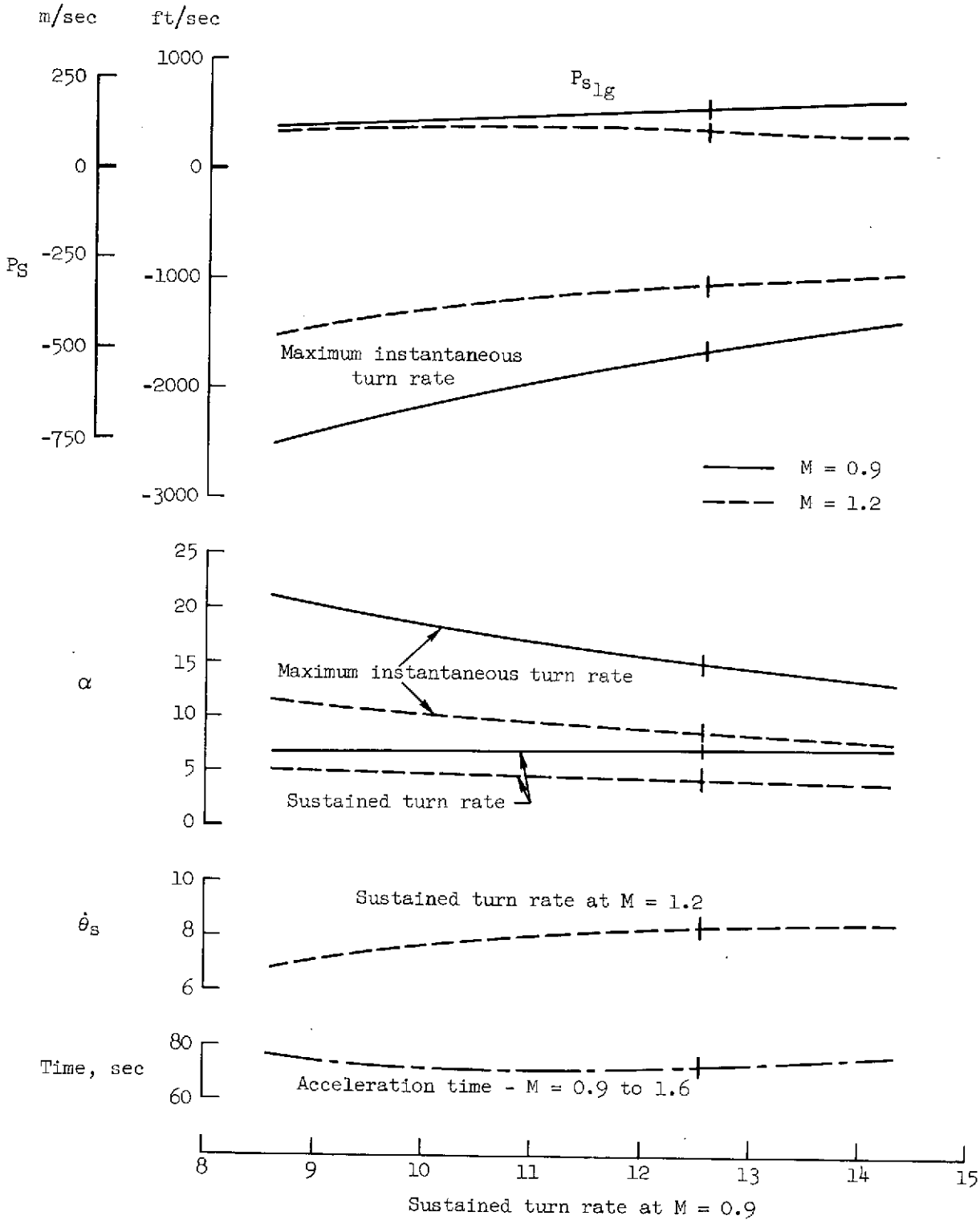

(c) Combat performance (concluded).

Figure 5.– Concluded.

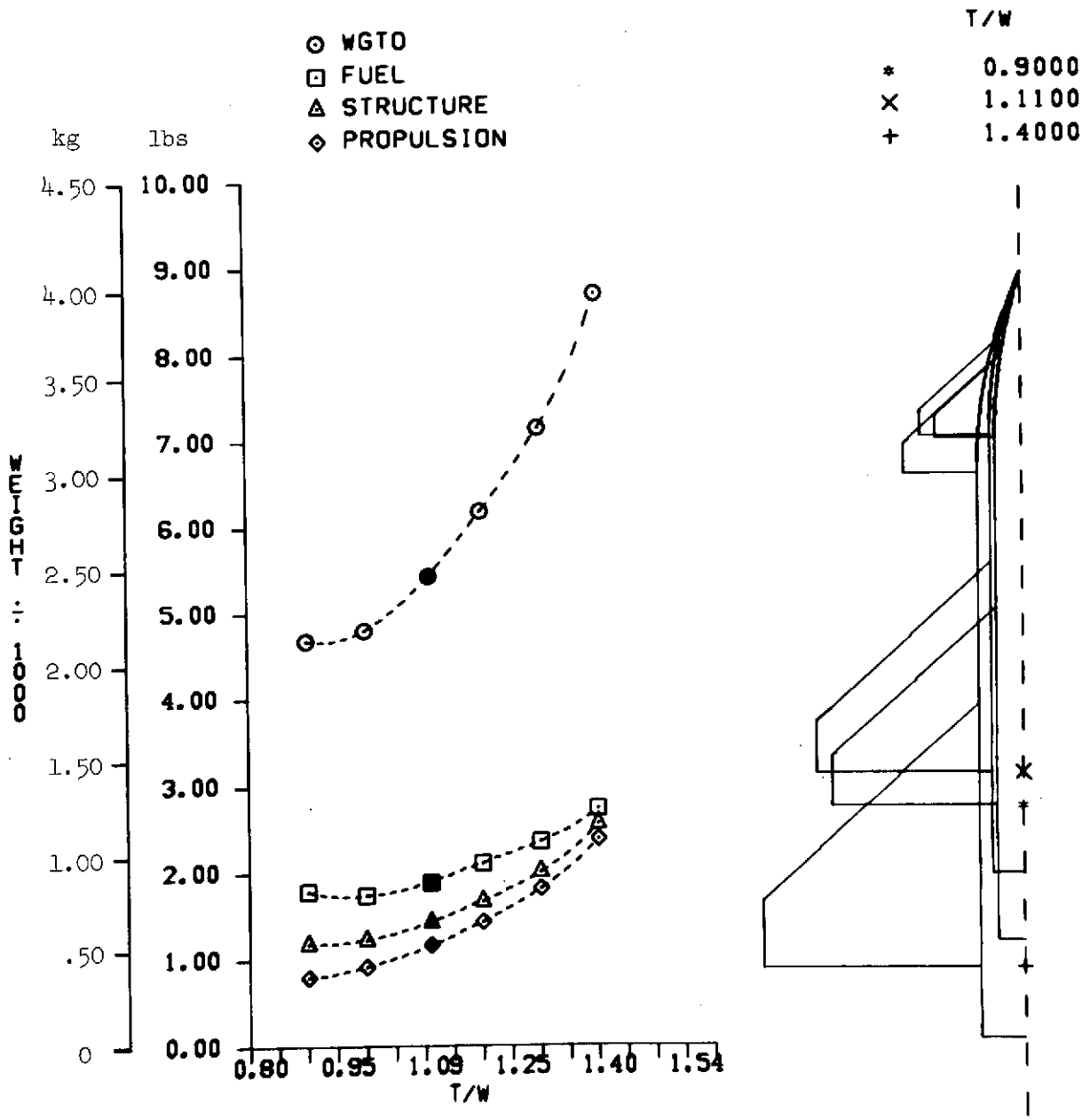

(a) Weights.

Figure 6.– Effect of thrust-to-weight ratio.

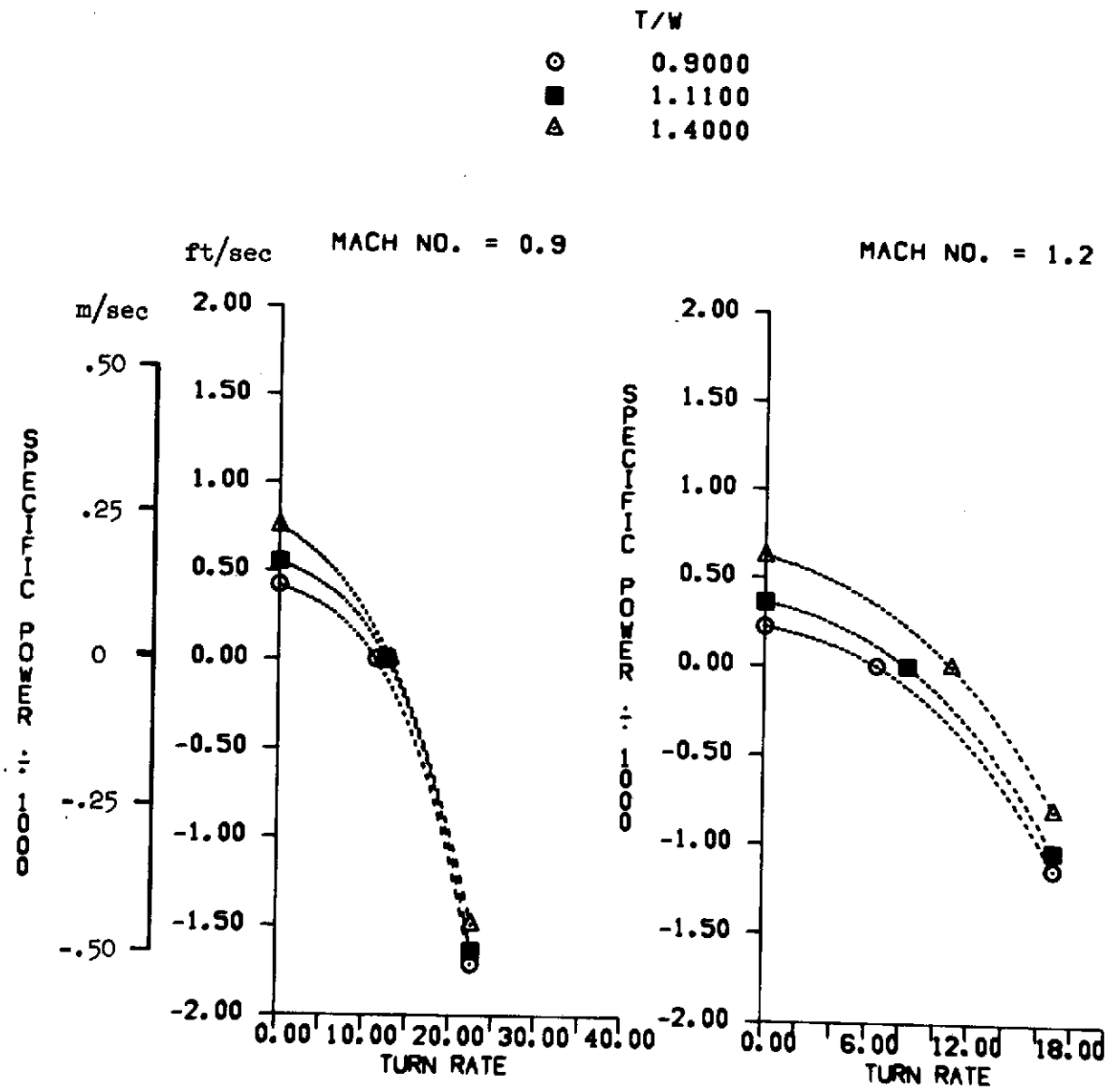

(b) Combat performance.

Figure 6.– Continued.

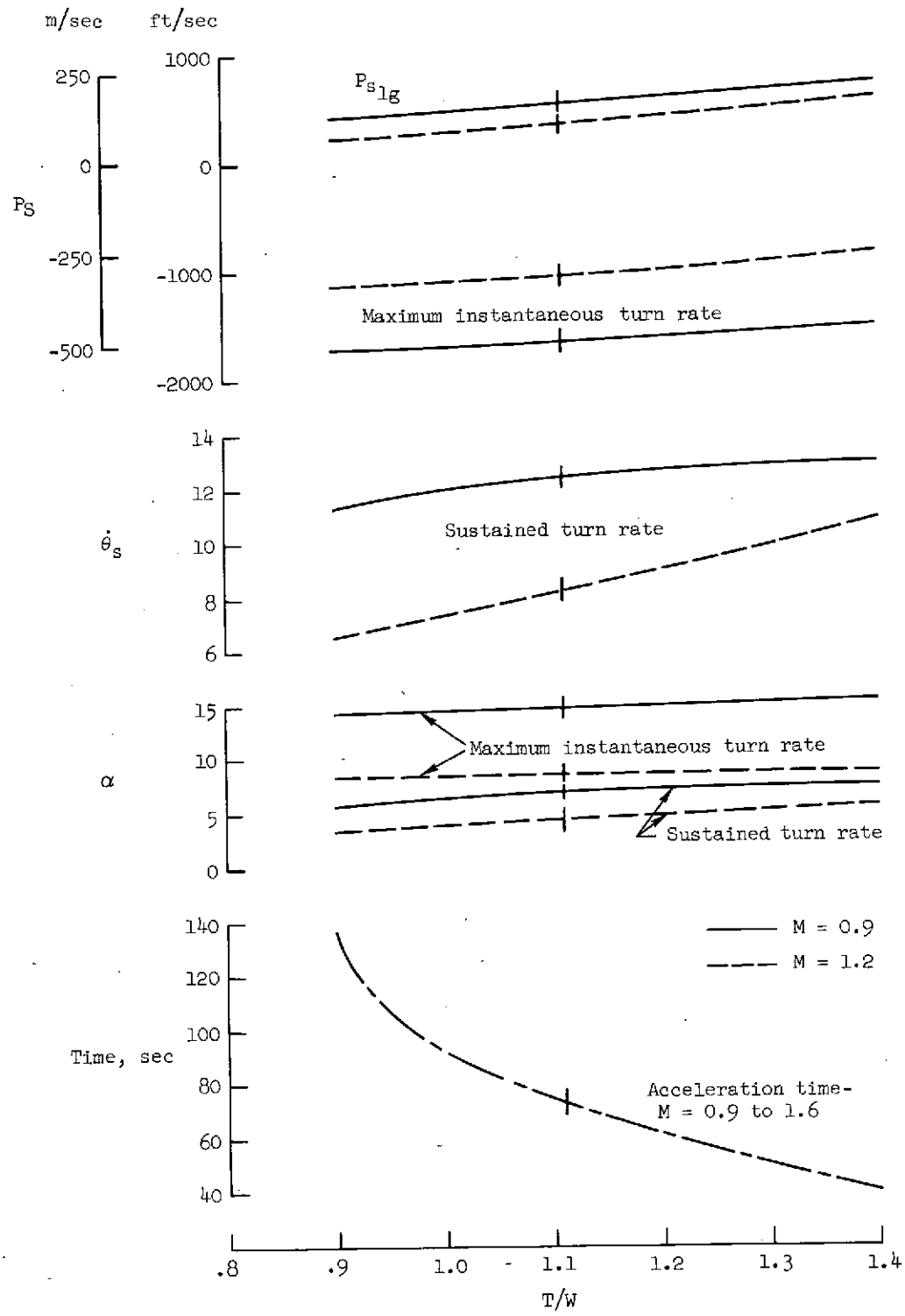

(b) Combat performance (concluded).

Figure 6.– Concluded.

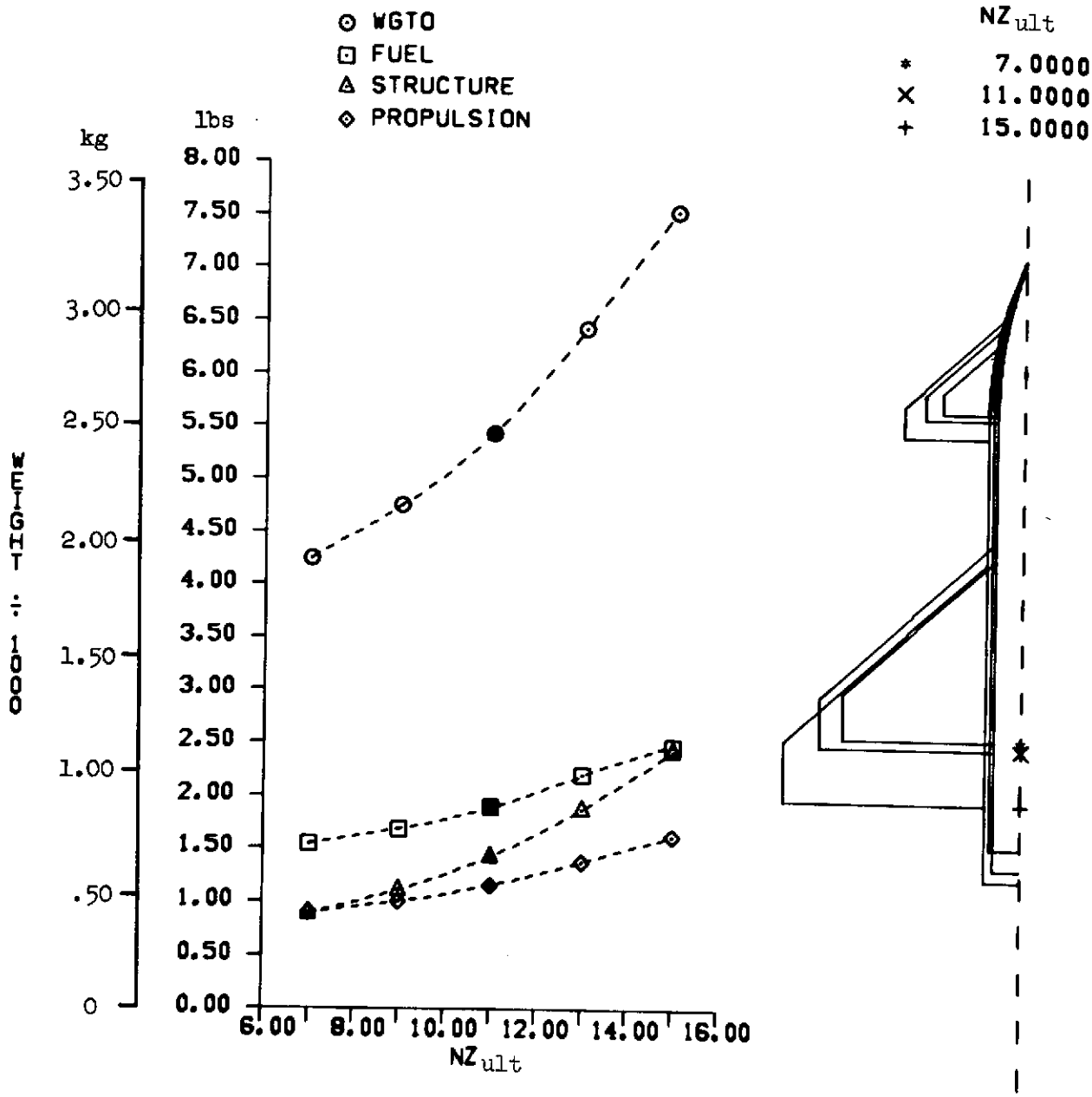

(a) Weights.

Figure 7.– Effect of ultimate load factor.

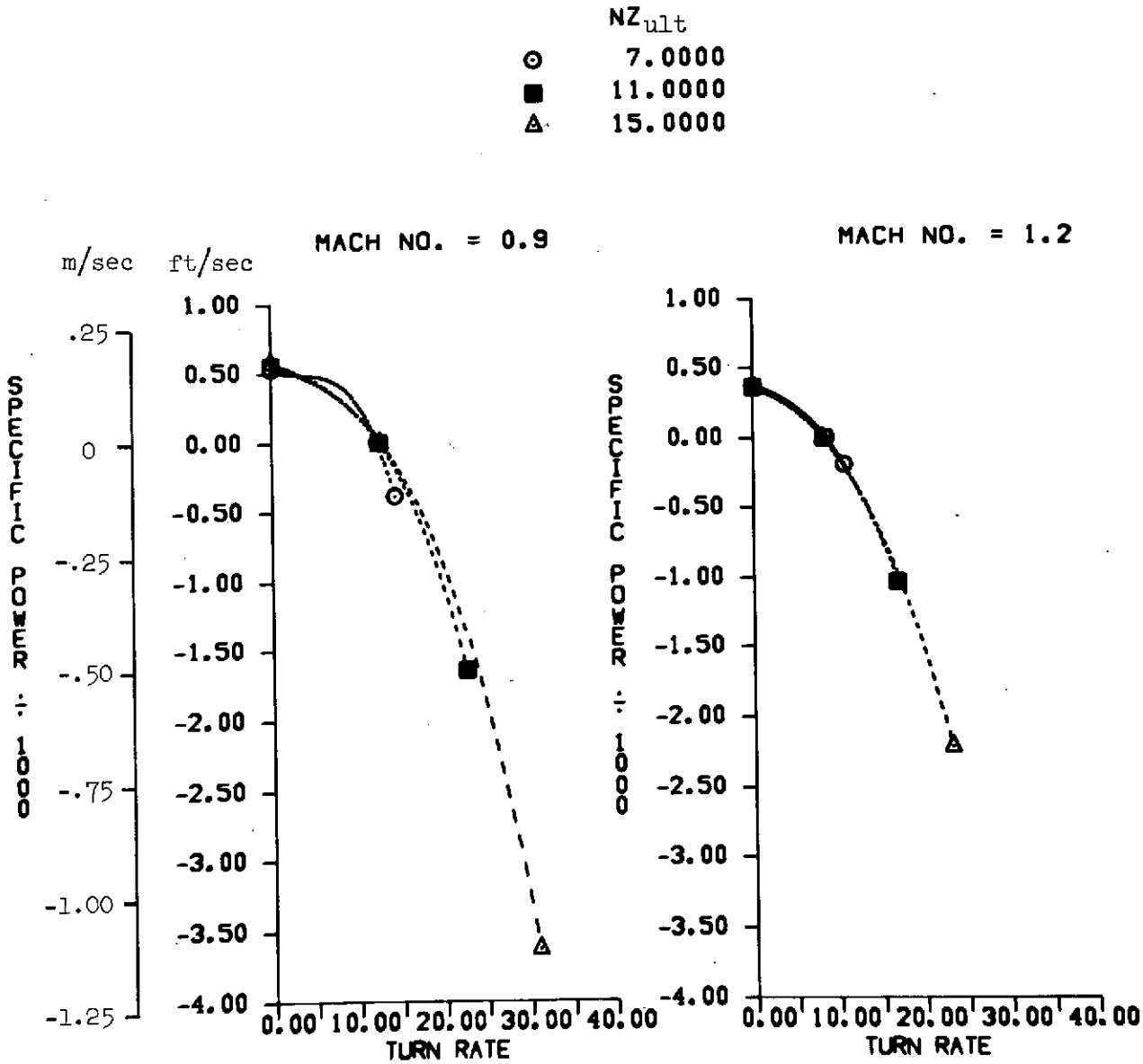

(b) Combat performance.

Figure 7.– Continued.

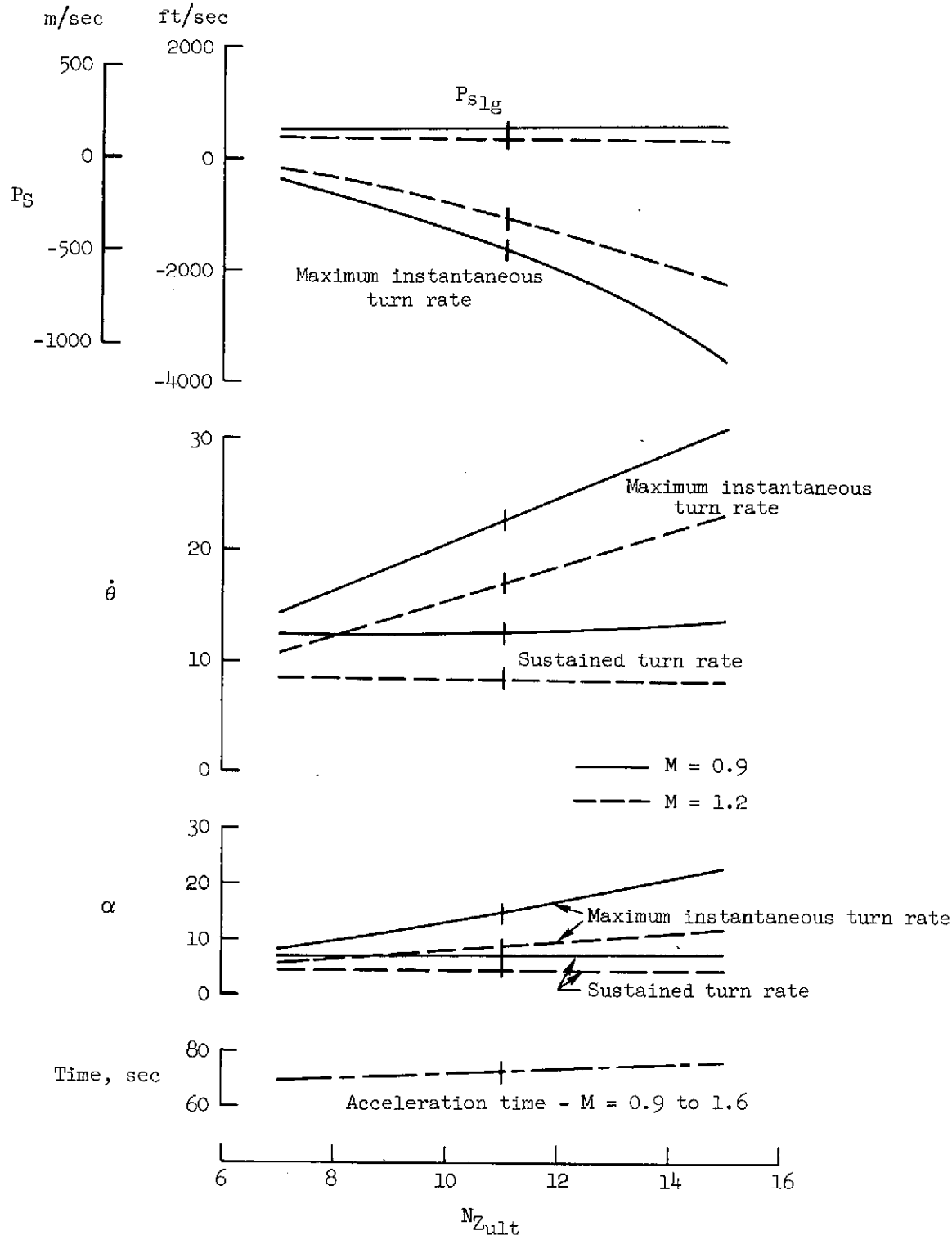

(b) Combat performance (concluded).

Figure 7.– Concluded.

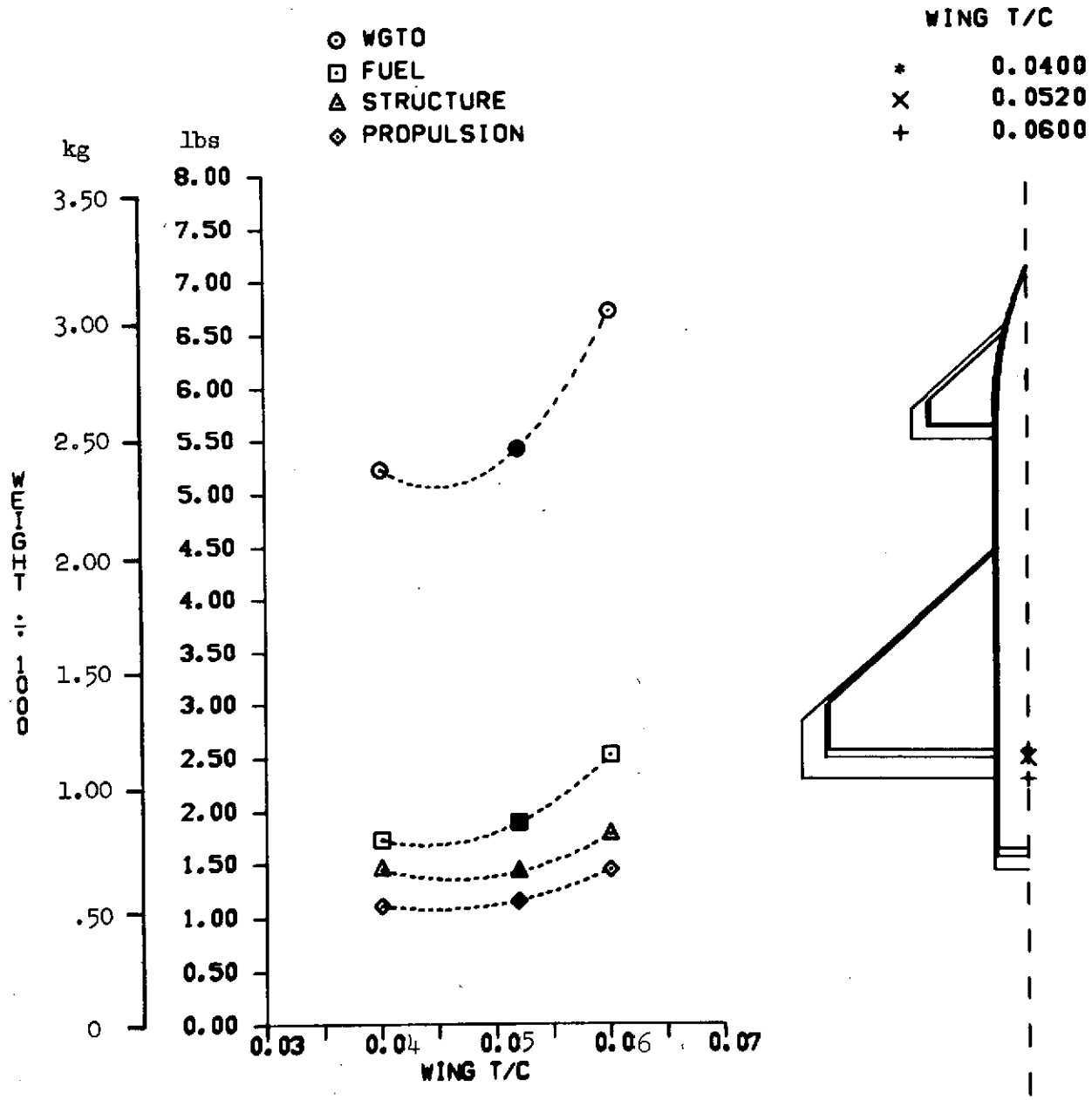

(a) Weights.

Figure 8.– Effect of wing thickness-to-chord ratio.

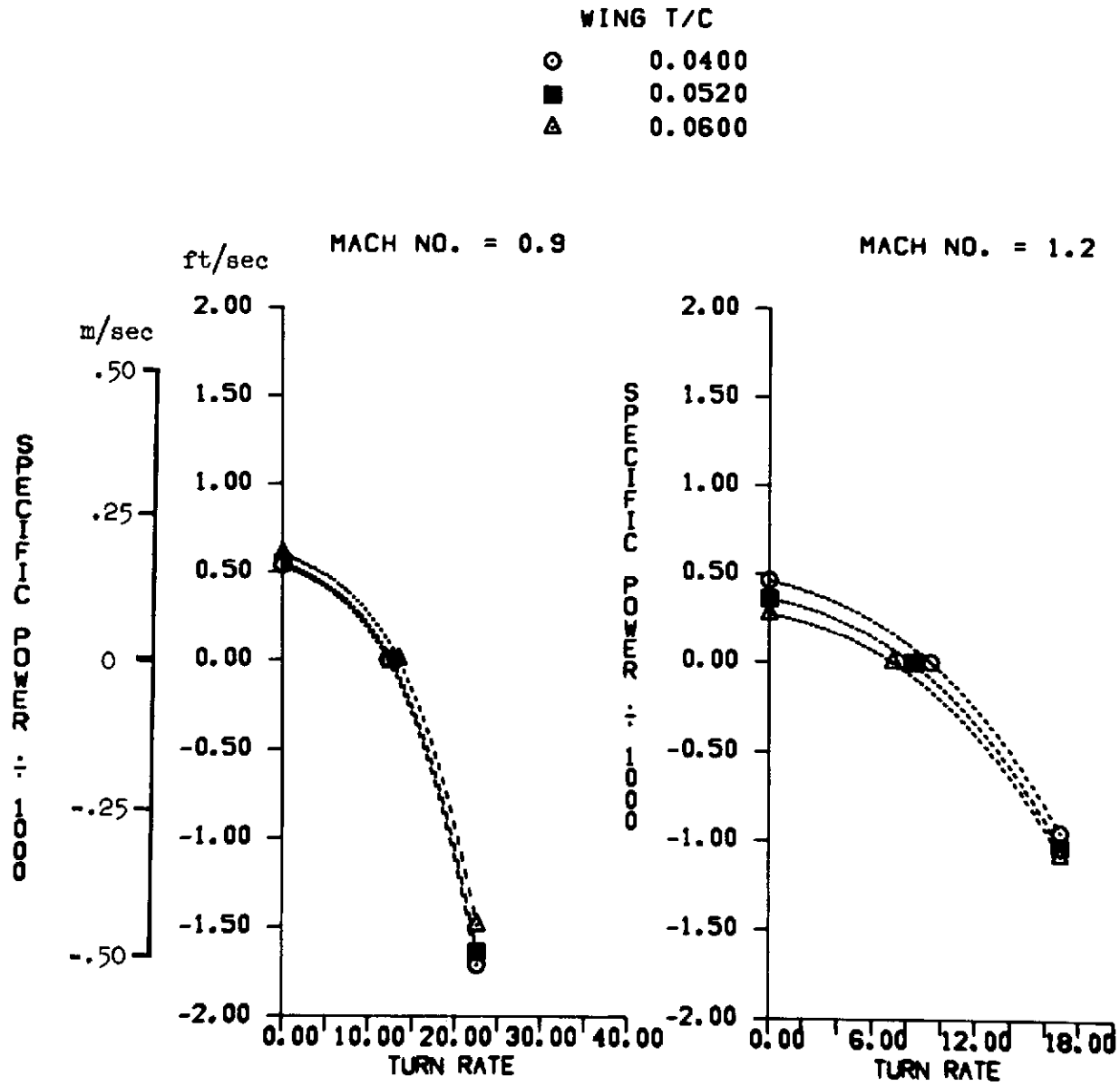

(b) Combat performance.

Figure 8.– Continued.

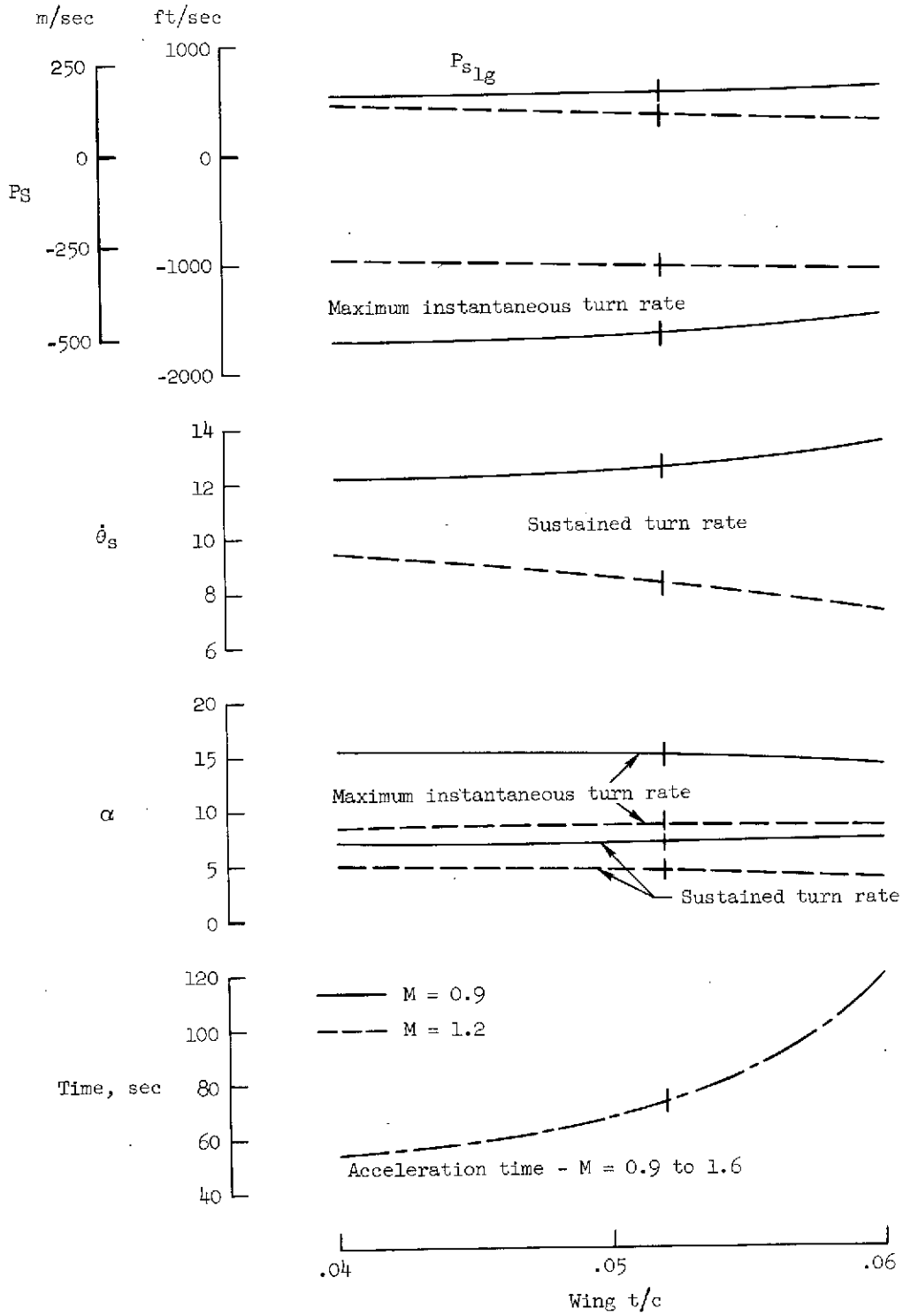

(b) Combat performance (concluded).

Figure 8.– Concluded.

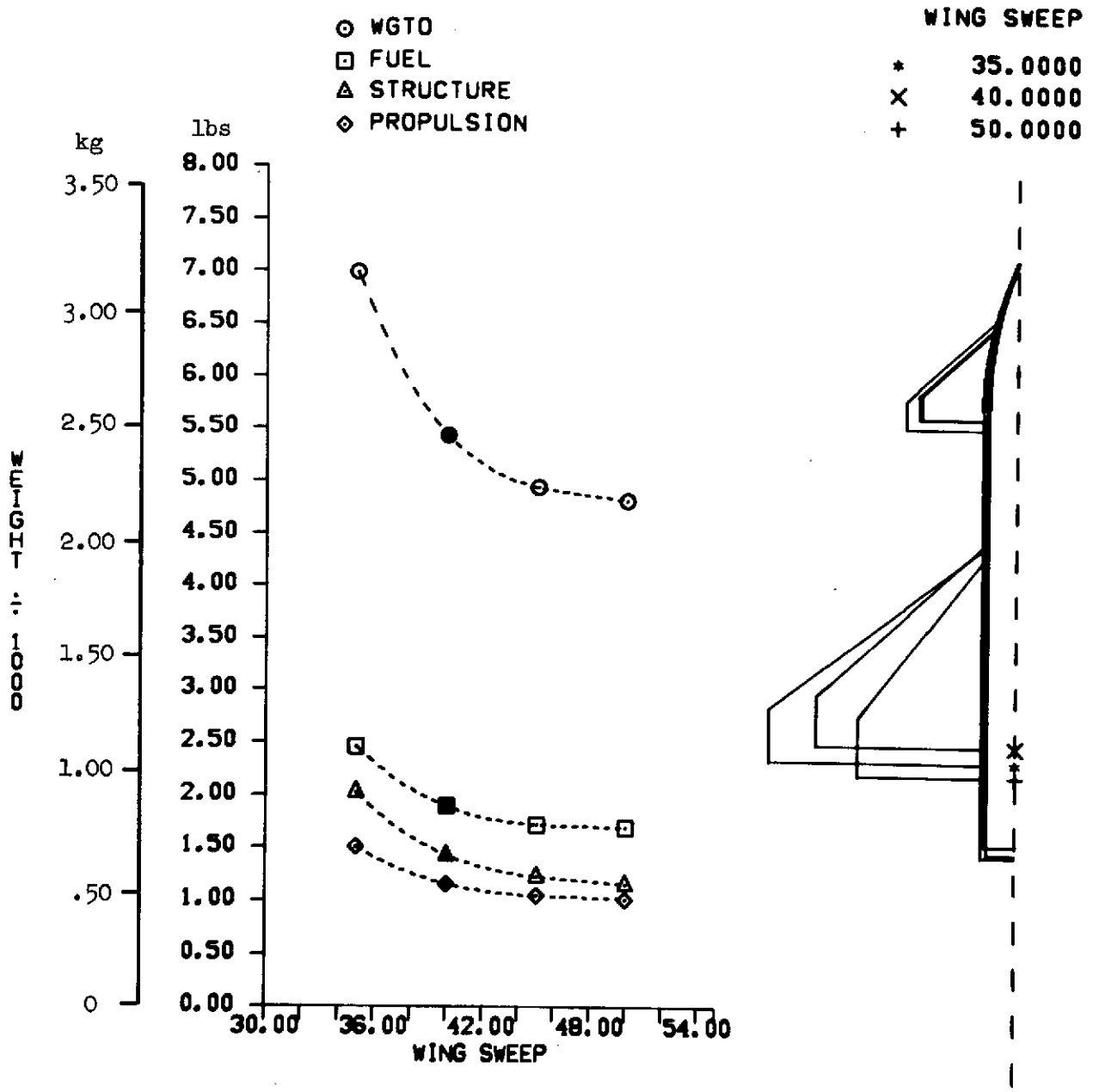

(a) Weights.

Figure 9.– Effect of wing leading-edge sweep.

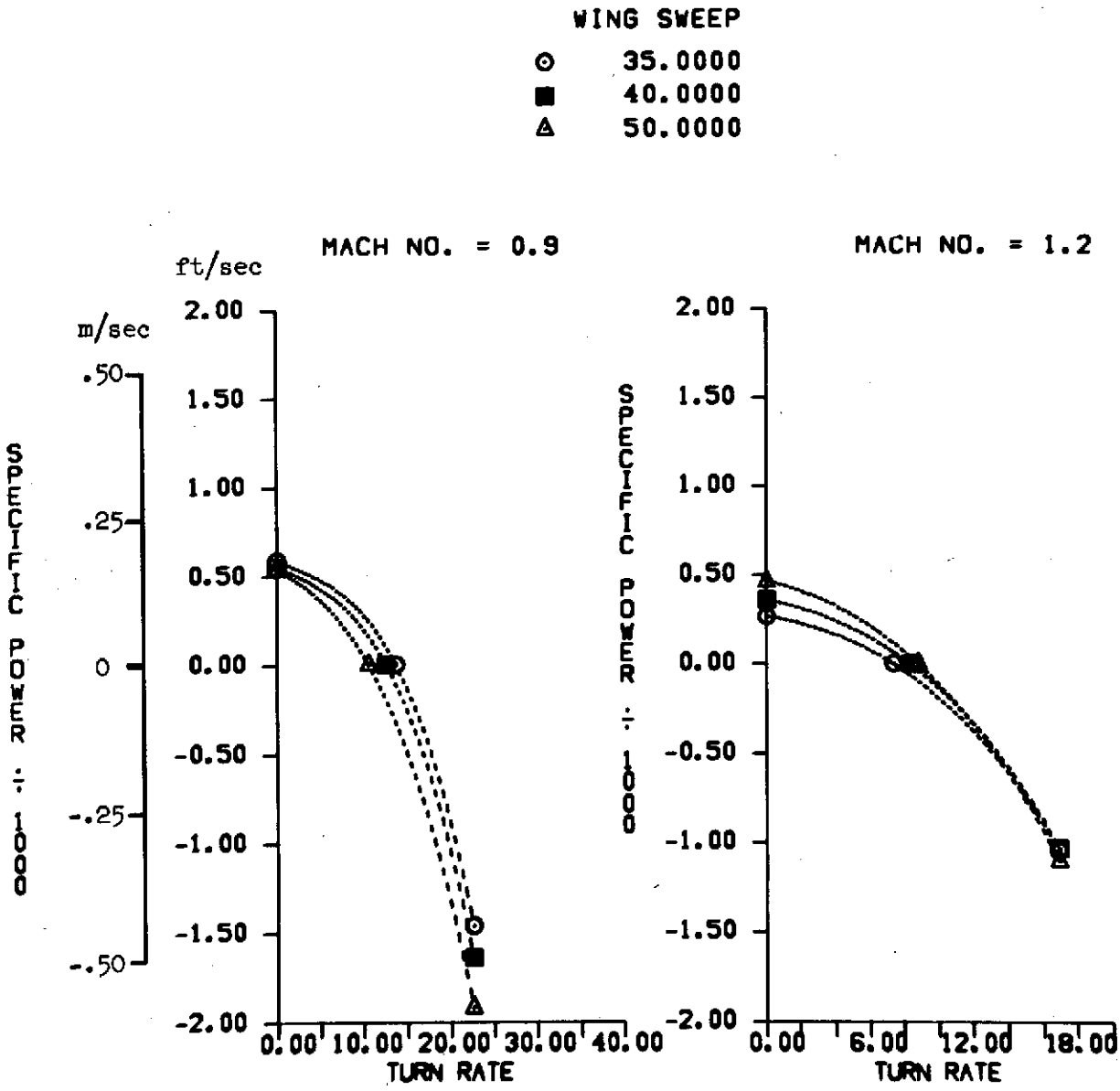

(b) Combat performance.

Figure 9.– Continued.

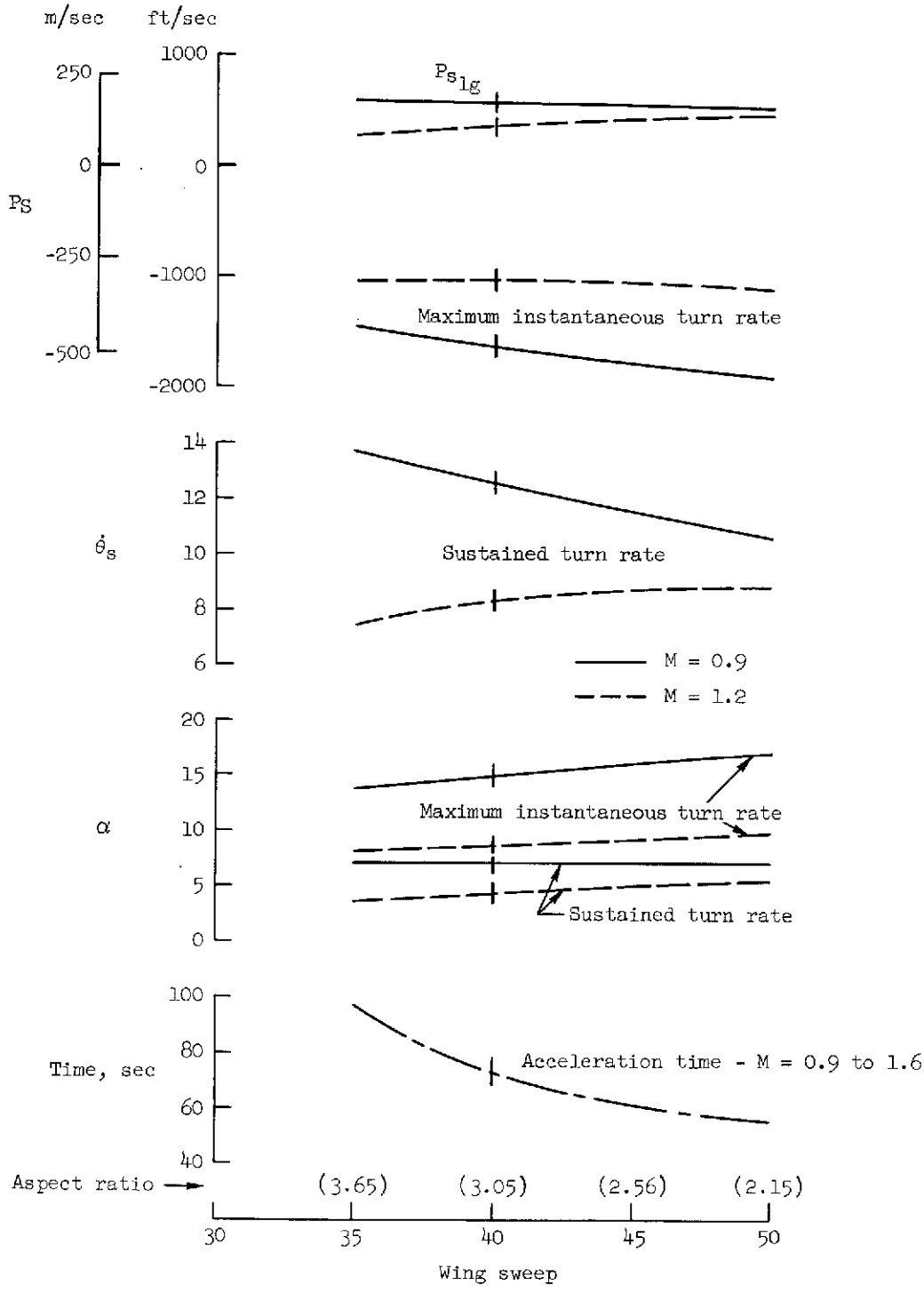

(b) Combat performance (concluded).

Figure 9.– Concluded.

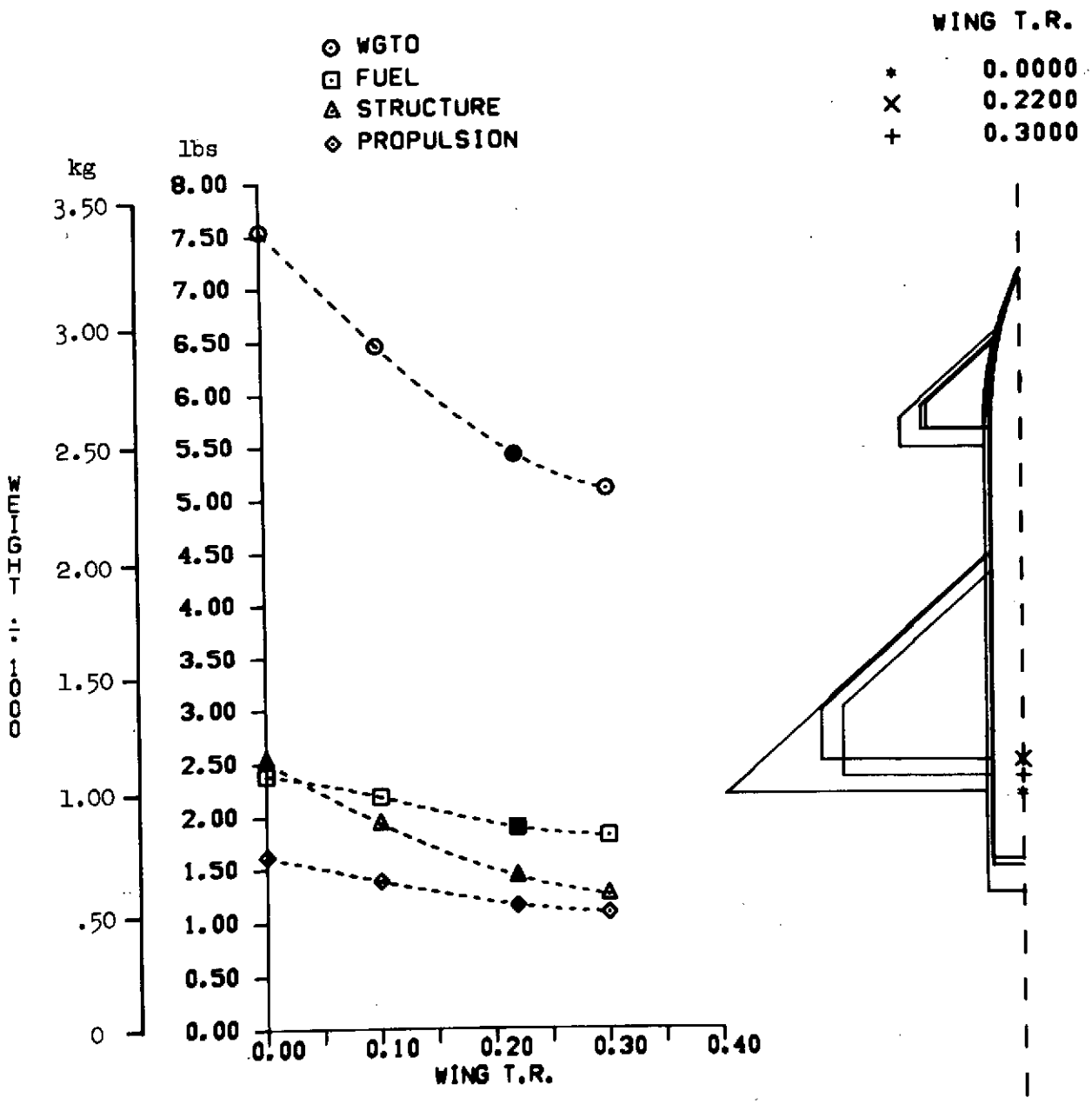

(a) Weights.

Figure 10.– Effect of wing taper ratio.

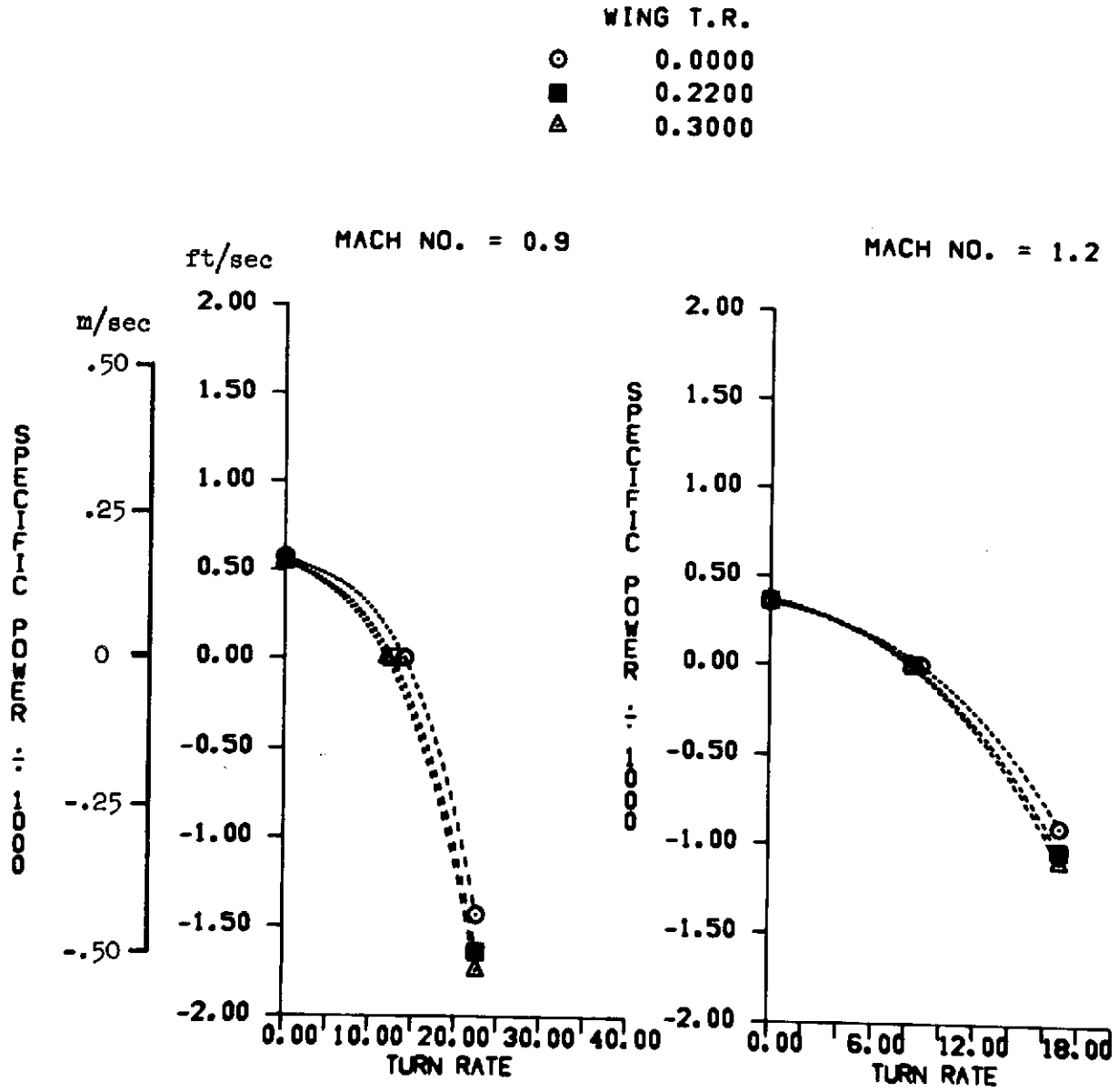

(b) Combat performance.

Figure 10.– Continued.

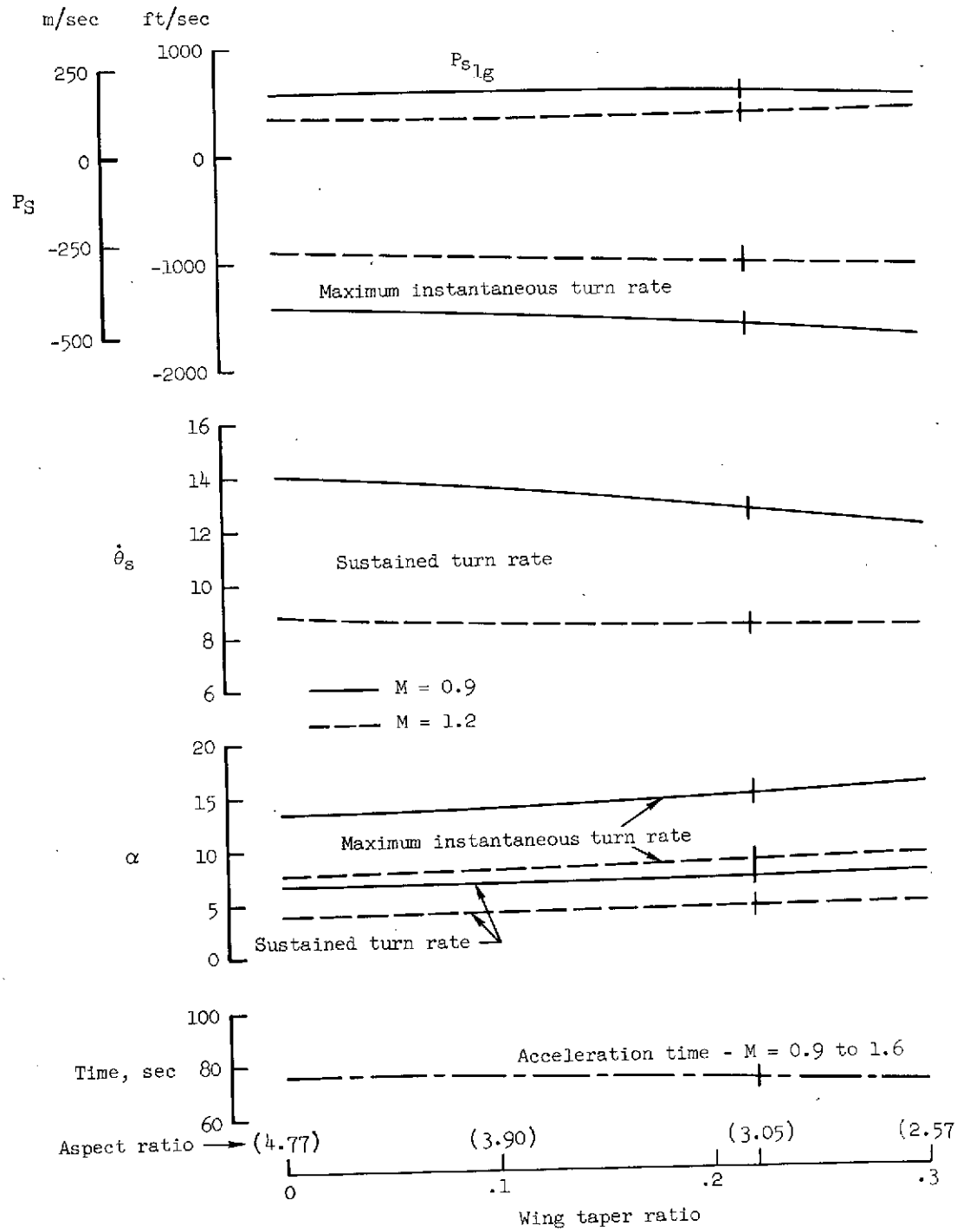

(b) Combat performance (concluded).

Figure 10.– Concluded.

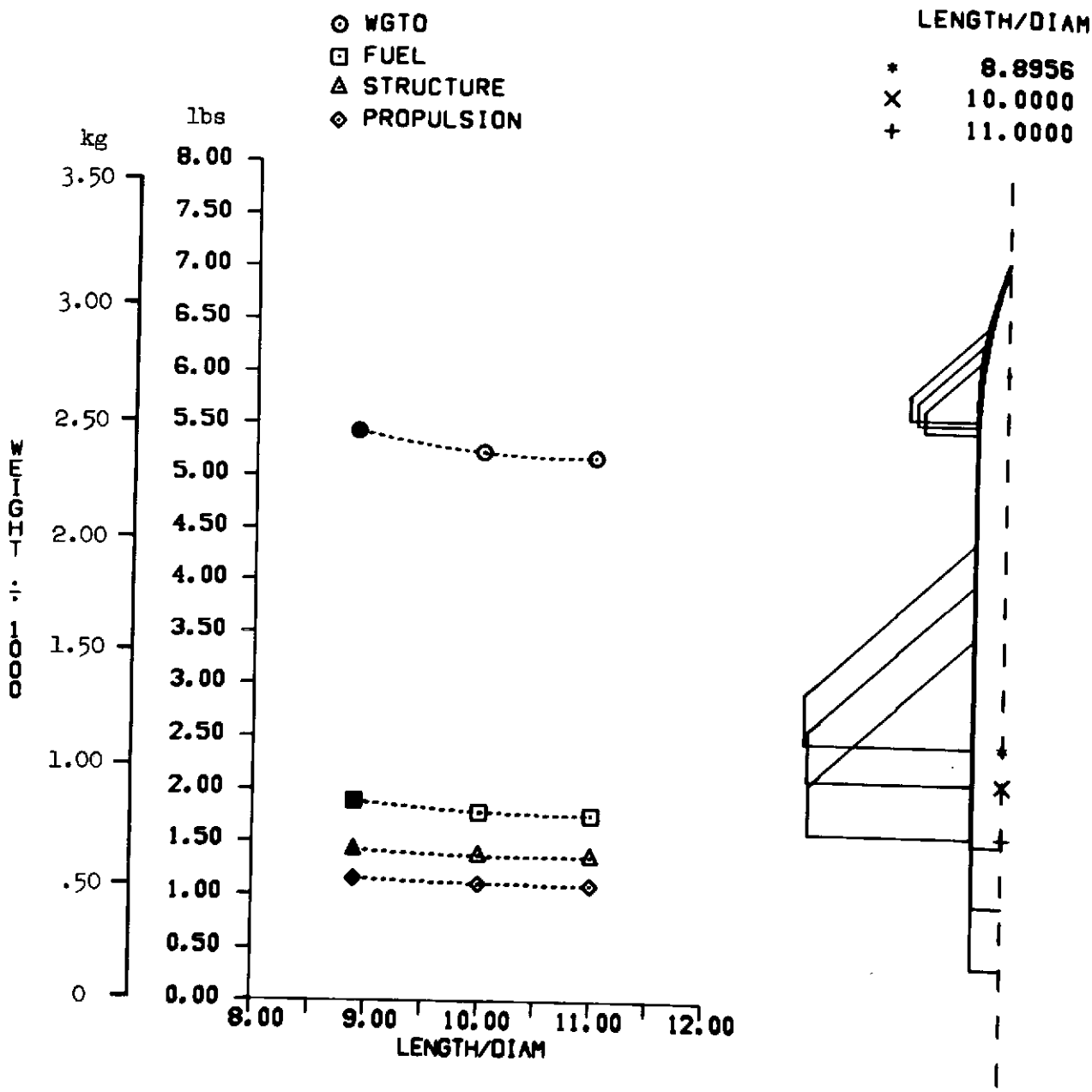

(a) Weights.

Figure 11.– Effect of body fineness ratio.

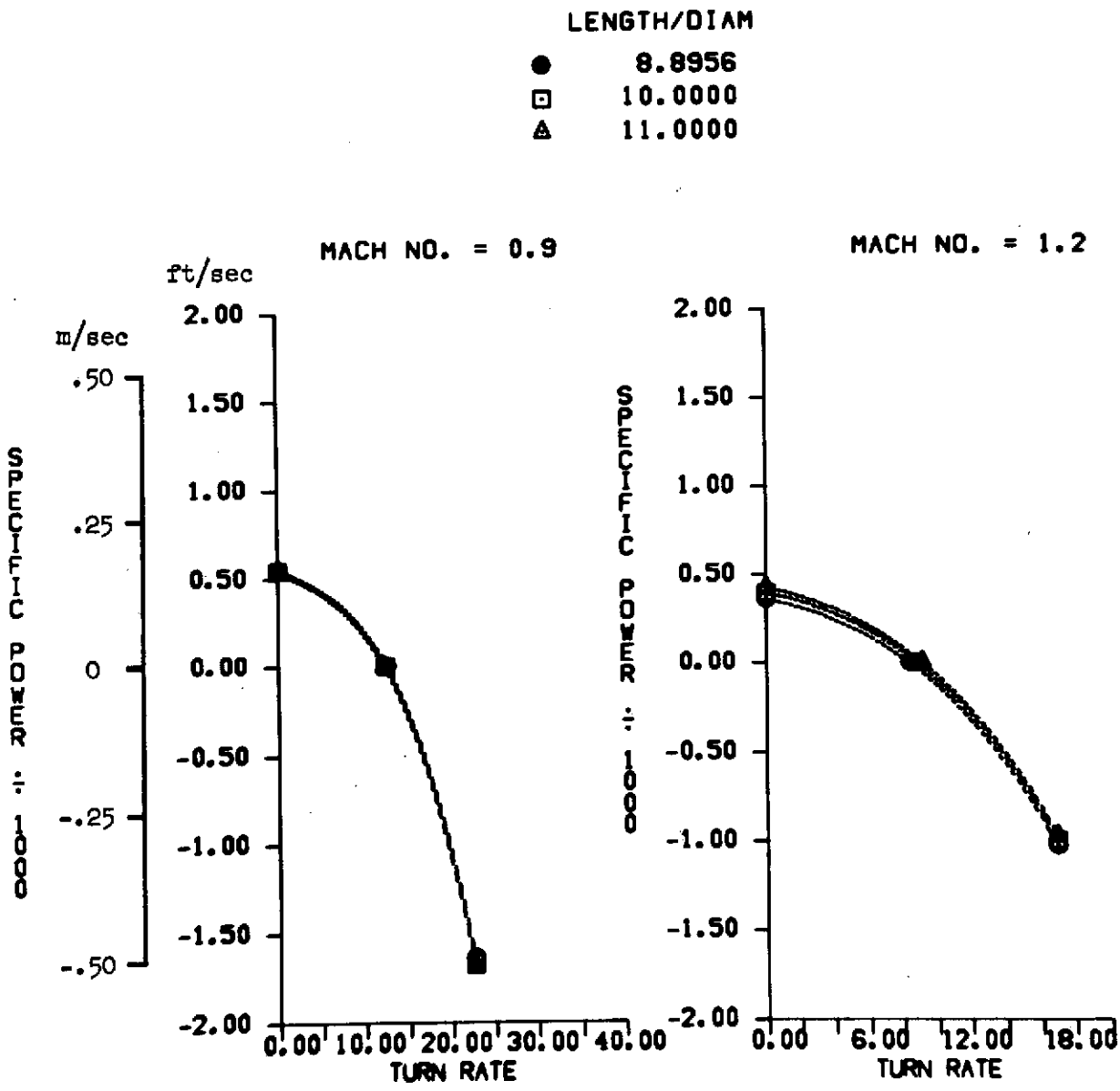

(b) Combat performance.

Figure 11.– Concluded.

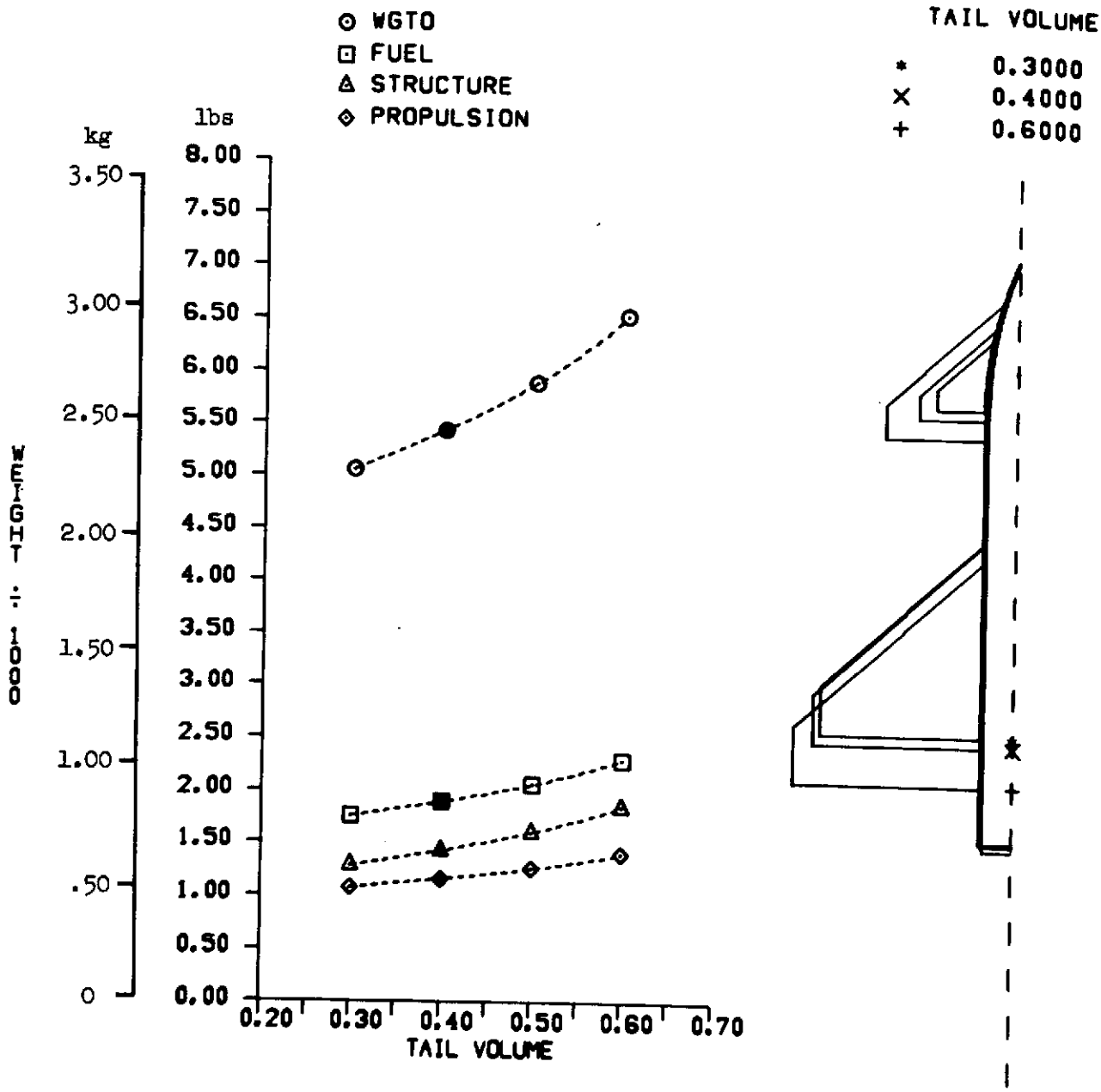

(a) Weights.

Figure 12.– Effect of canard-volume coefficient.

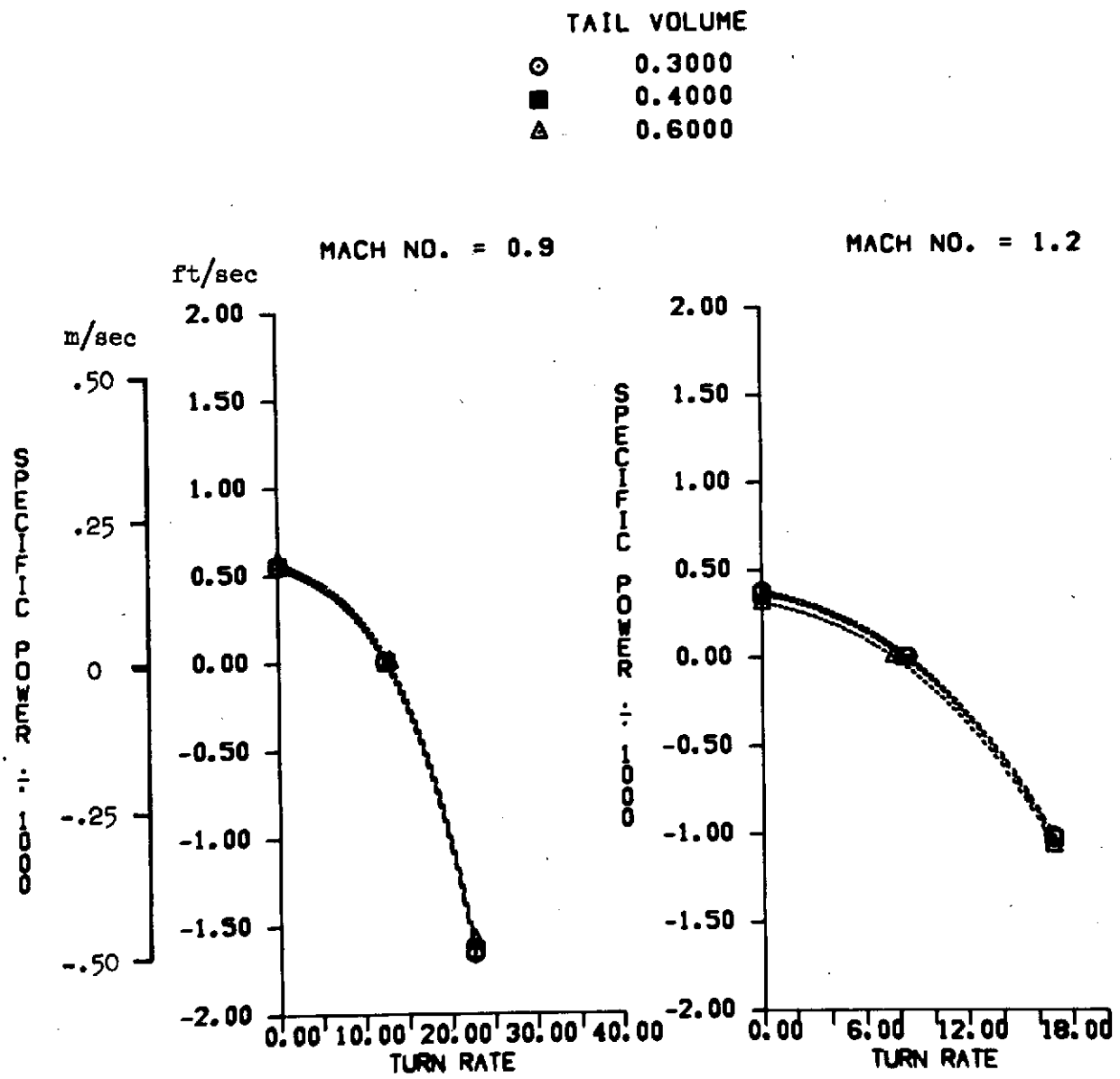

(b) Combat performance.

Figure 12.– Concluded.

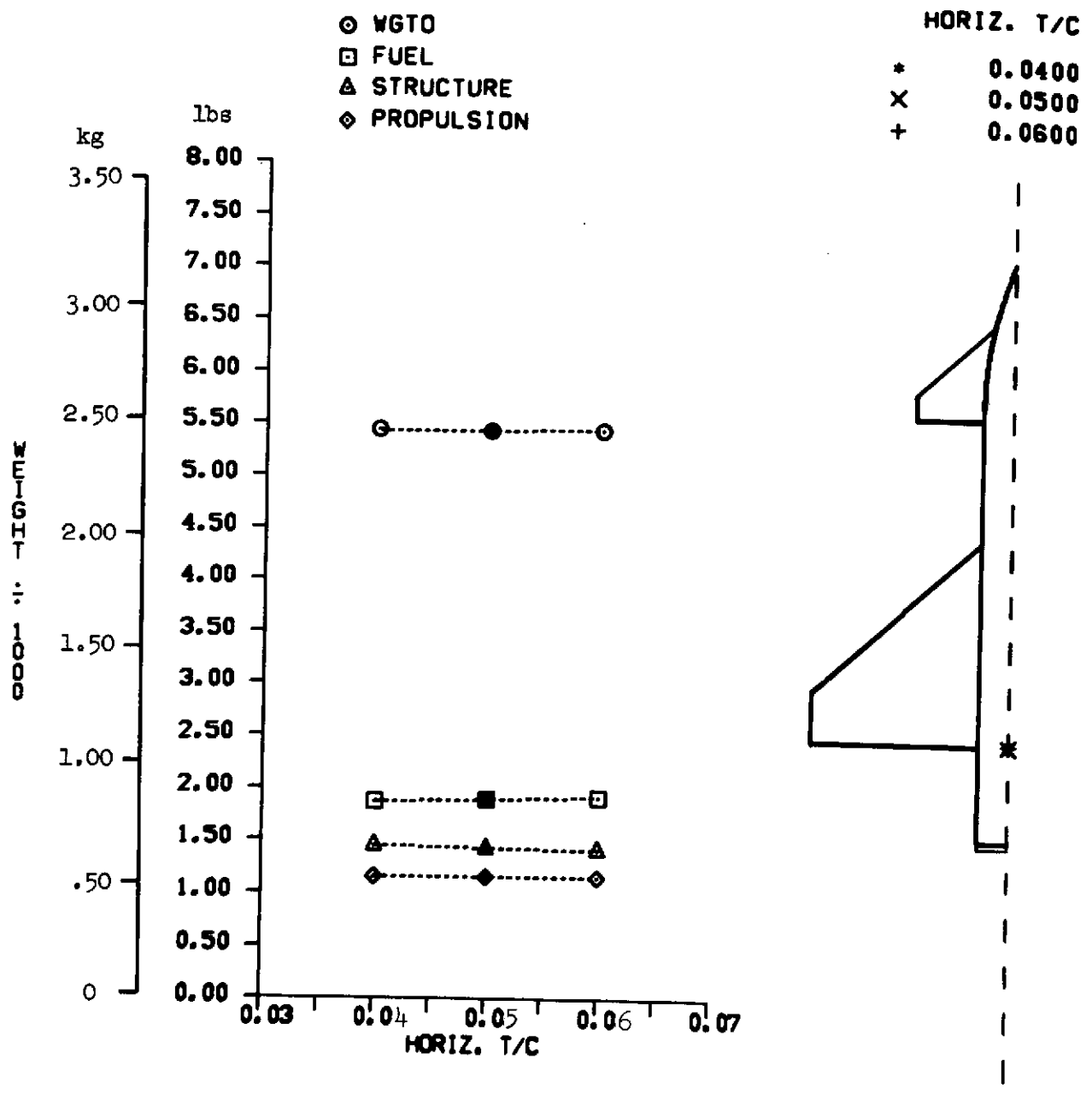

(a) Weights.

Figure 13.– Effect of canard thickness-to-chord ratio.

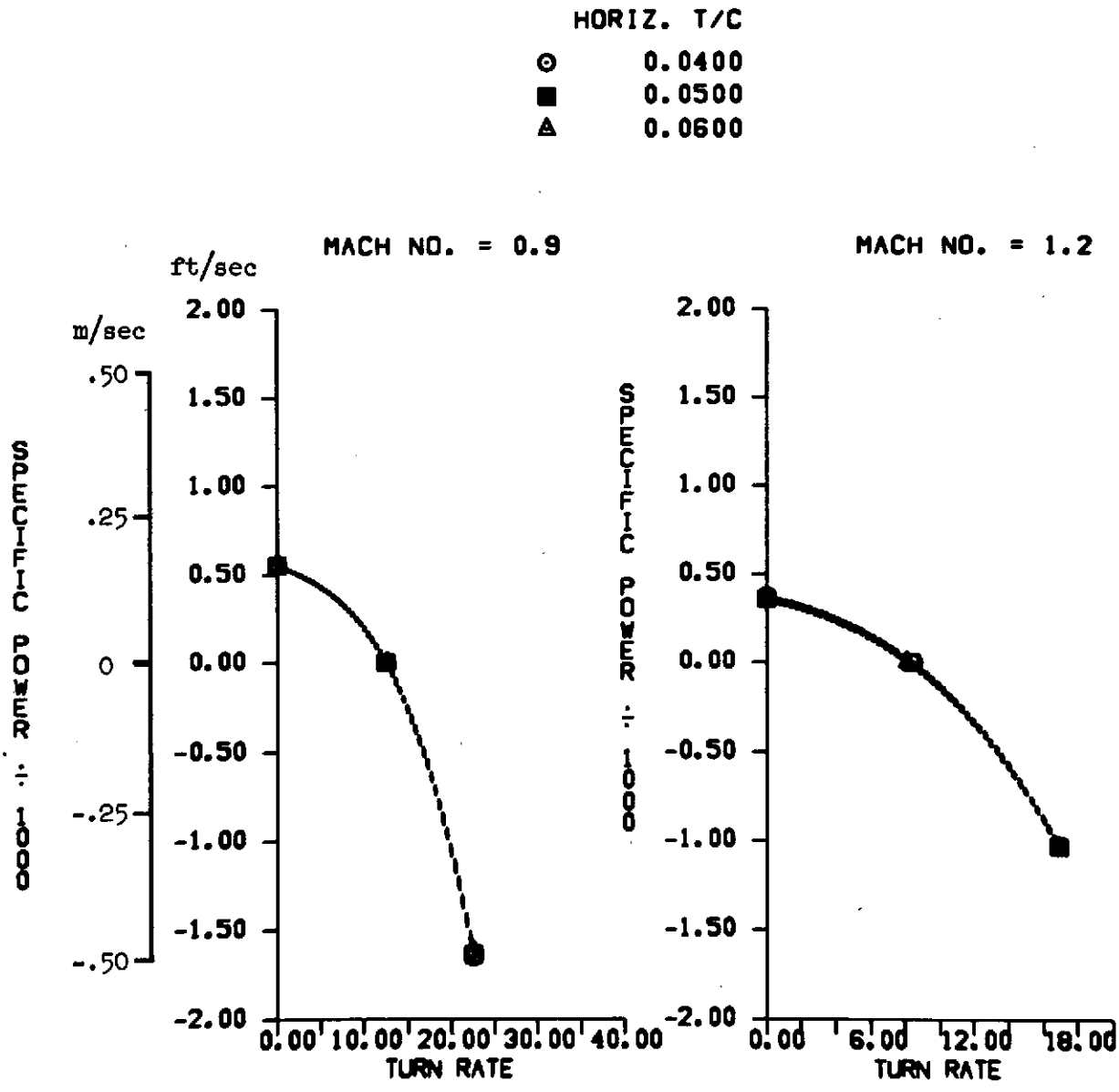

(b) Combat performance.

Figure 13.– Concluded.

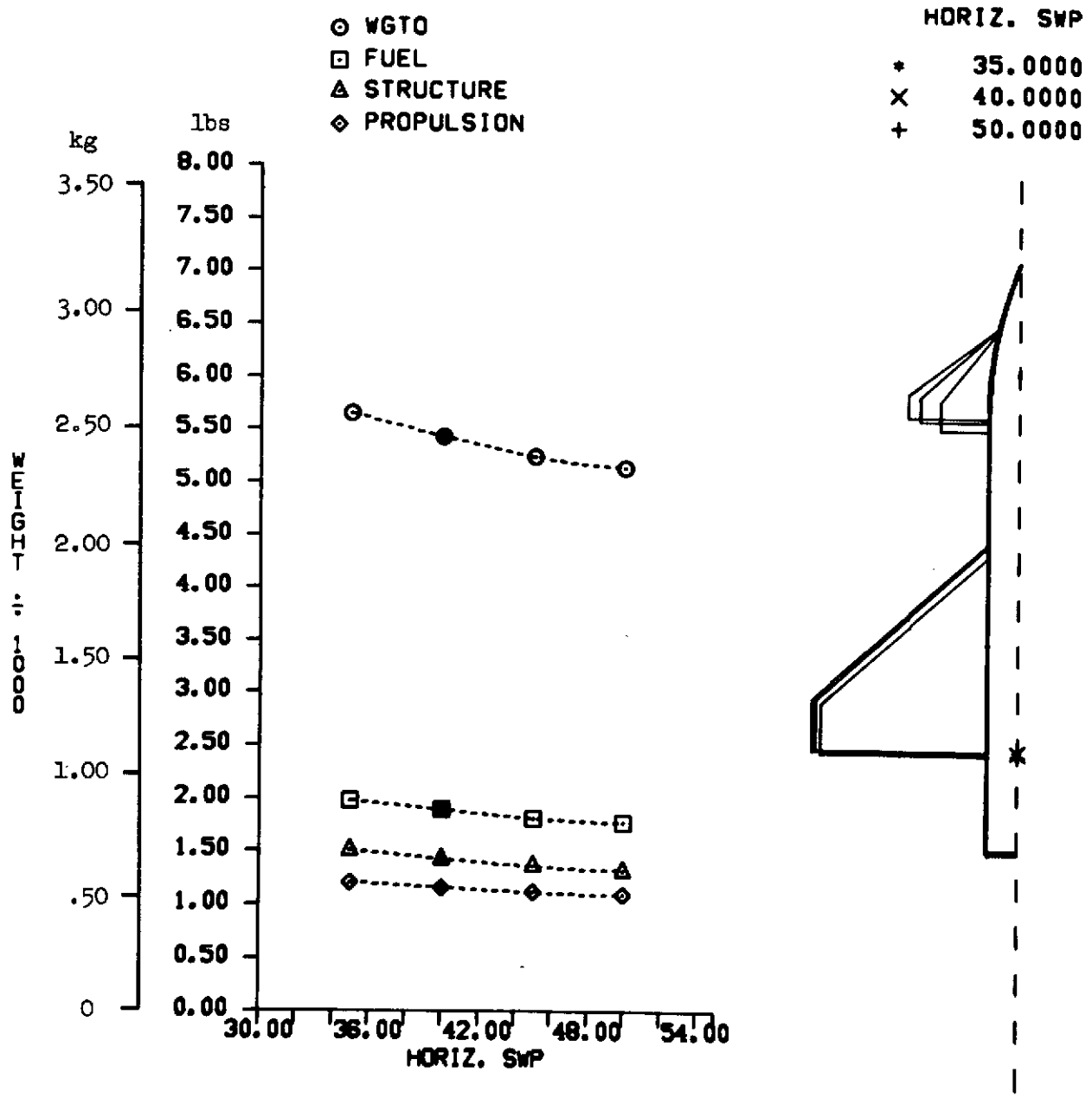

(a) Weights.

Figure 14.– Effect of canard leading-edge sweep.

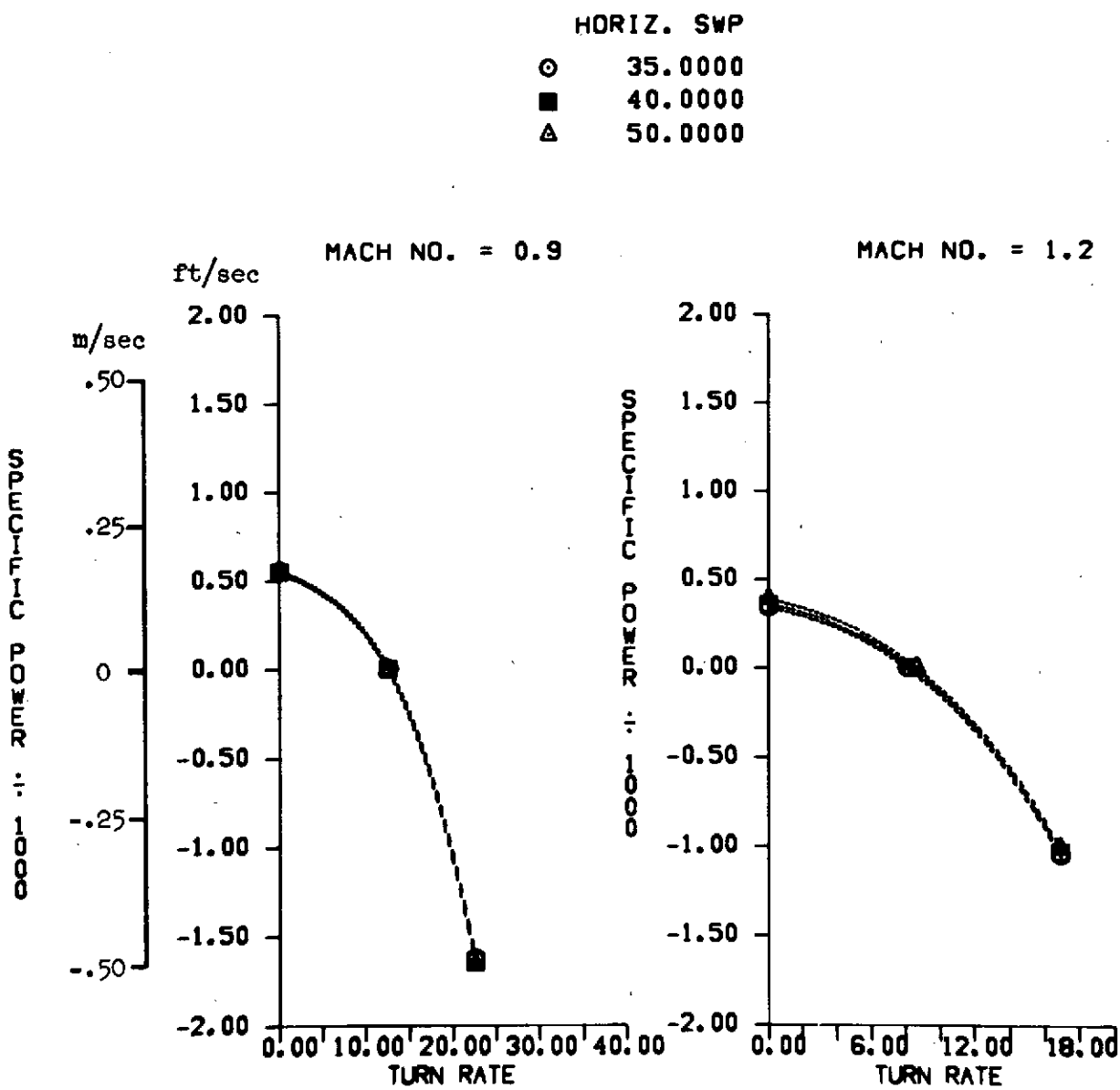

(b) Combat performance.

Figure 14.– Concluded.

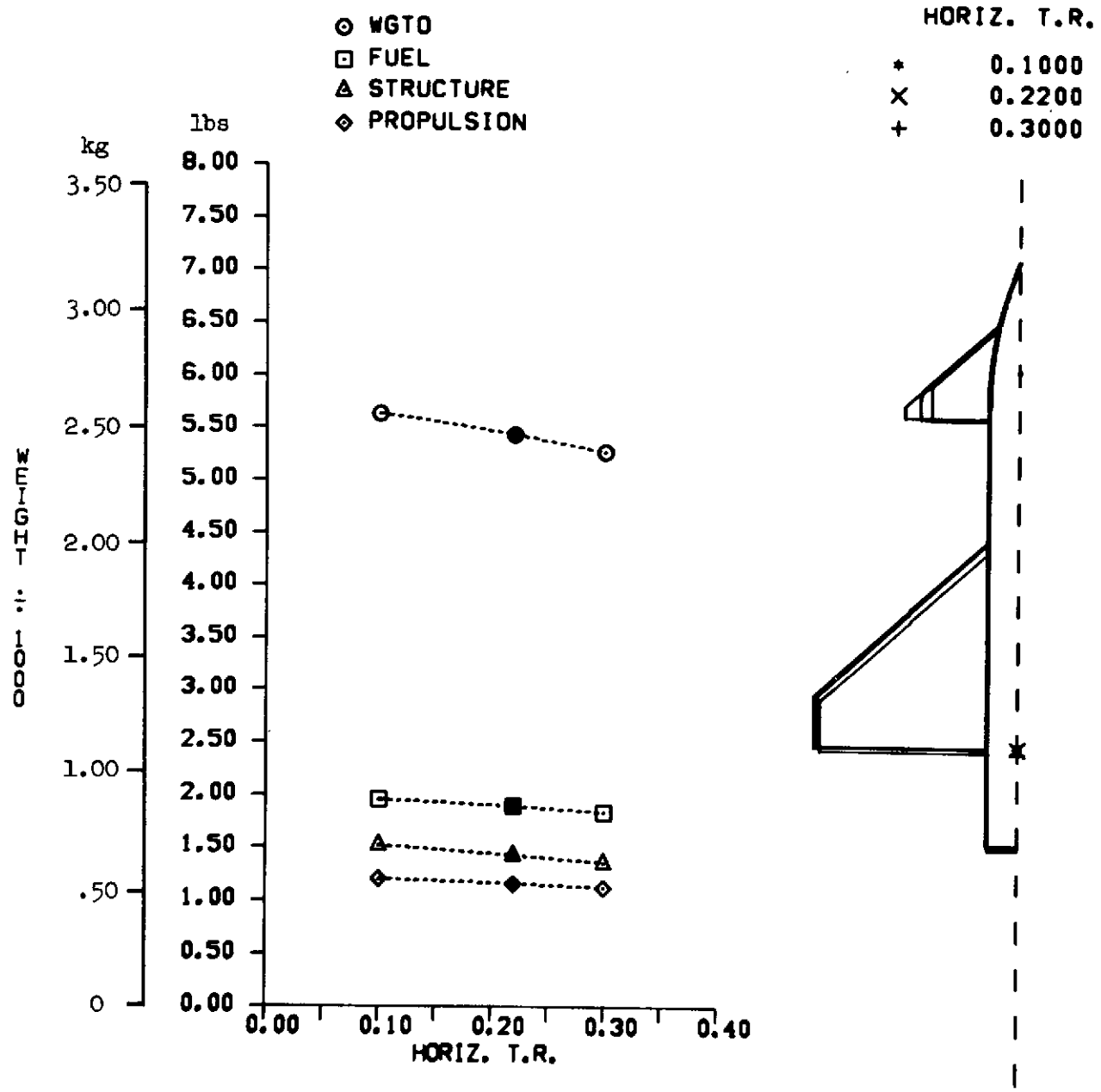

(a) Weights.

Figure 15.– Effect of canard taper ratio.

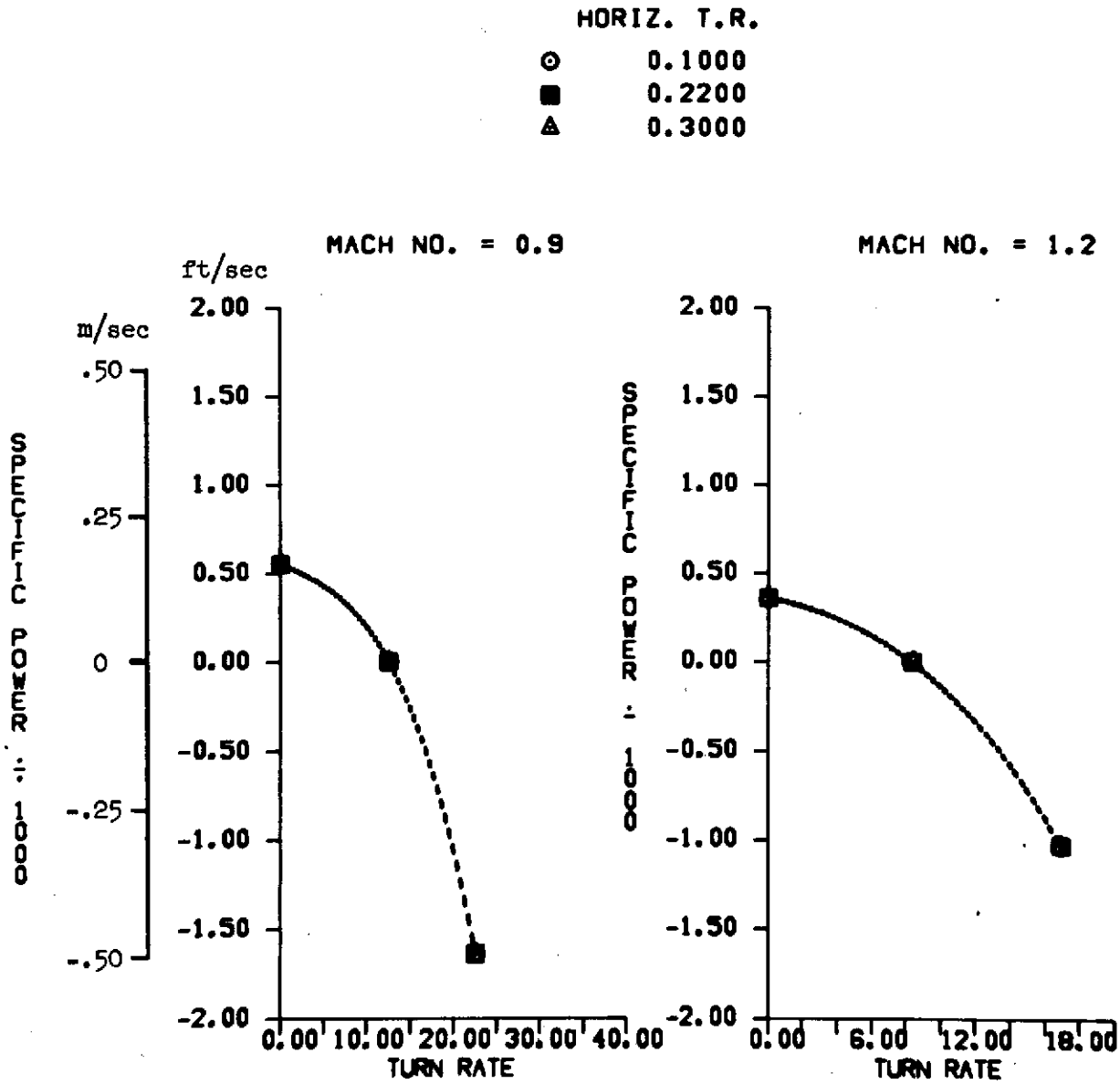

(b) Combat performance.

Figure 15.– Concluded.

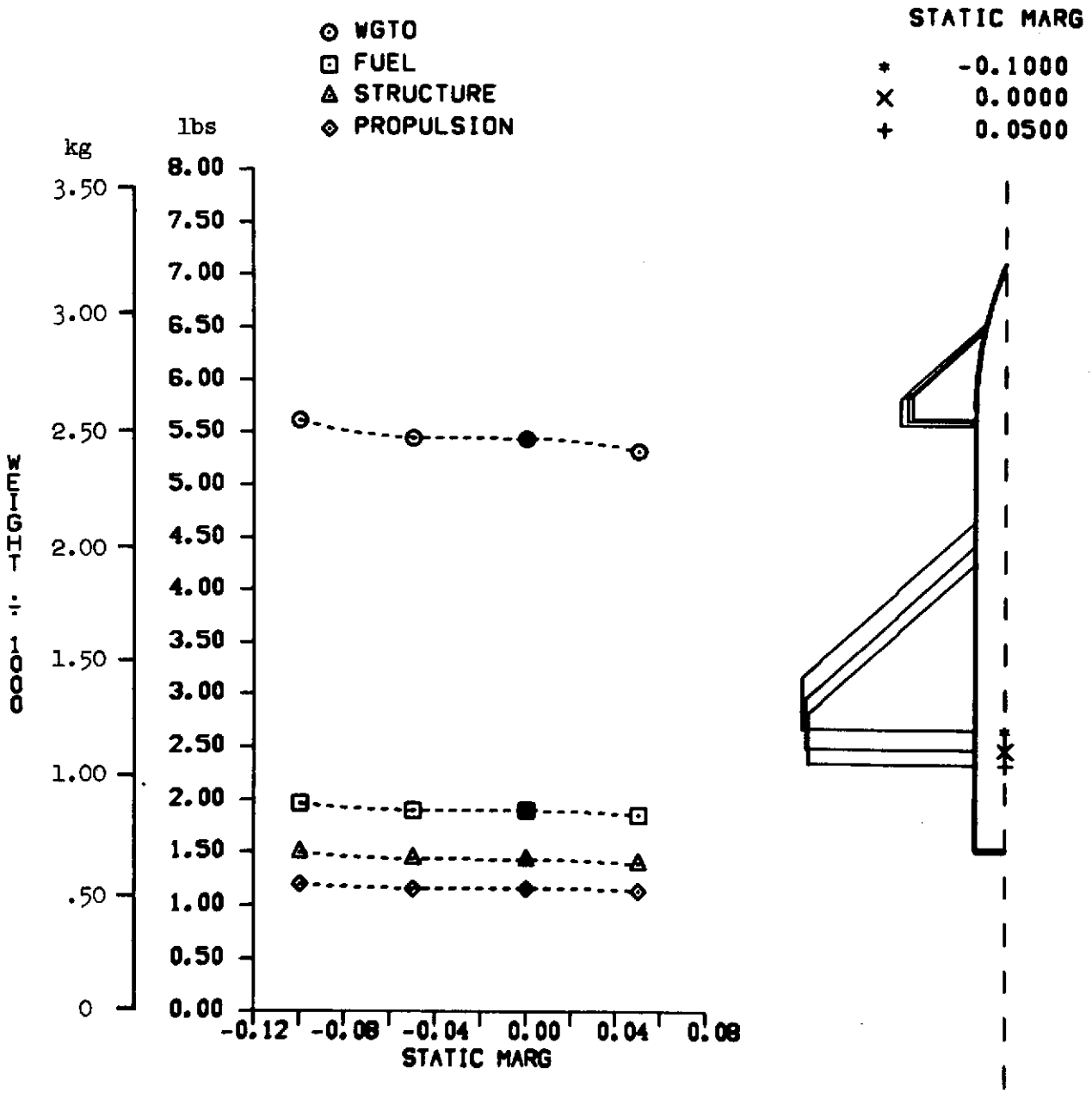

(a) Weights.

Figure 16.– Effect of static margin.

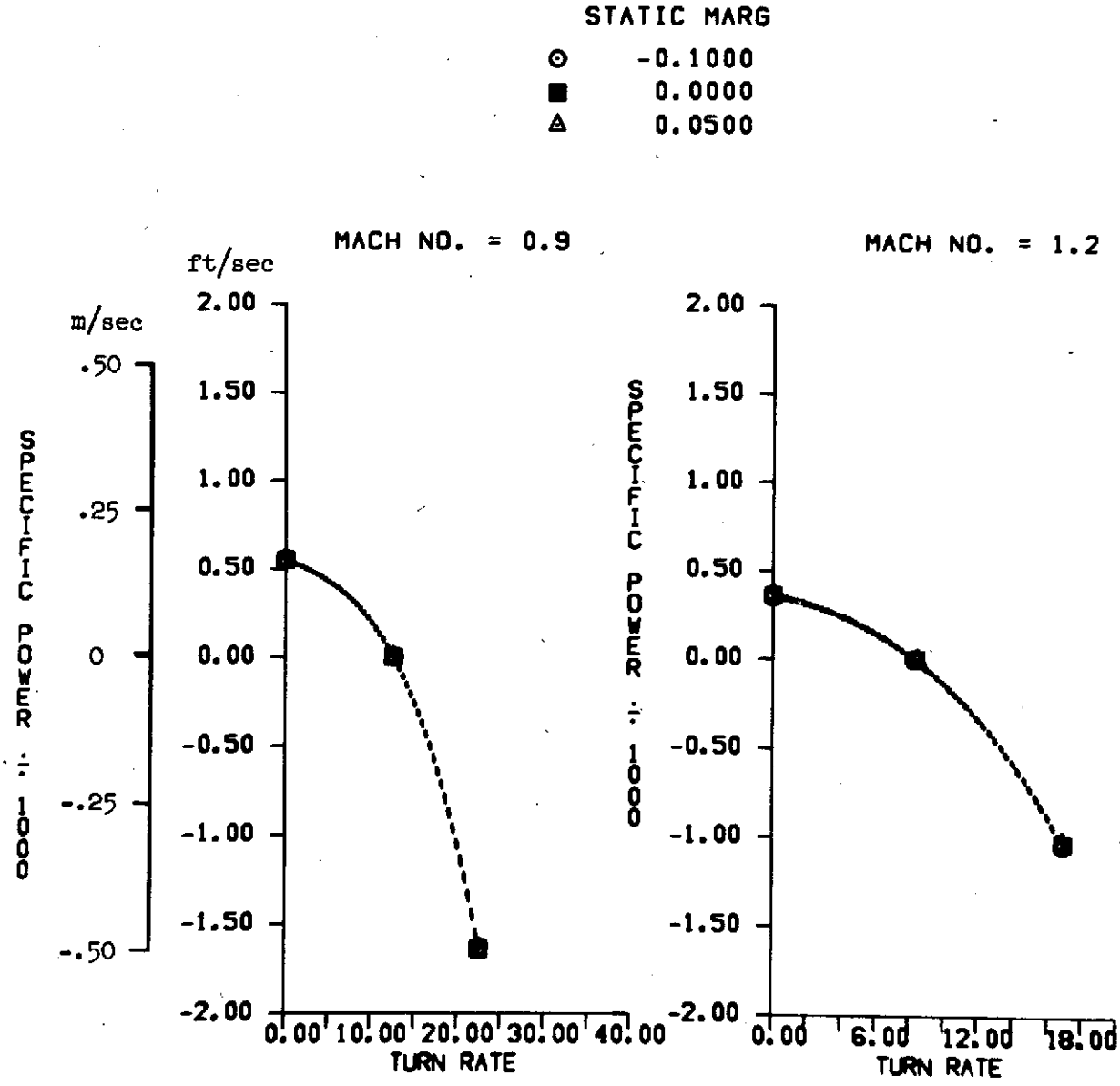

(b) Combat performance.

Figure 16.– Concluded.

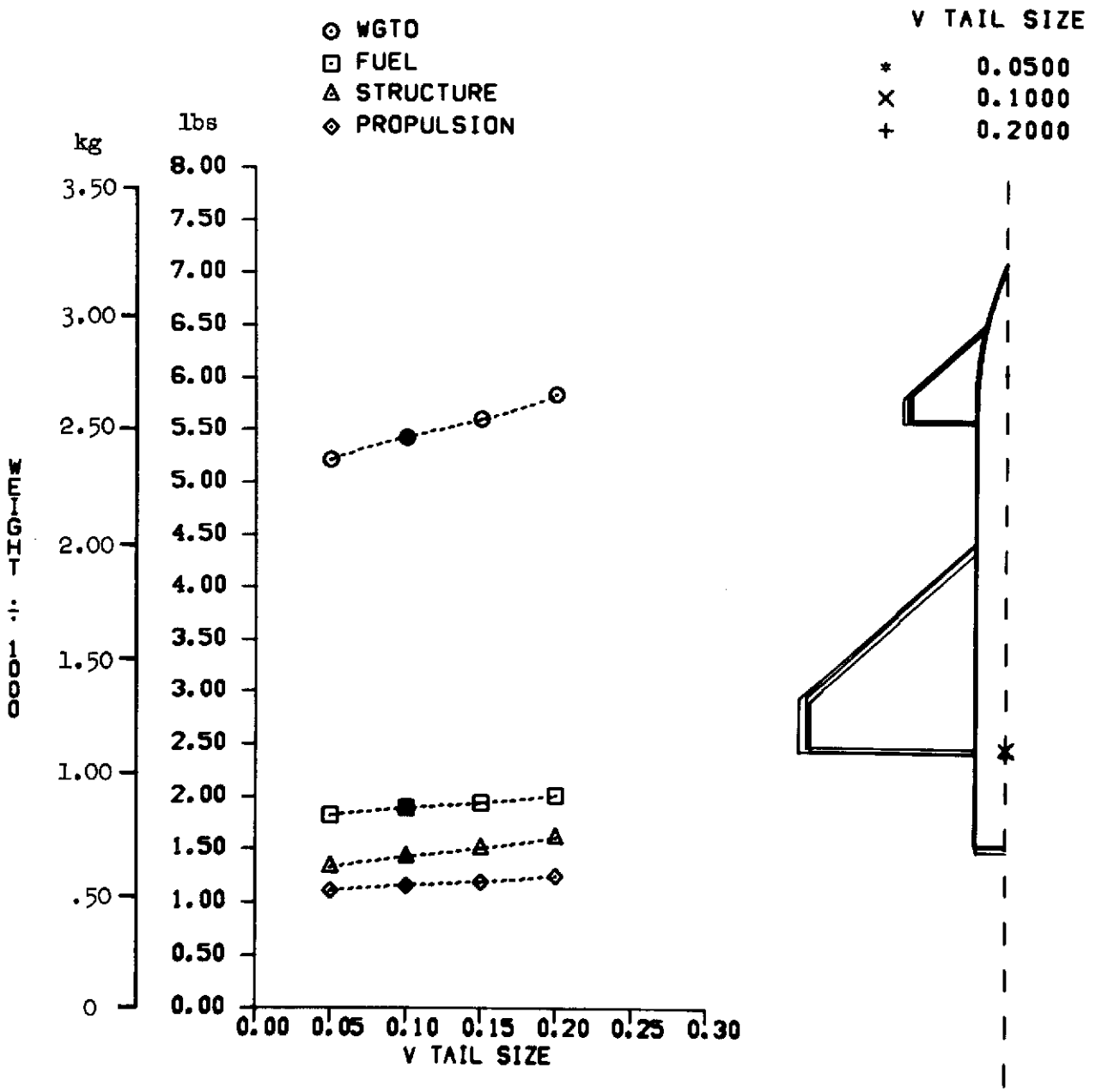

(a) Weights.

Figure 17.– Effect of vertical-surface size.

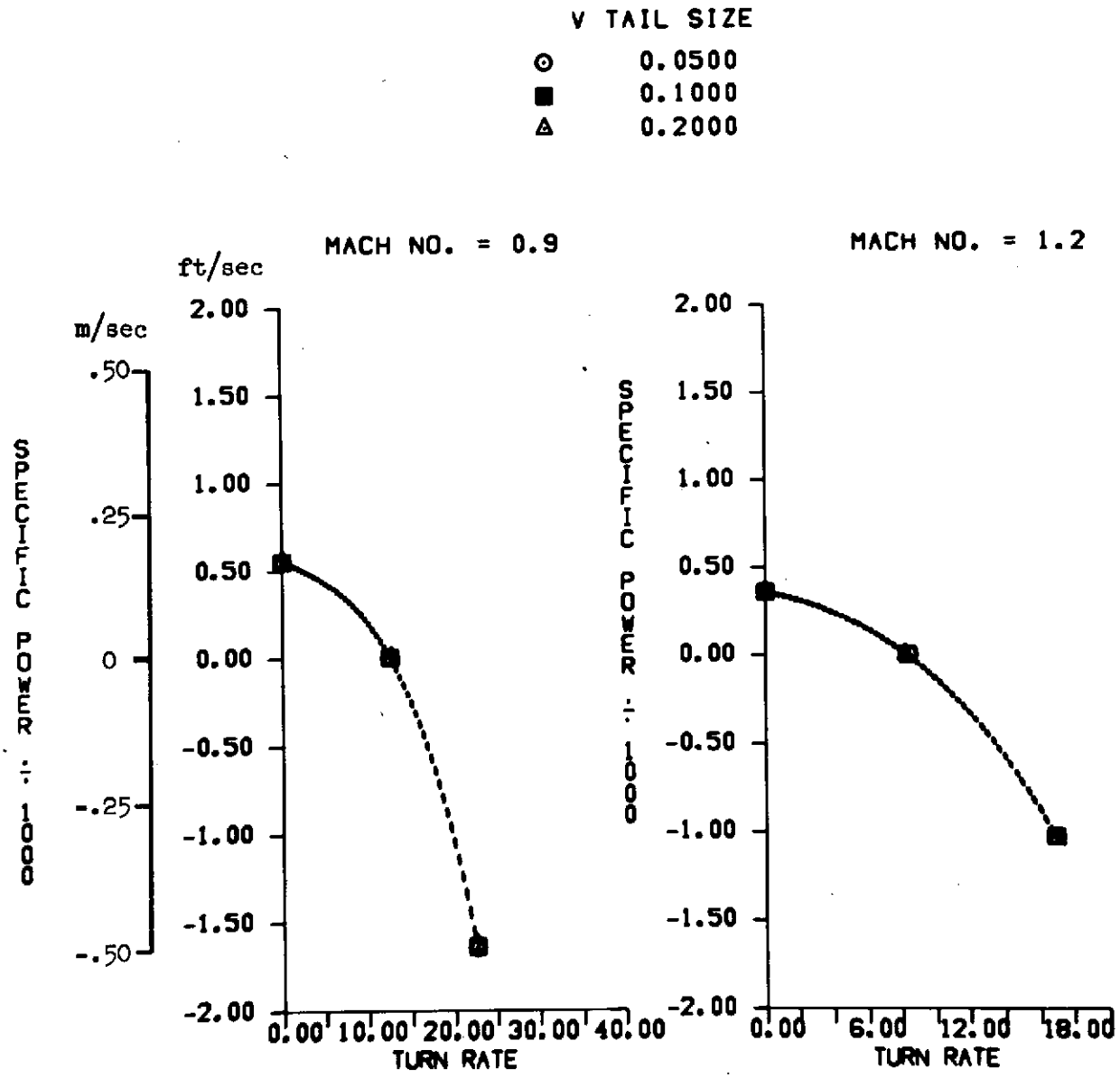

(b) Combat performance.

Figure 17.– Concluded.

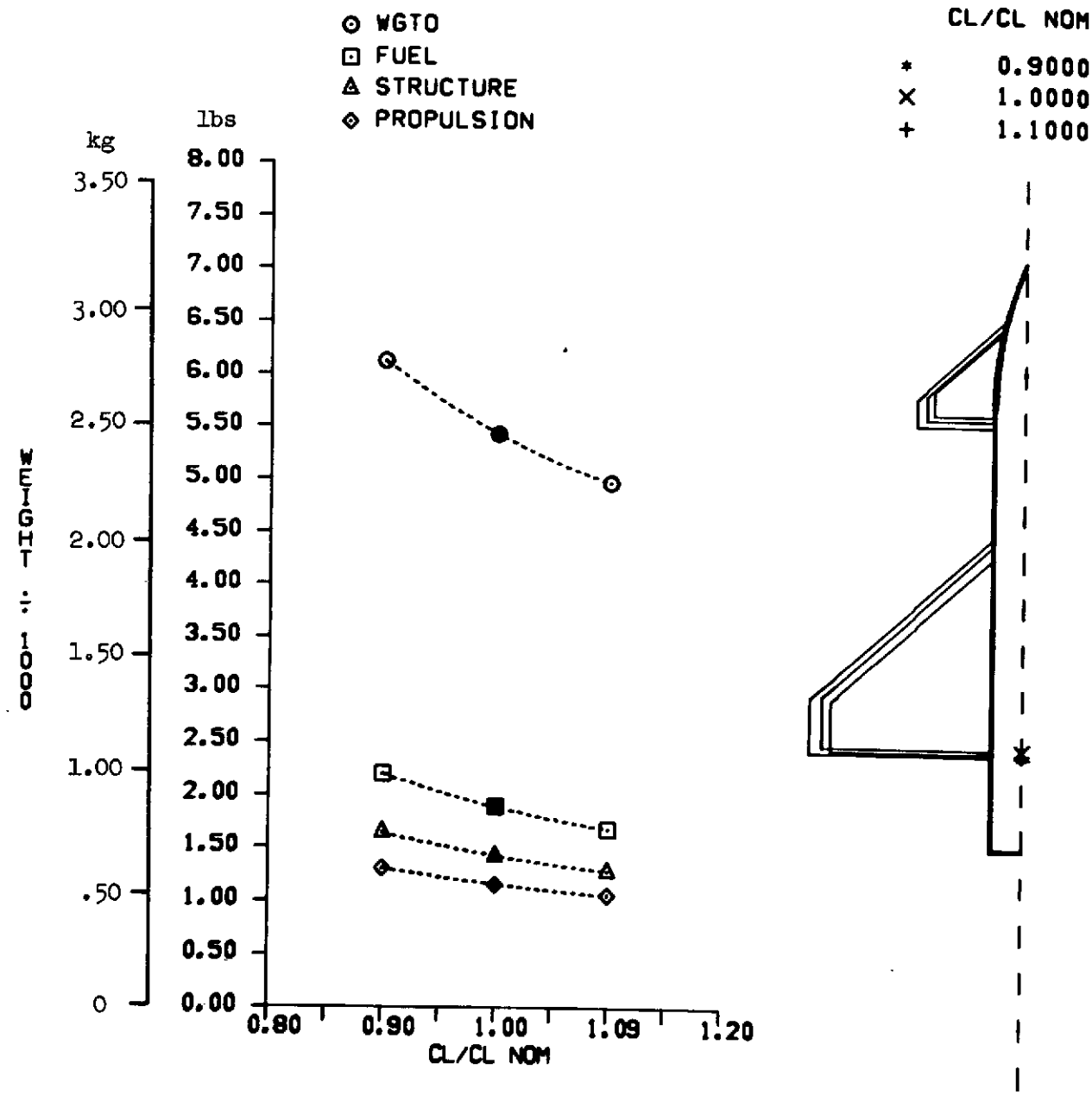

(a) Weights.

Figure 18.– Effect of a change in lift coefficient.

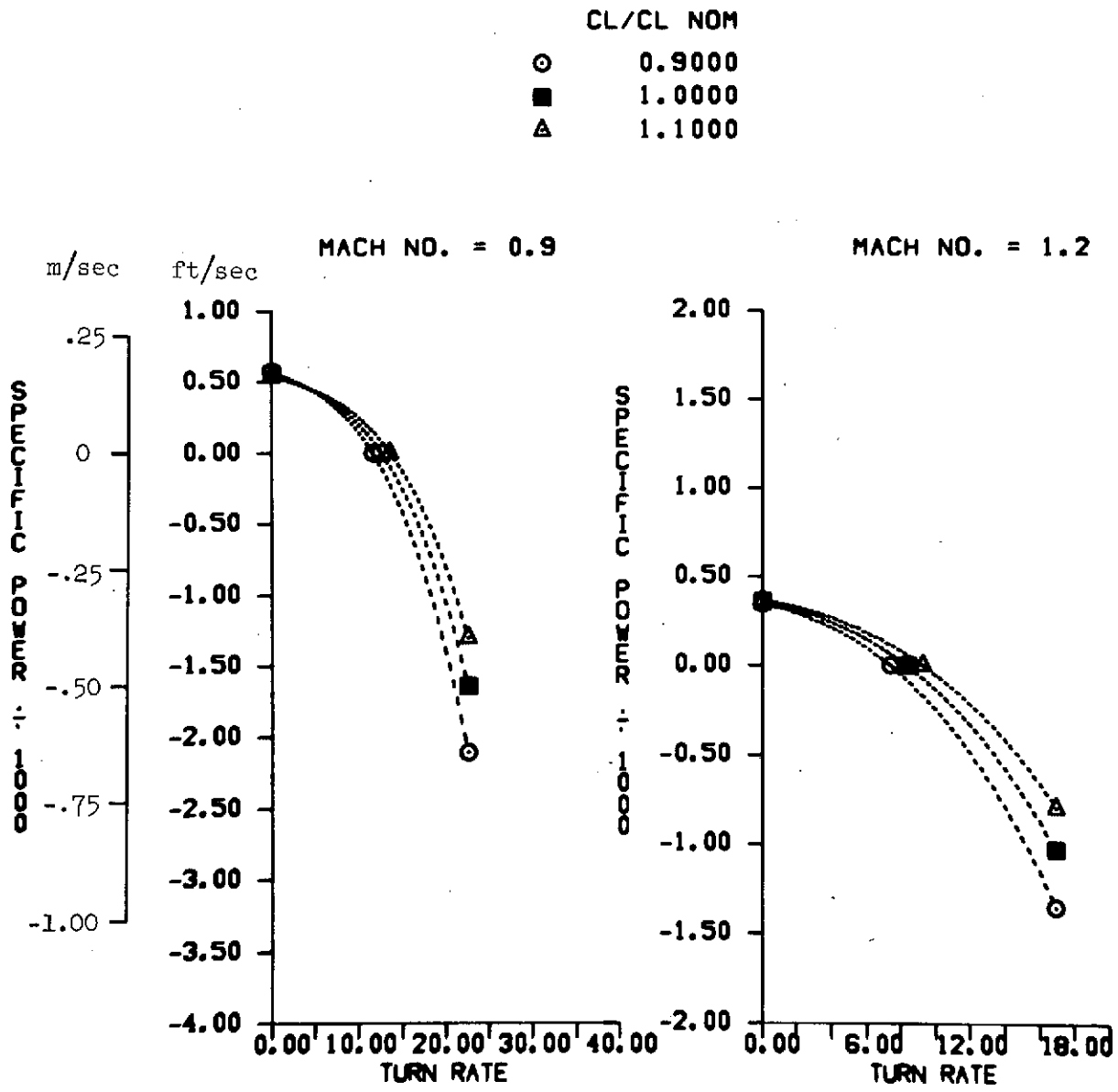

(b) Combat performance.

Figure 18.– Continued.

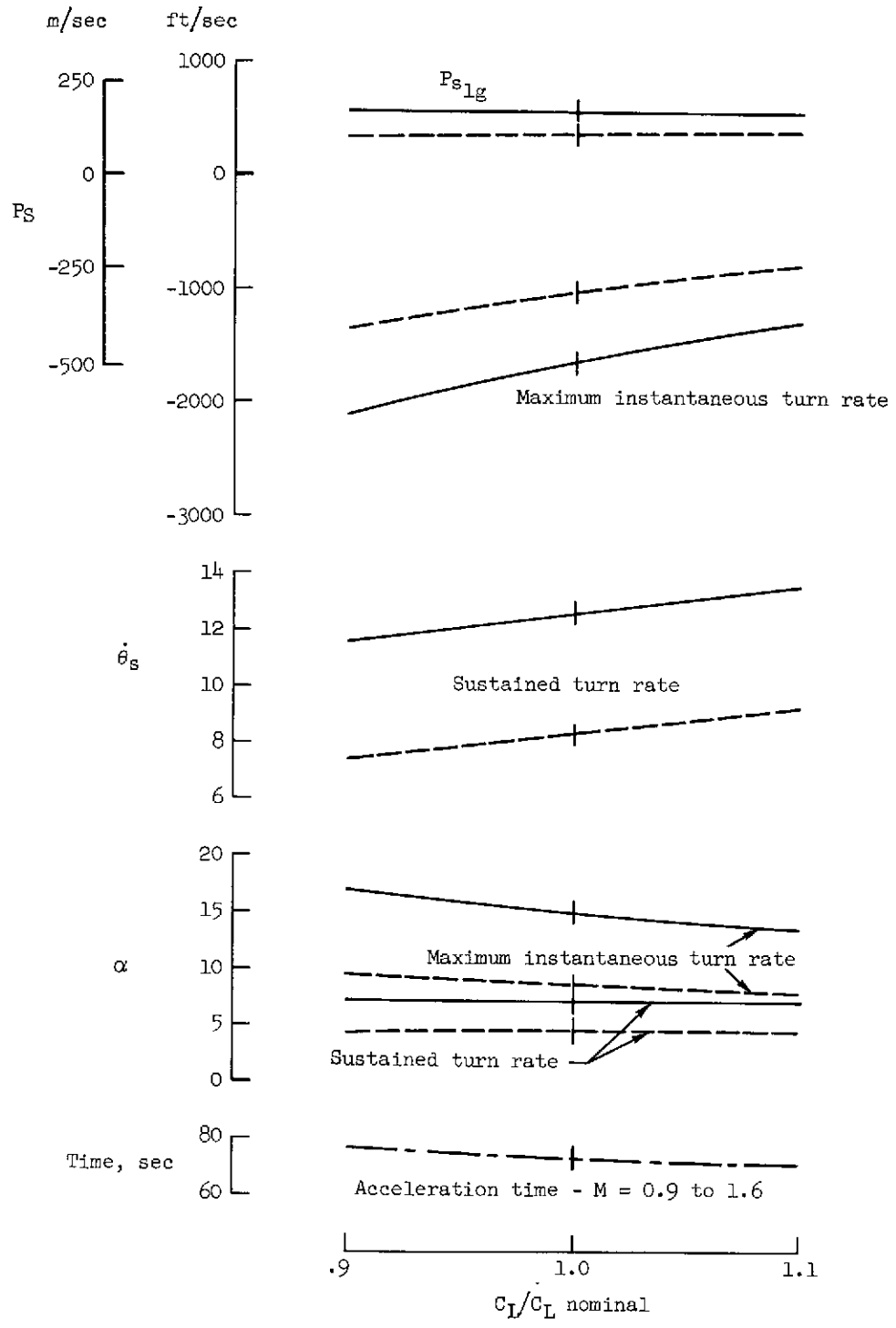

(b) Combat performance (concluded).

Figure 18.– Concluded.

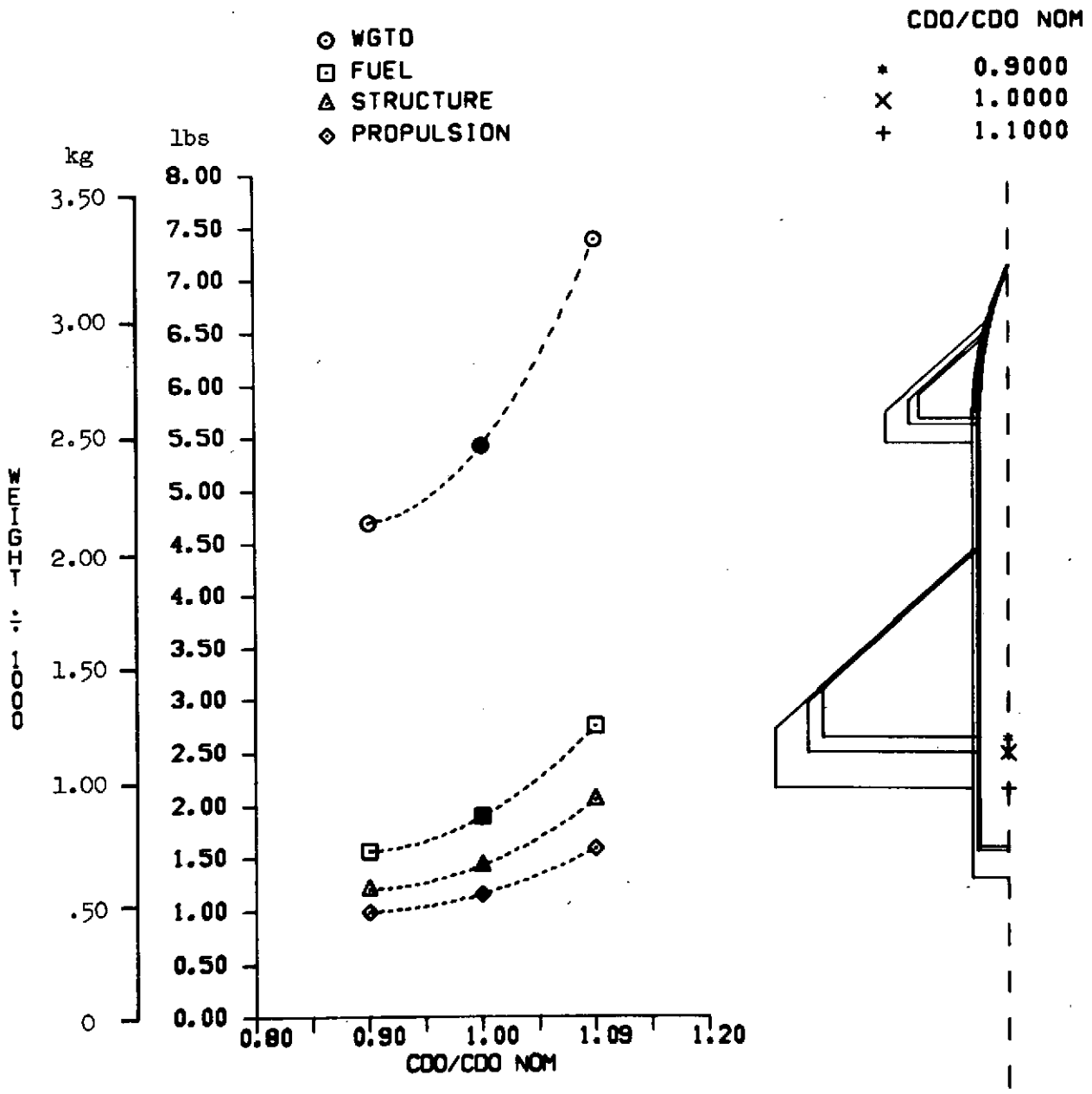

(a) Weights.

Figure 19.– Effect of a change in zero-lift drag coefficient.

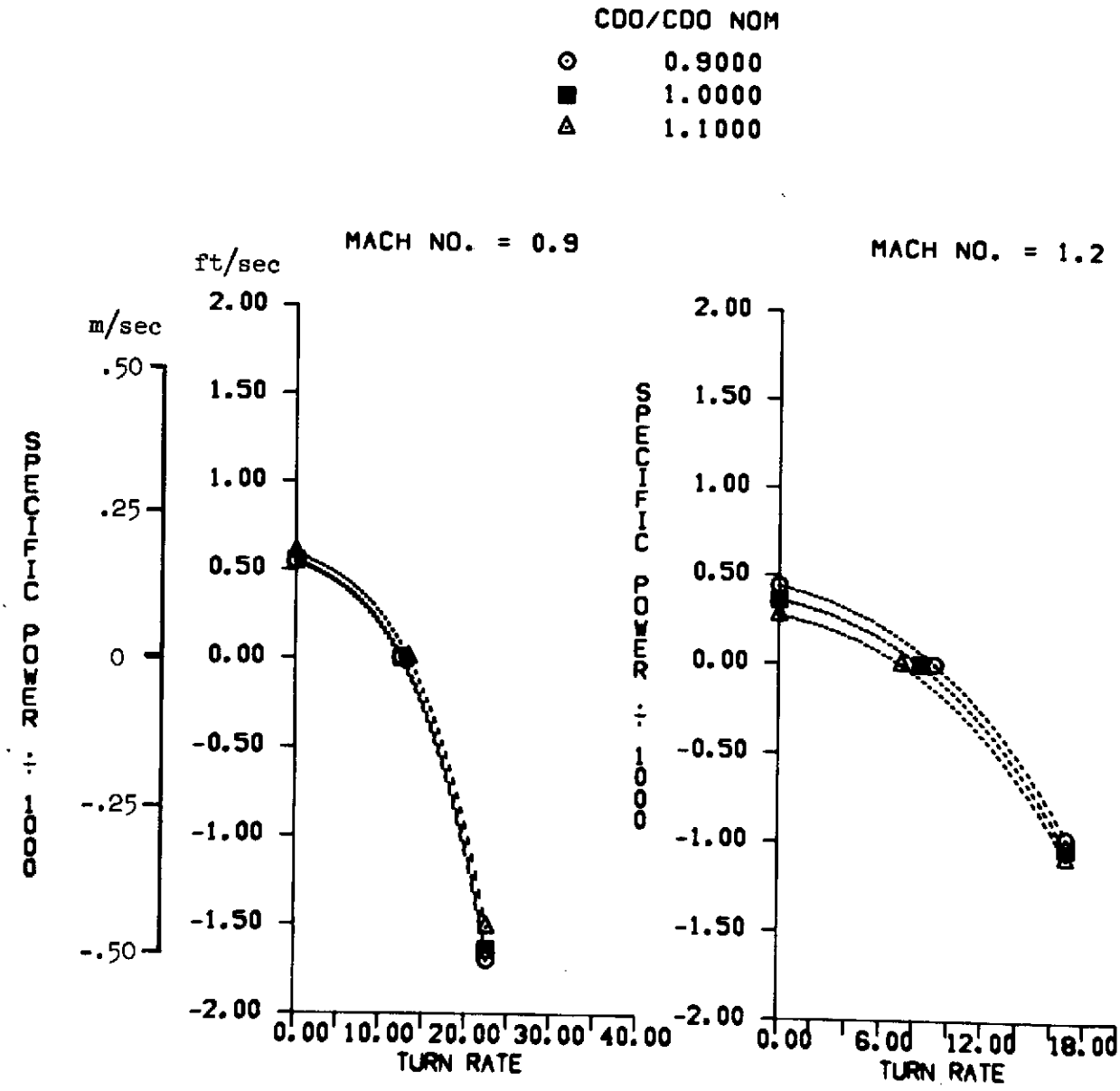

(b) Combat performance.

Figure 19.– Continued.

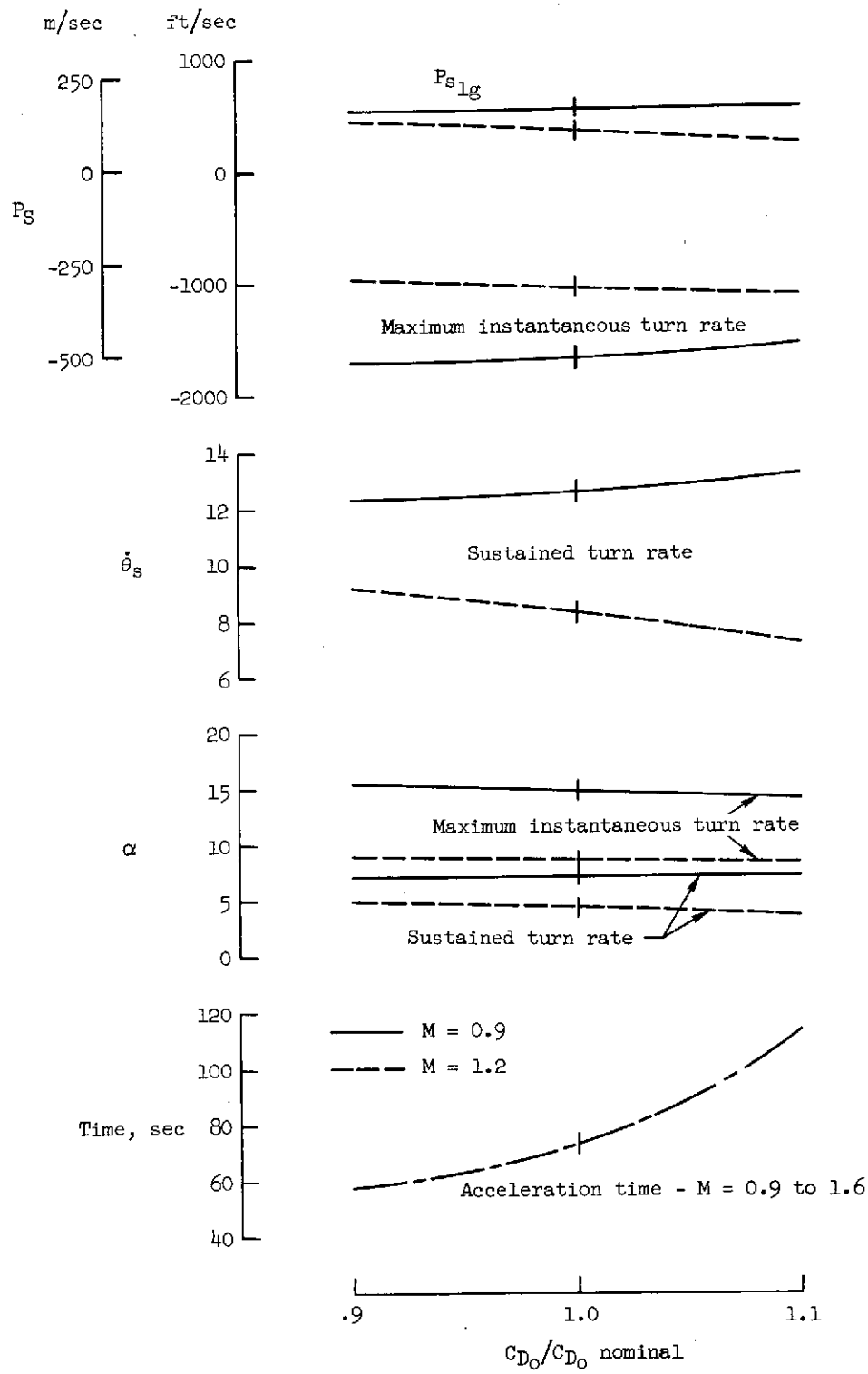

(b) Combat performance (concluded).

Figure 19.– Concluded.

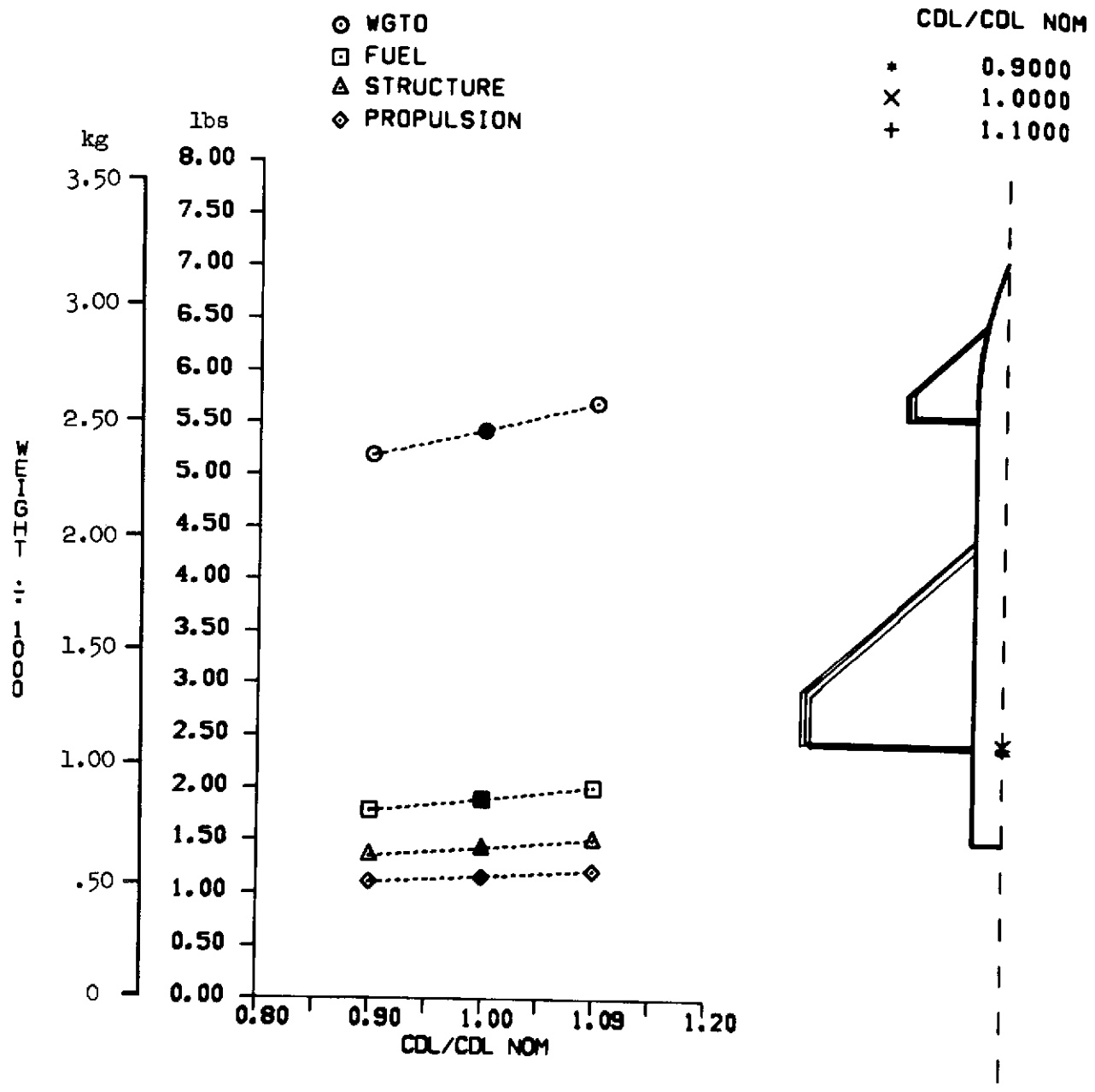

(a) Weights.

Figure 20.– Effect of a change in drag-due-to-lift coefficient.

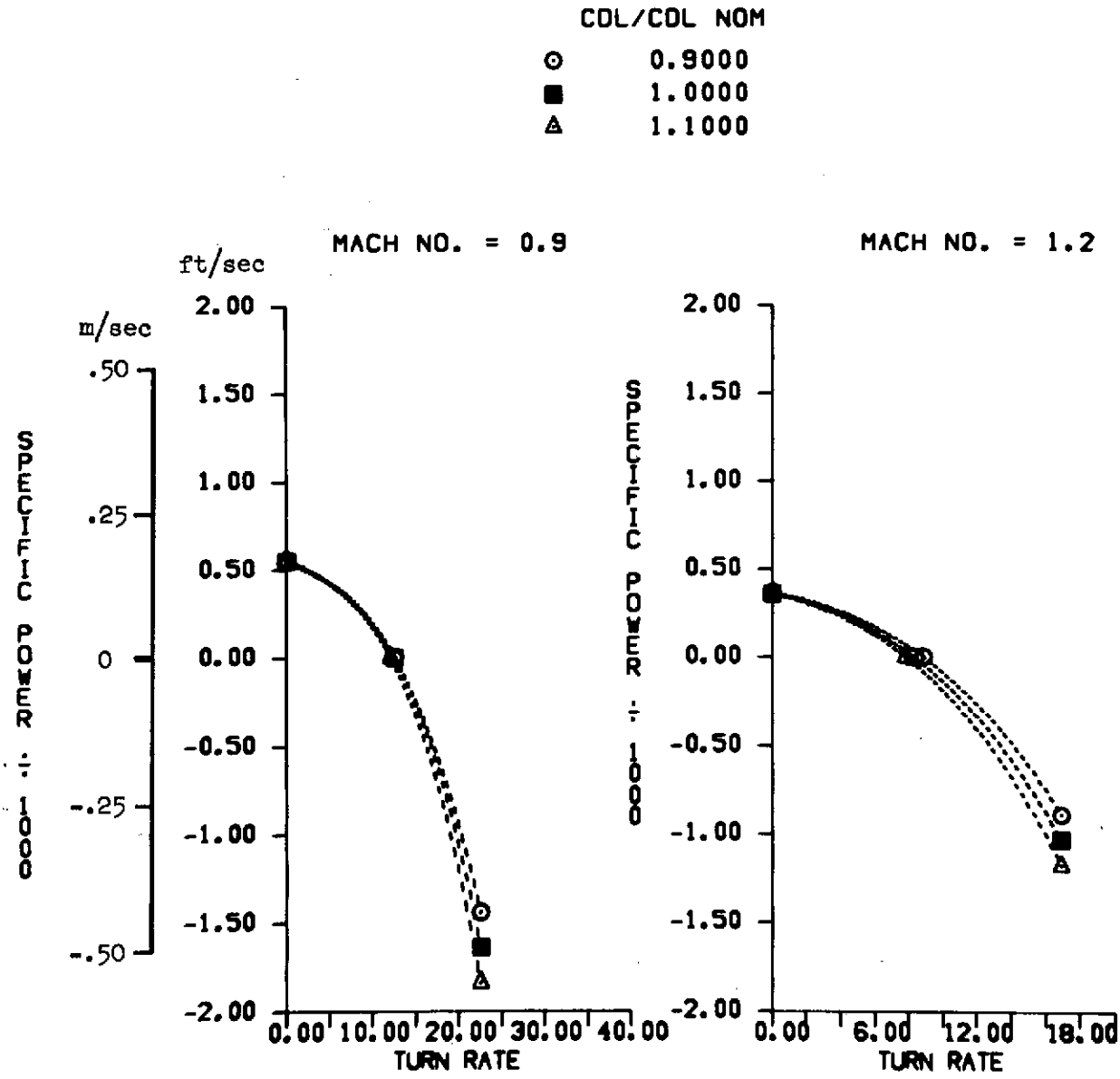

(b) Combat performance.

Figure 20.– Continued.

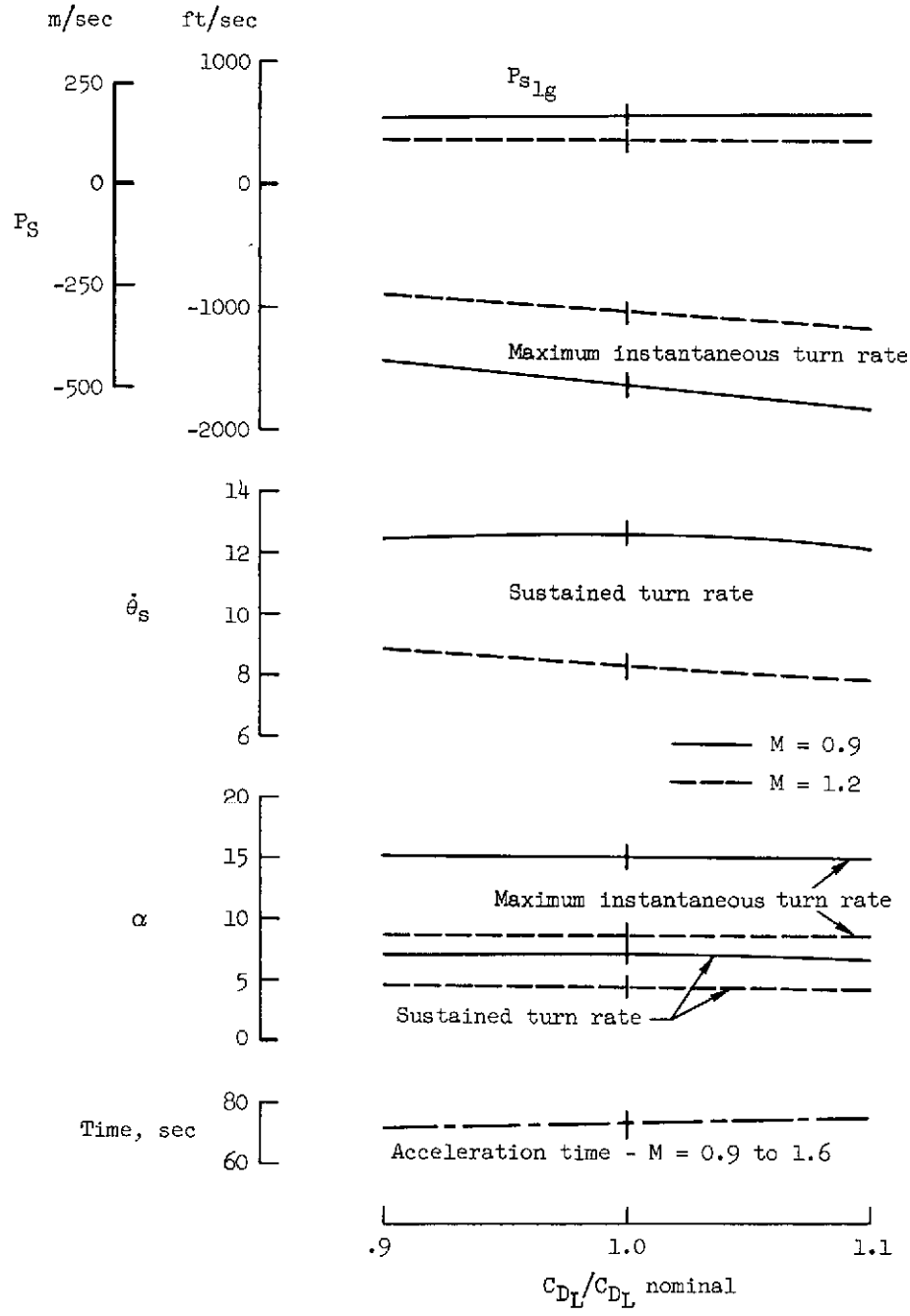

(b) Combat performance (concluded).

Figure 20.–Concluded.

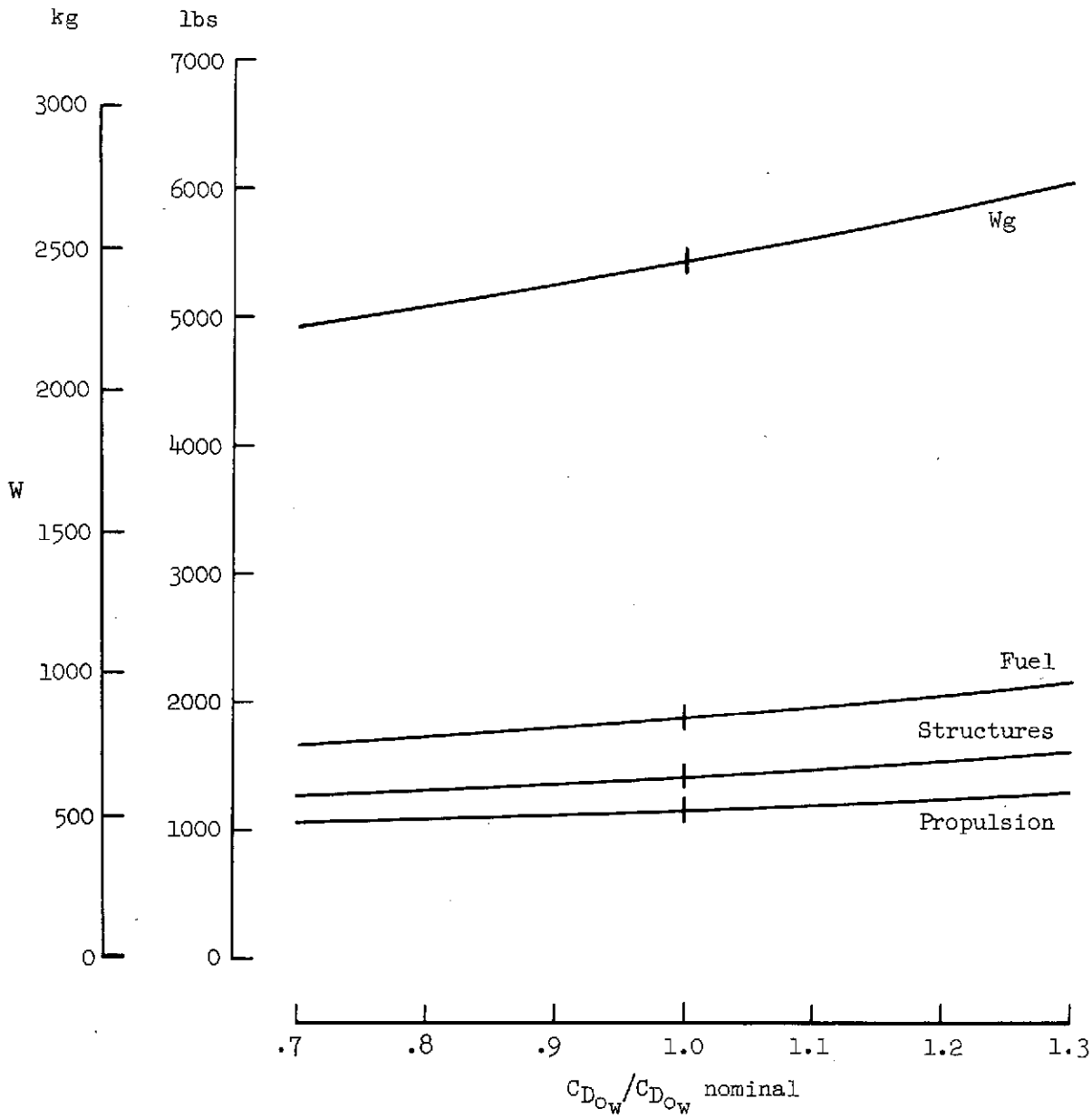

(a) Weights.

Figure 21.– Effect of a change in weapons drag coefficient.

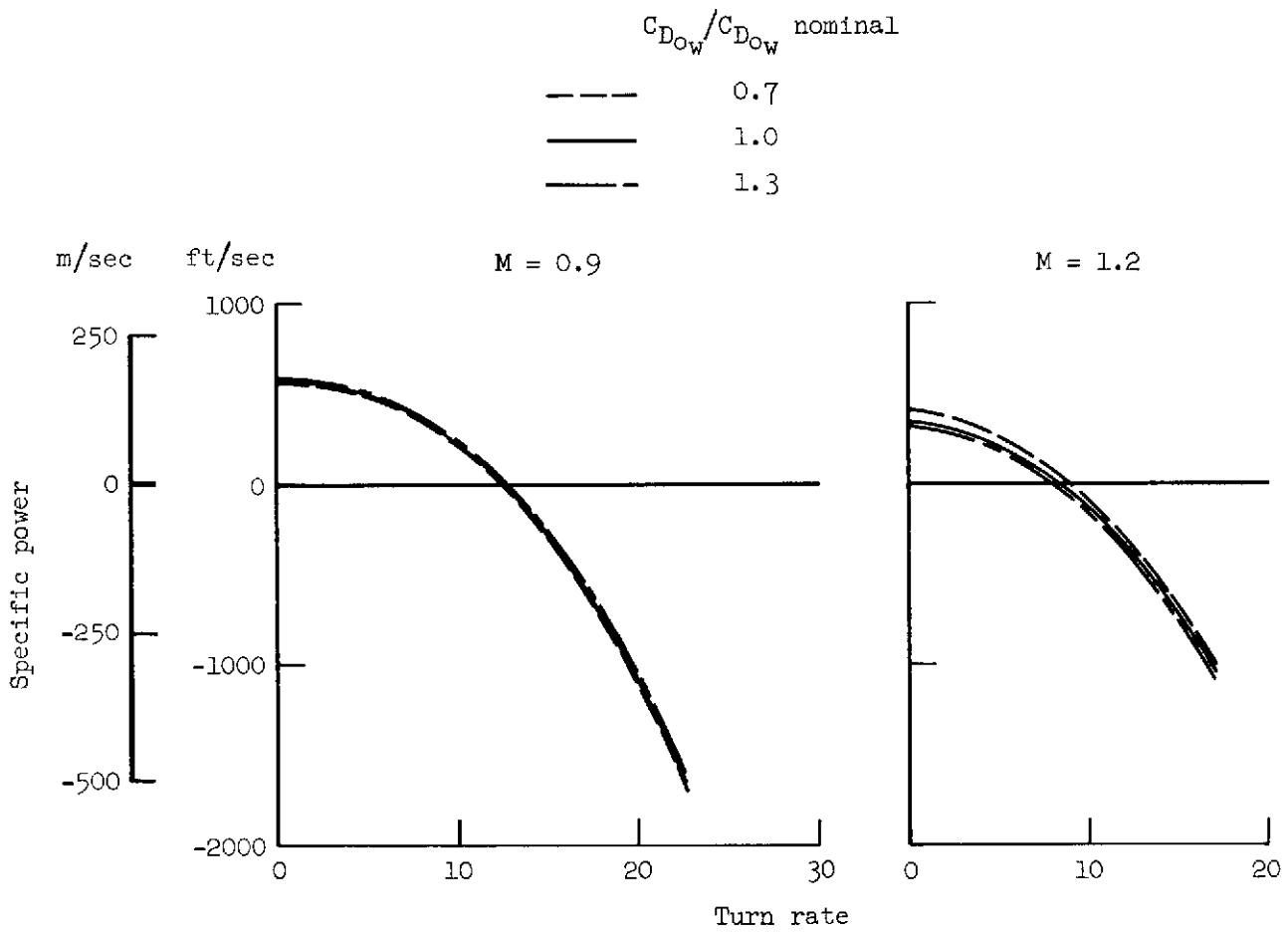

(b) Combat performance.

Figure 21.– Concluded.

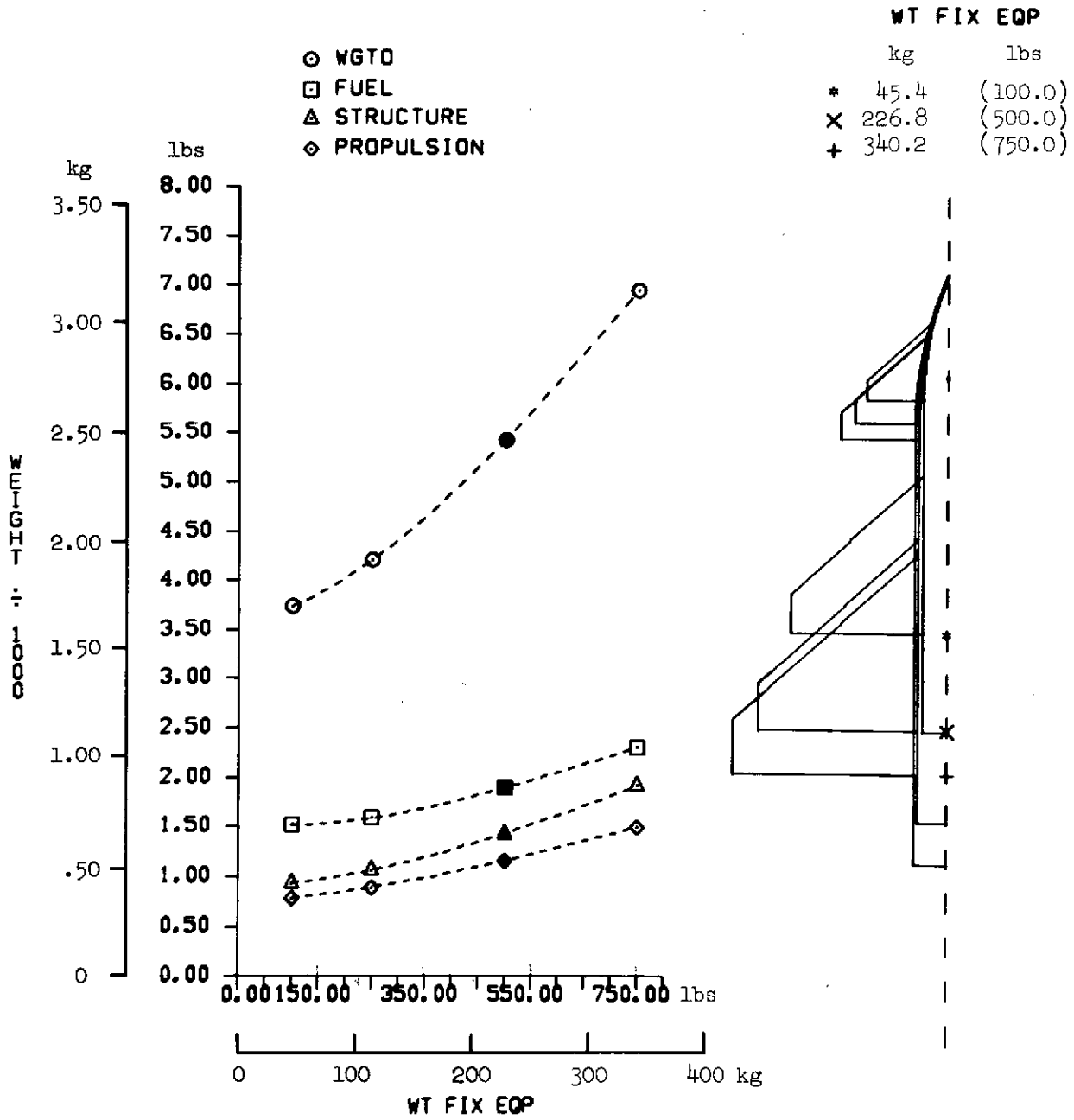

(a) Weights.

Figure 22.– Effect of weight of fixed equipment.

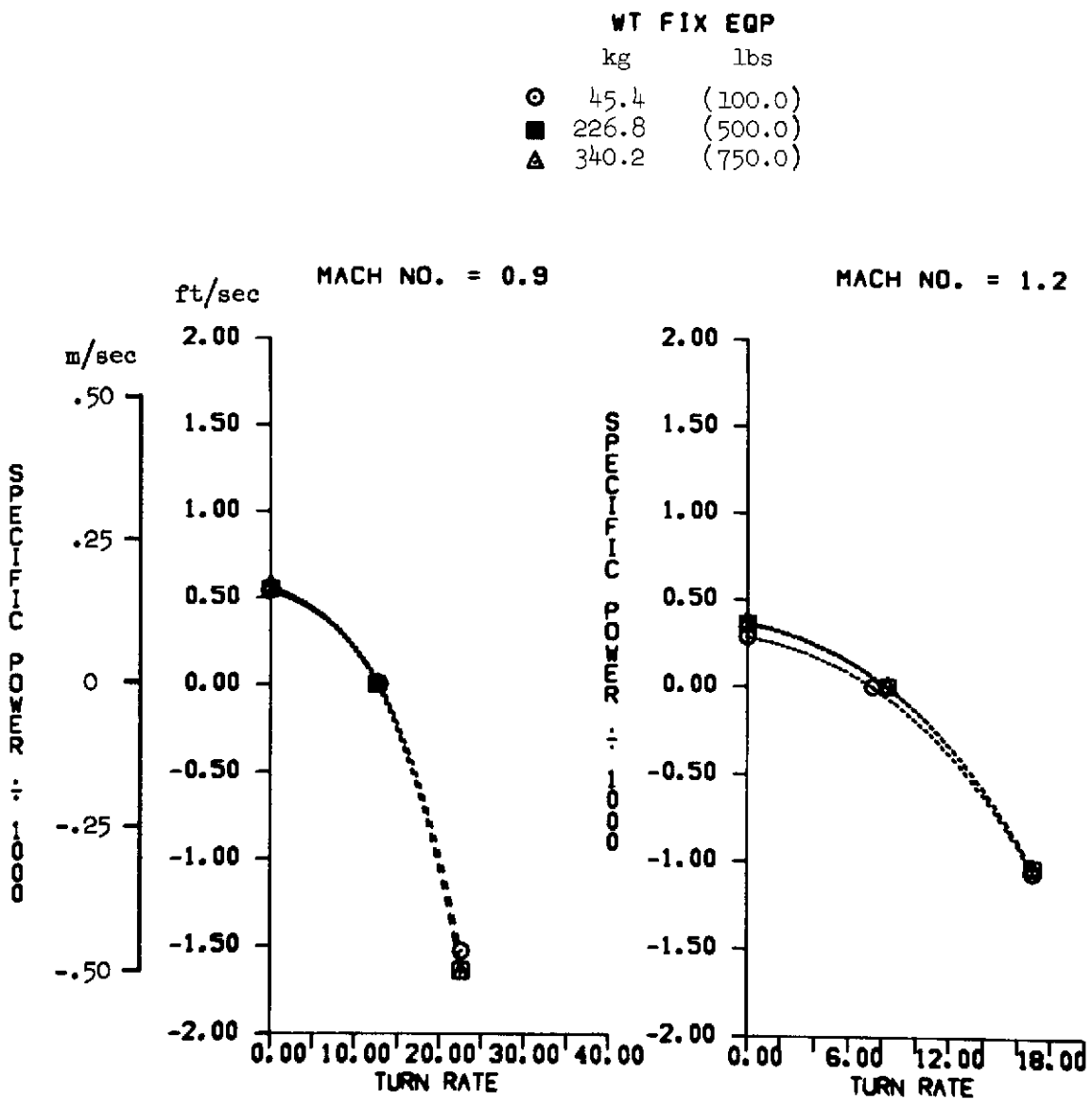

(b) Combat performance.

Figure 22.– Concluded.

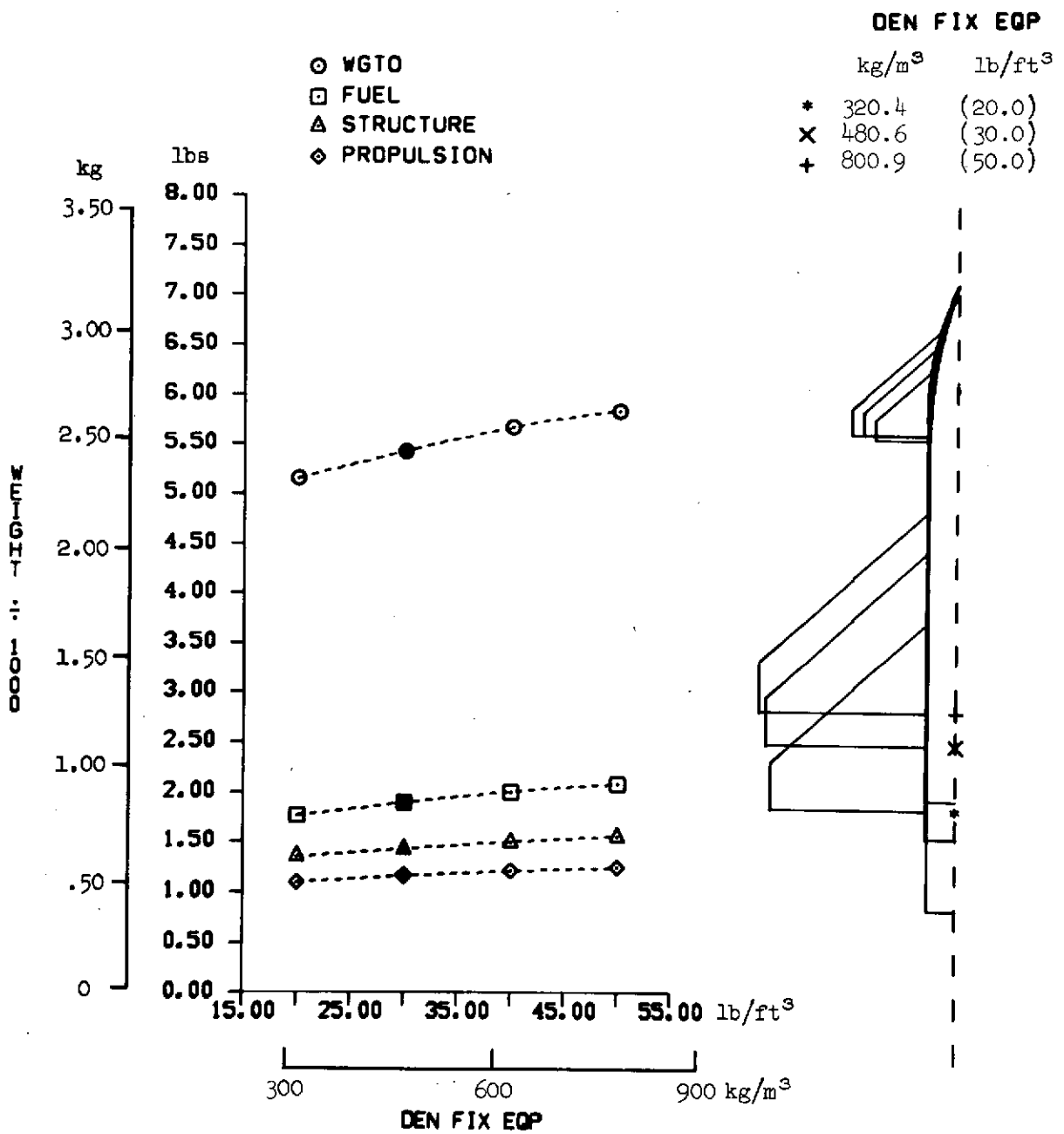

(a) Weights.

Figure 23.– Effect of density of fixed equipment.

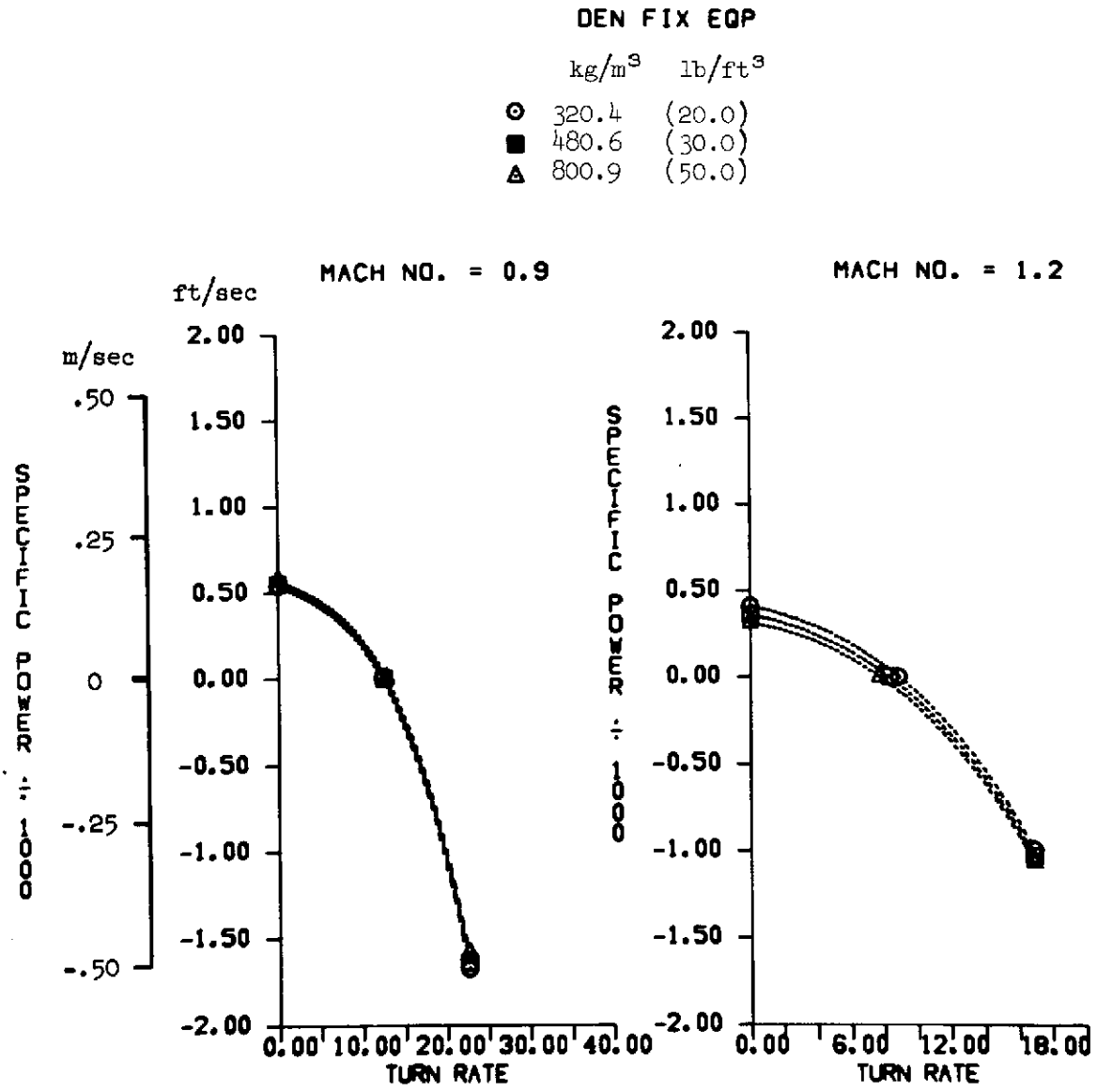

(b) Combat performance.

Figure 23.– Concluded.

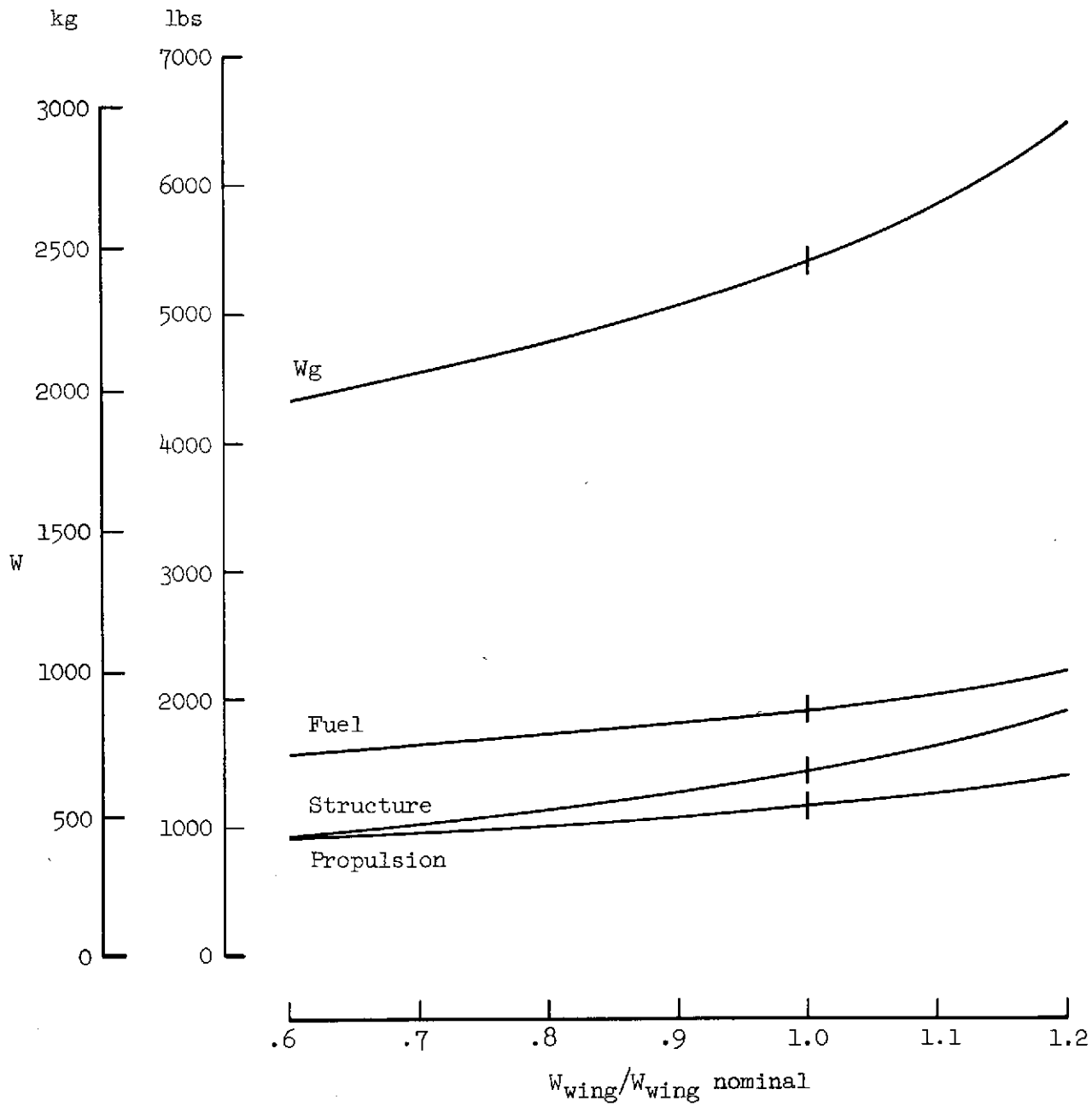

(a) Weights.

Figure 24.– Effect of a change in wing weight.

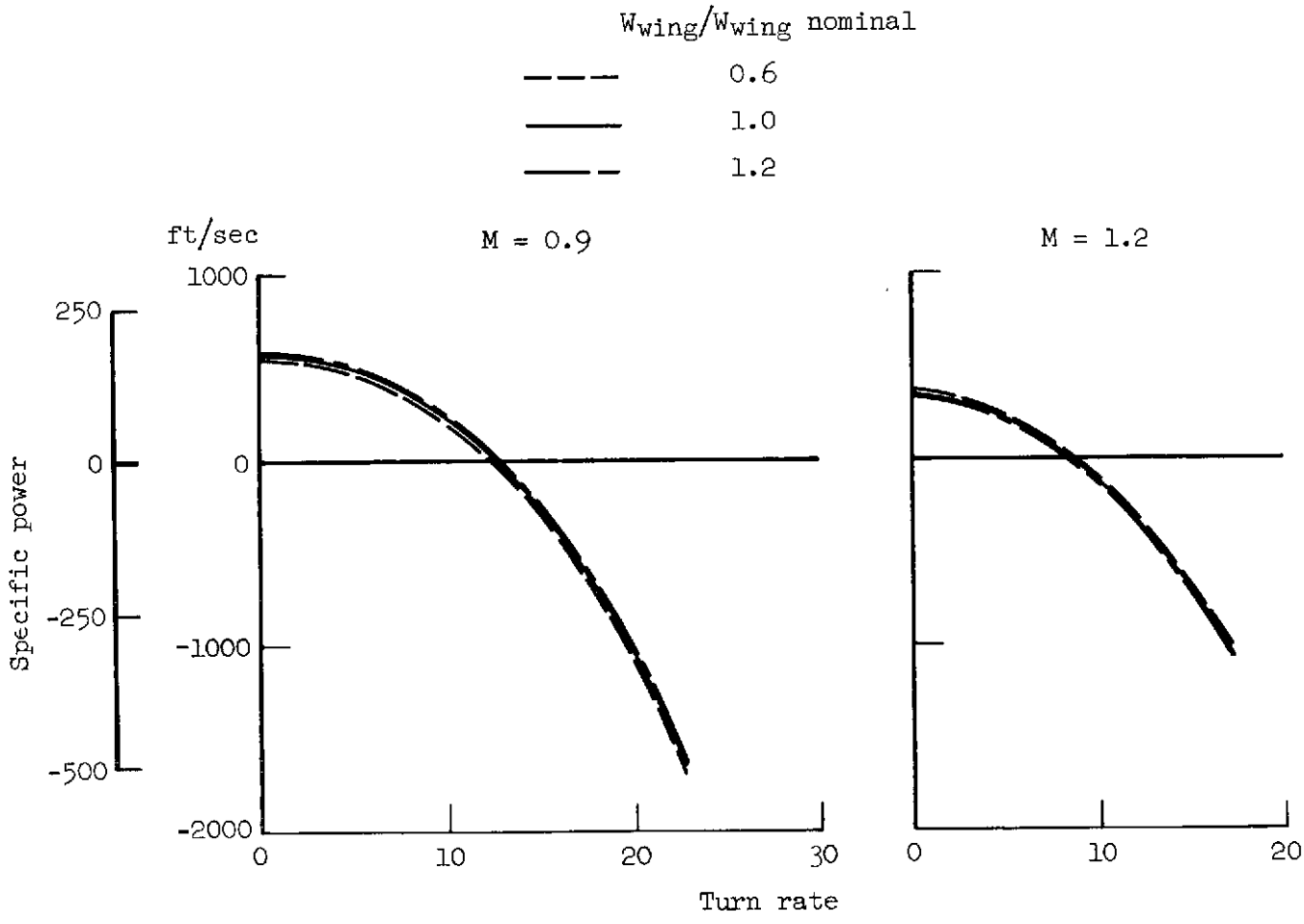

(b) Combat performance.

Figure 24.– Concluded.

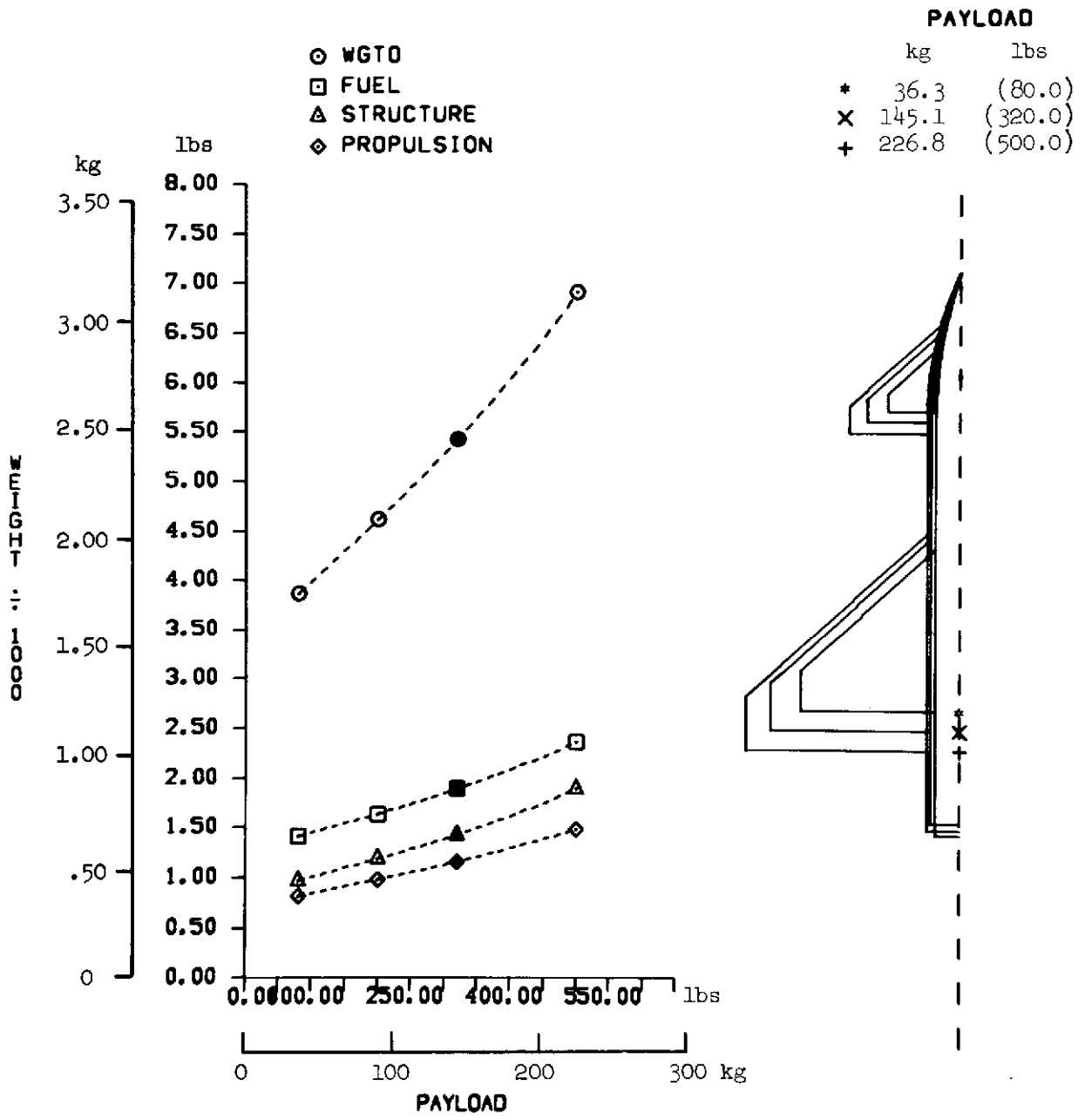

(a) Weights.

Figure 25.– Effect of weight of payload.

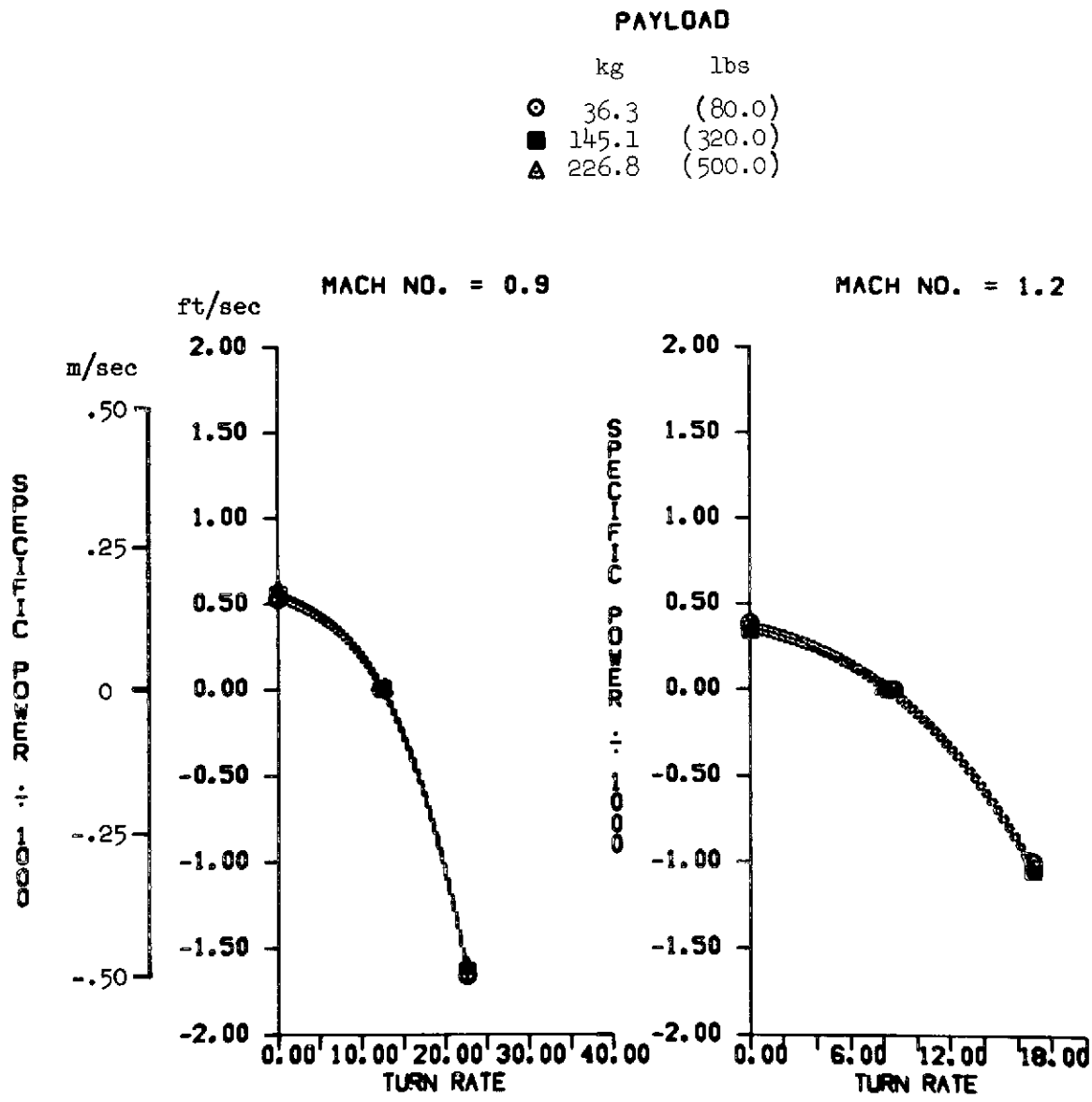

(b) Combat performance.

Figure 25.– Concluded.

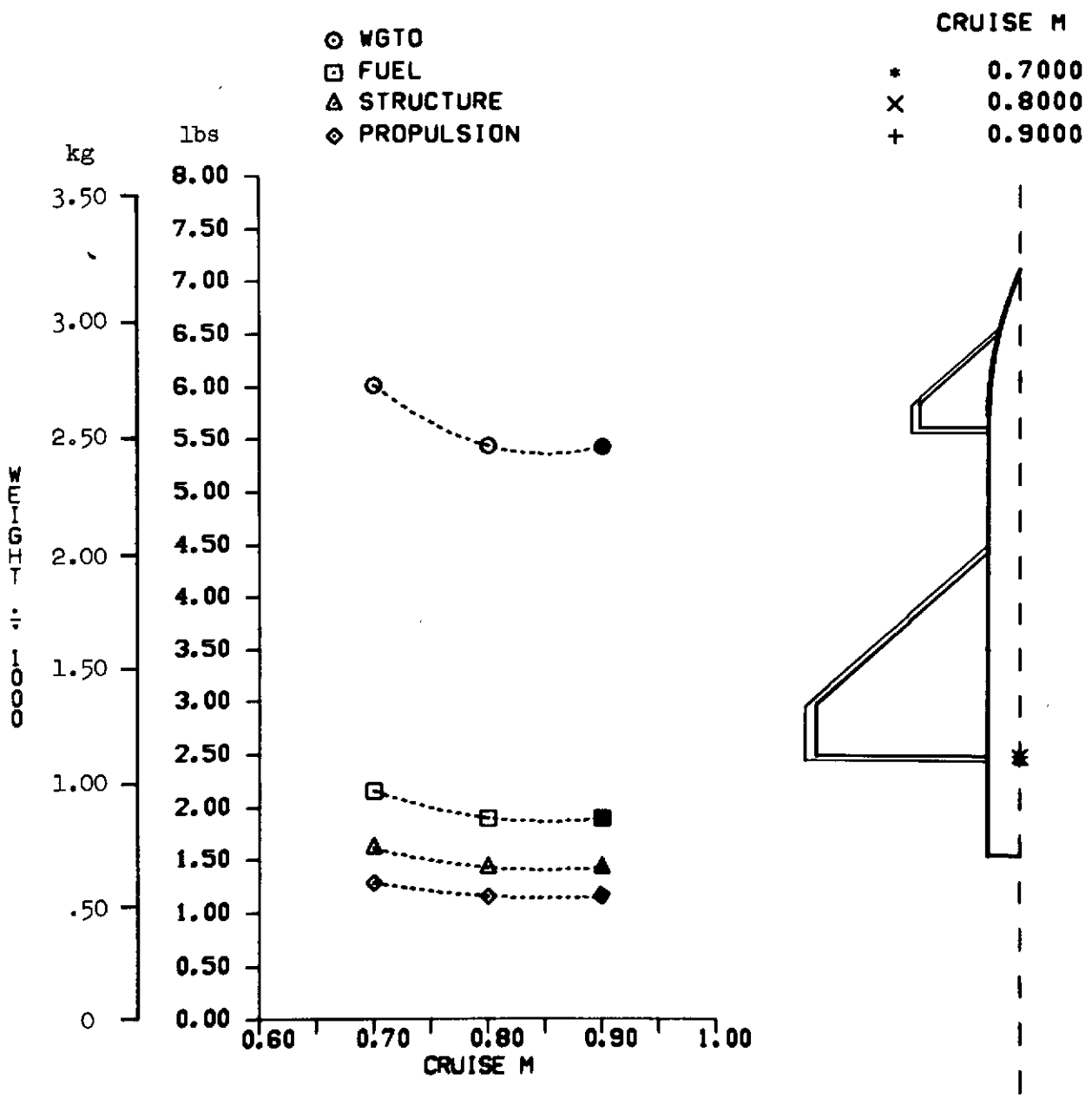

(a) Weights.

Figure 26.– Effect of cruise Mach number.

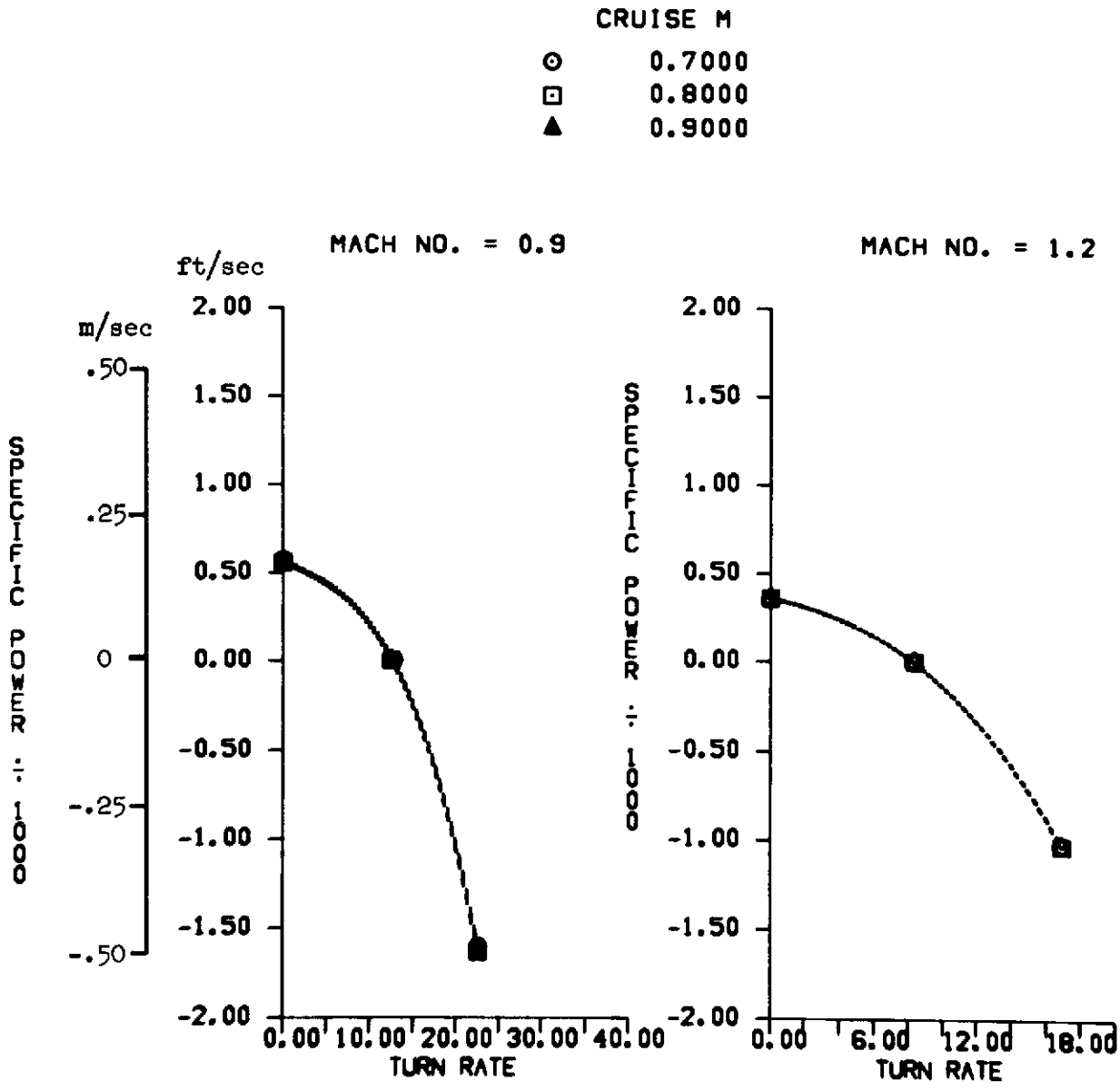

(b) Combat performance.

Figure 26.– Concluded.

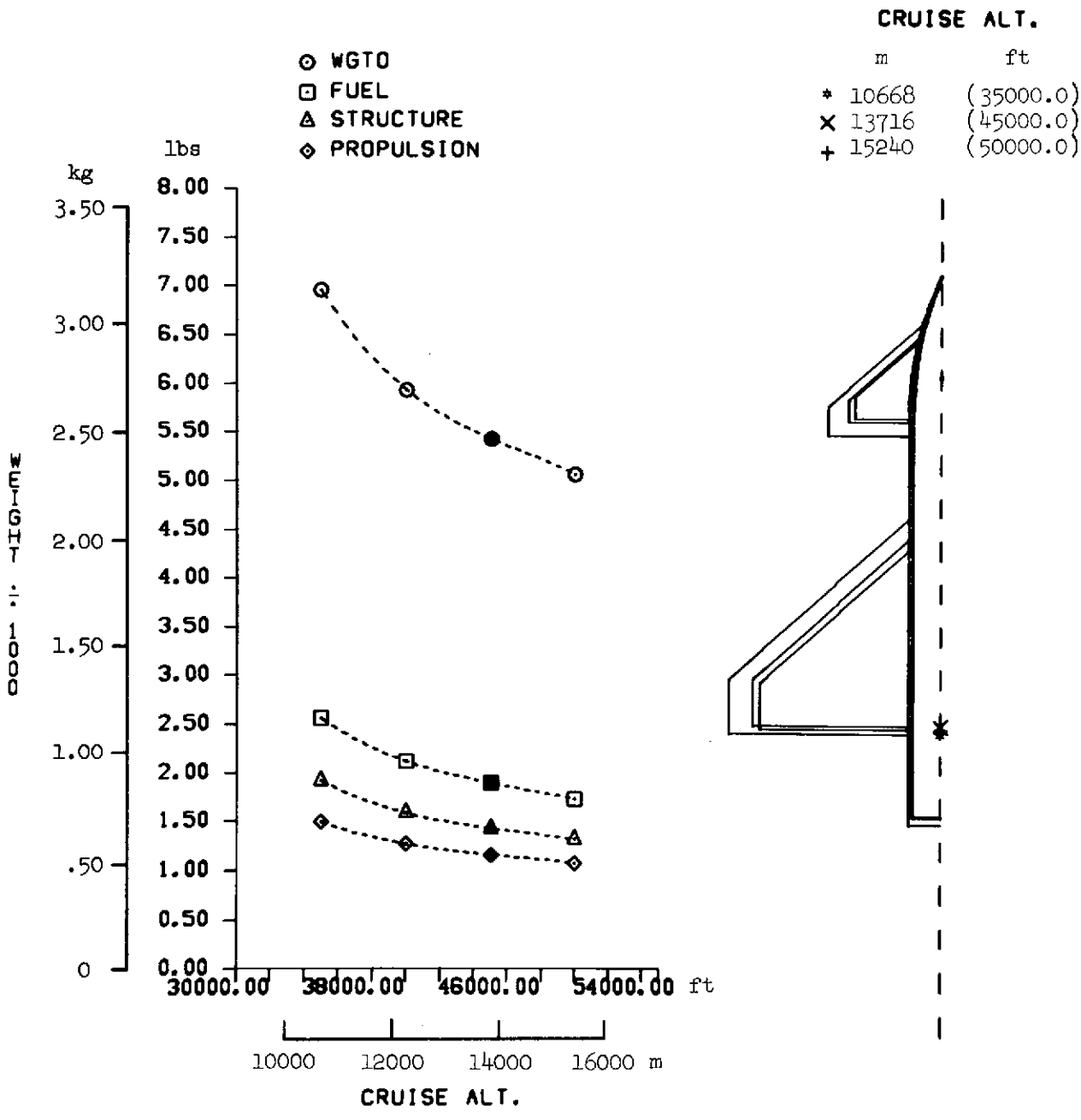

(a) Weights.

Figure 27.– Effect of cruise altitude.

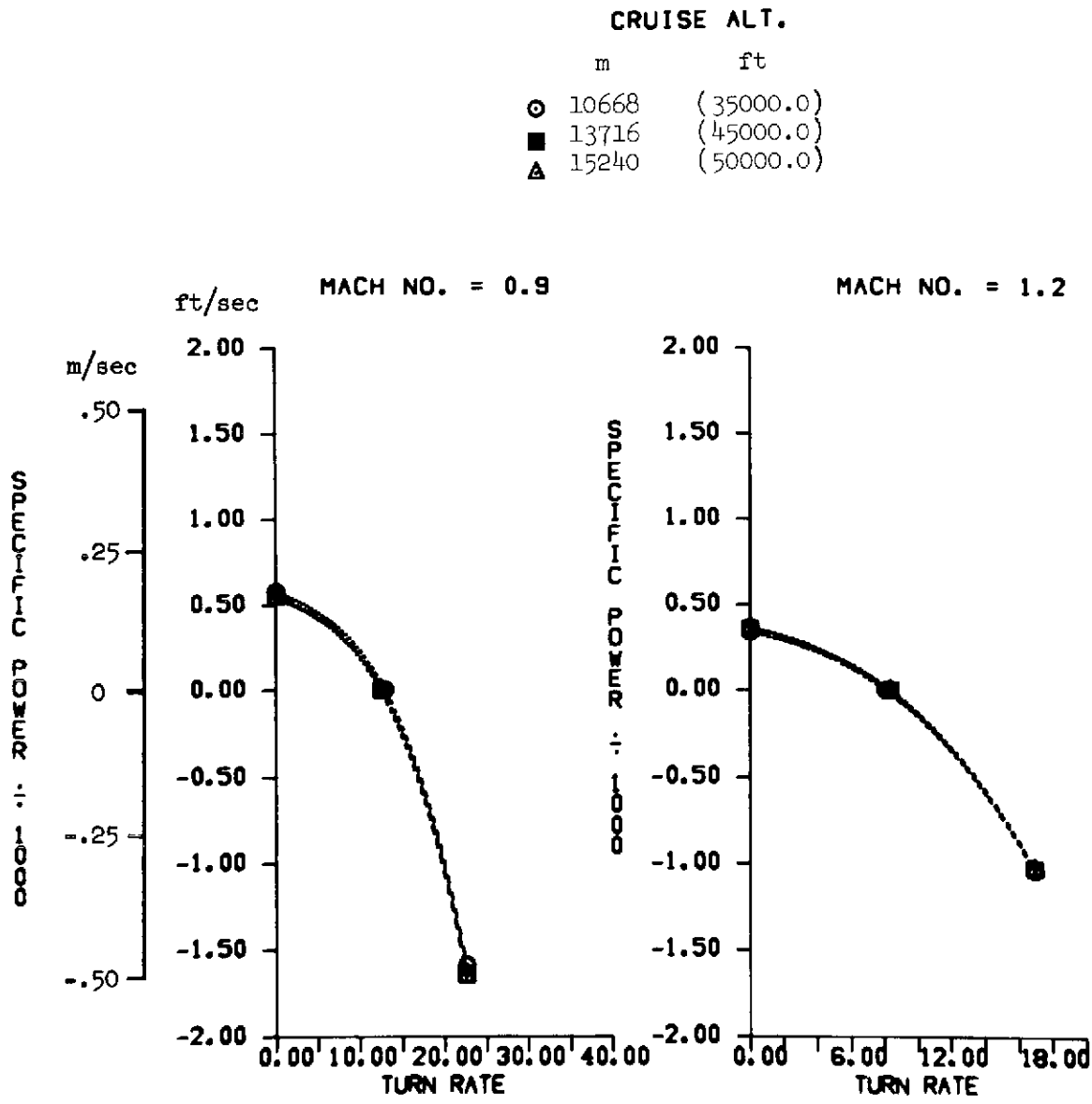

(b) Combat performance.

Figure 27.– Concluded.

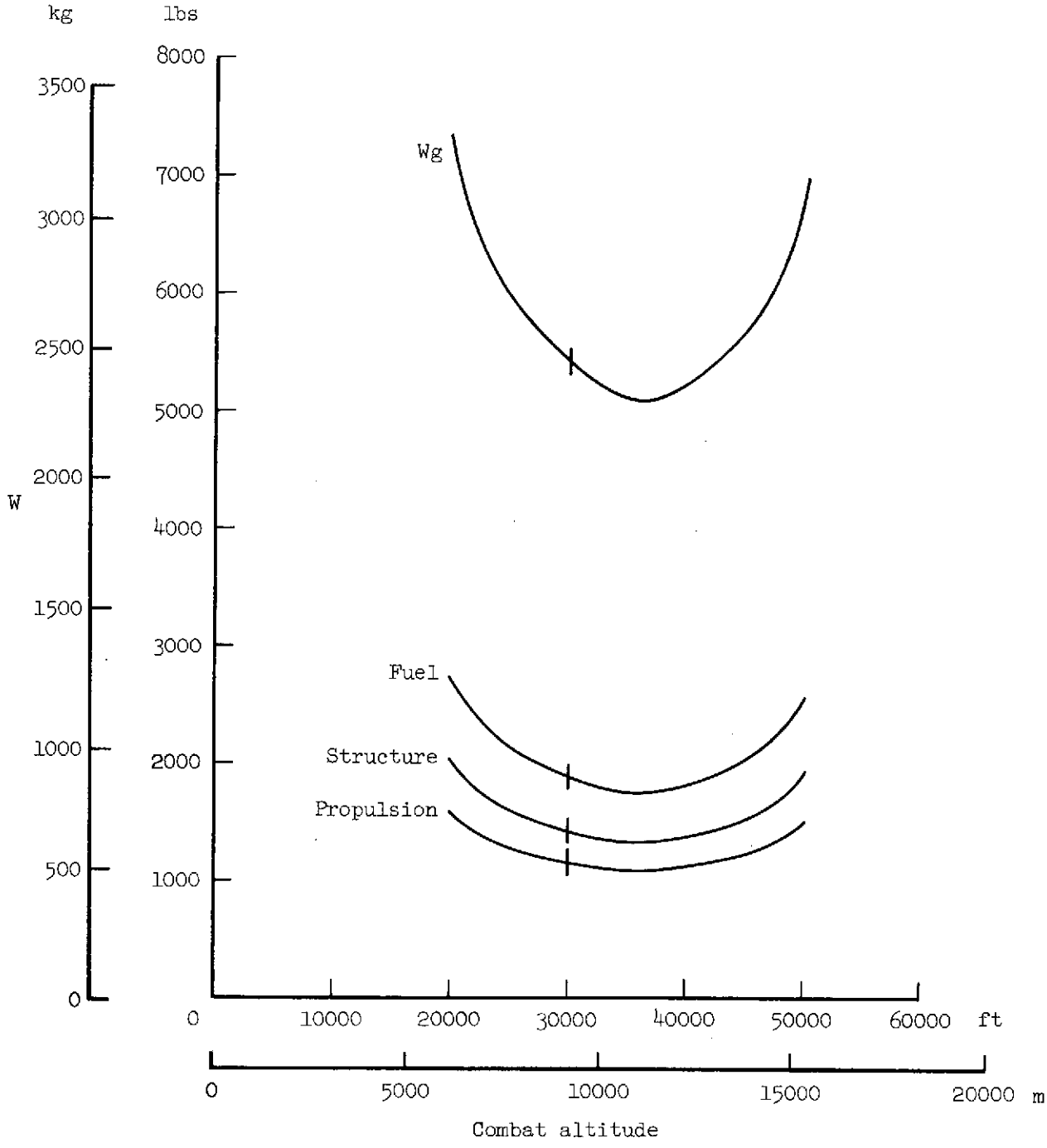

(a) Weights.

Figure 28.– Effect of combat altitude.

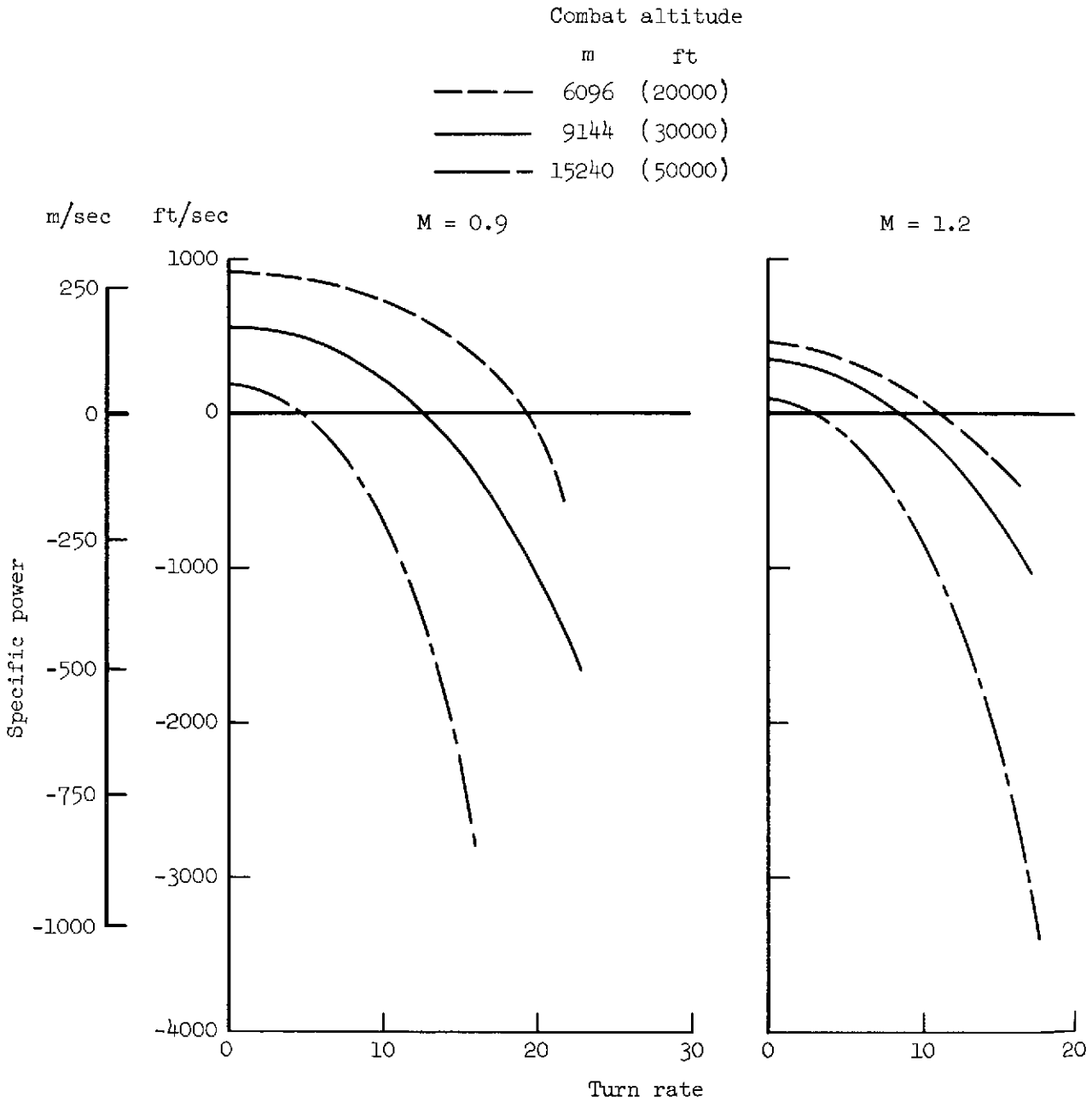

(b) Combat performance.

Figure 28.– Continued.

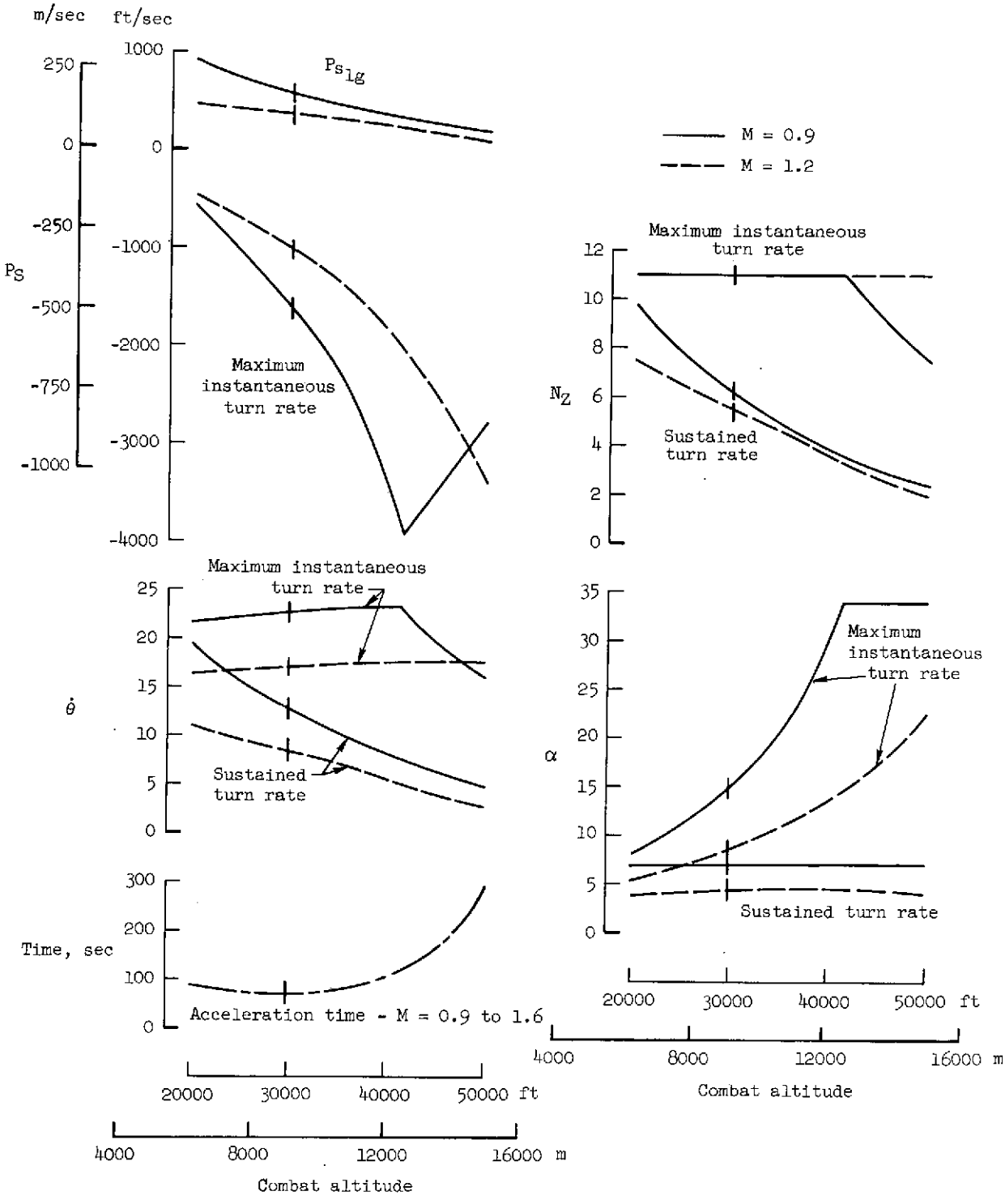

(b) Combat performance (concluded).

Figure 28.– Concluded.

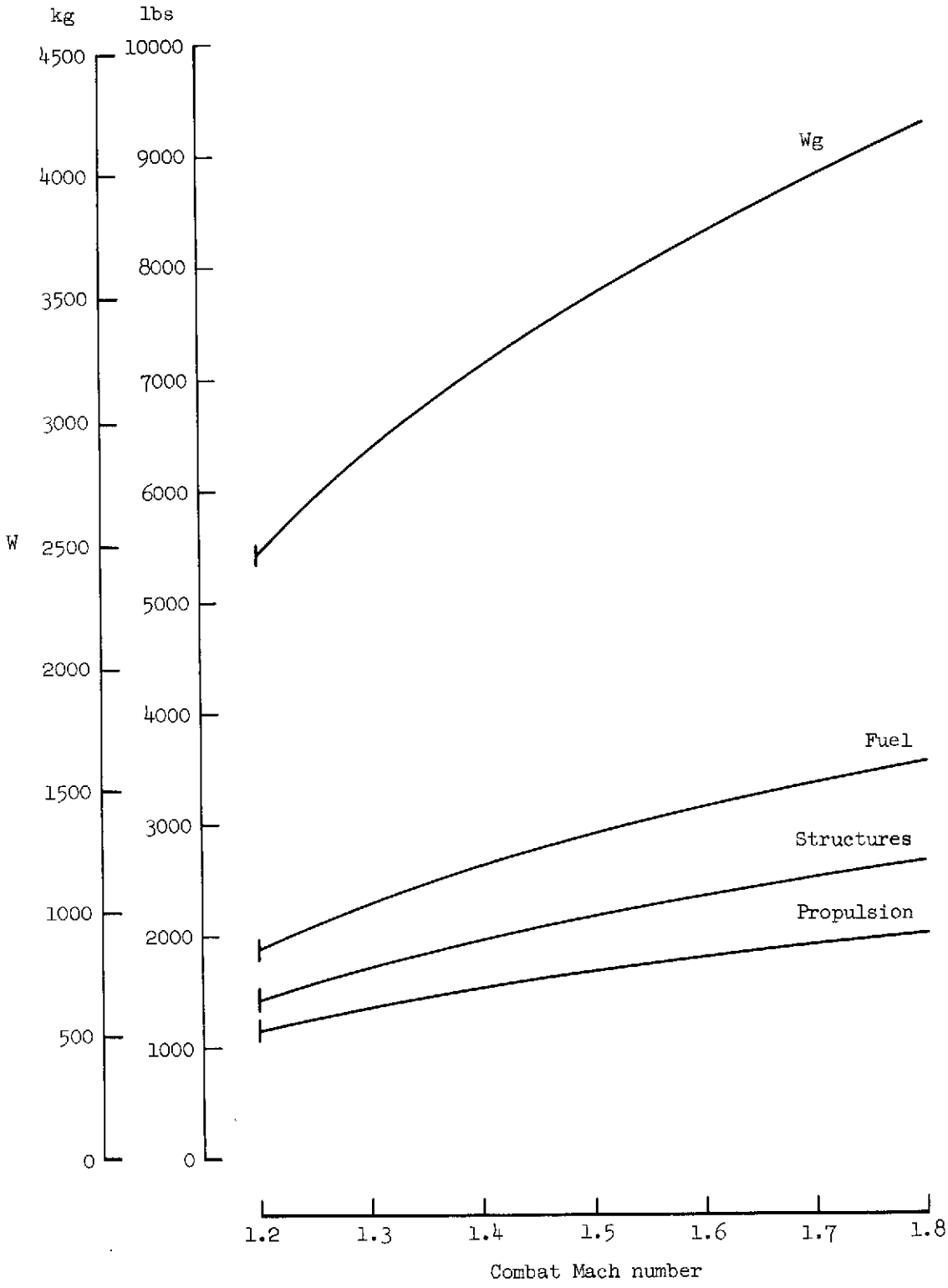

(a) Weights.

Figure 29.– Effect of supersonic combat Mach number.

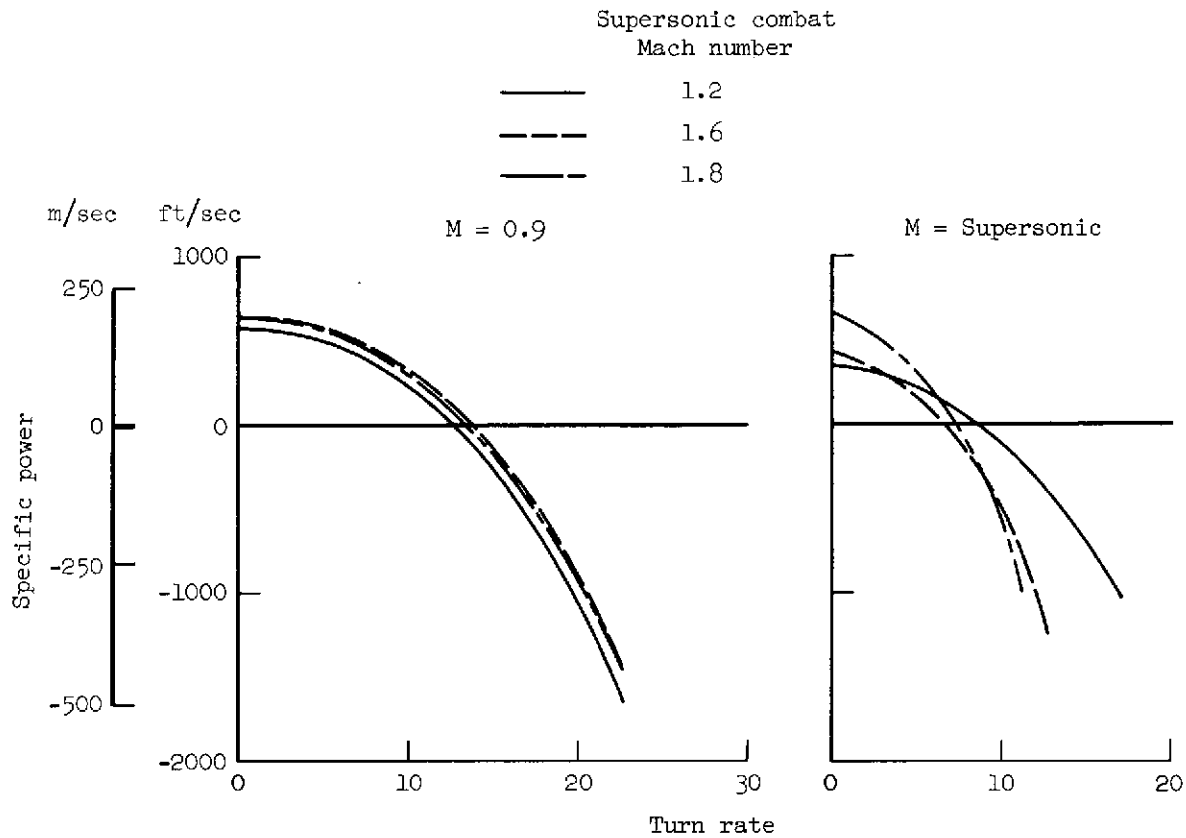

(b) Combat performance.

Figure 29.– Continued.

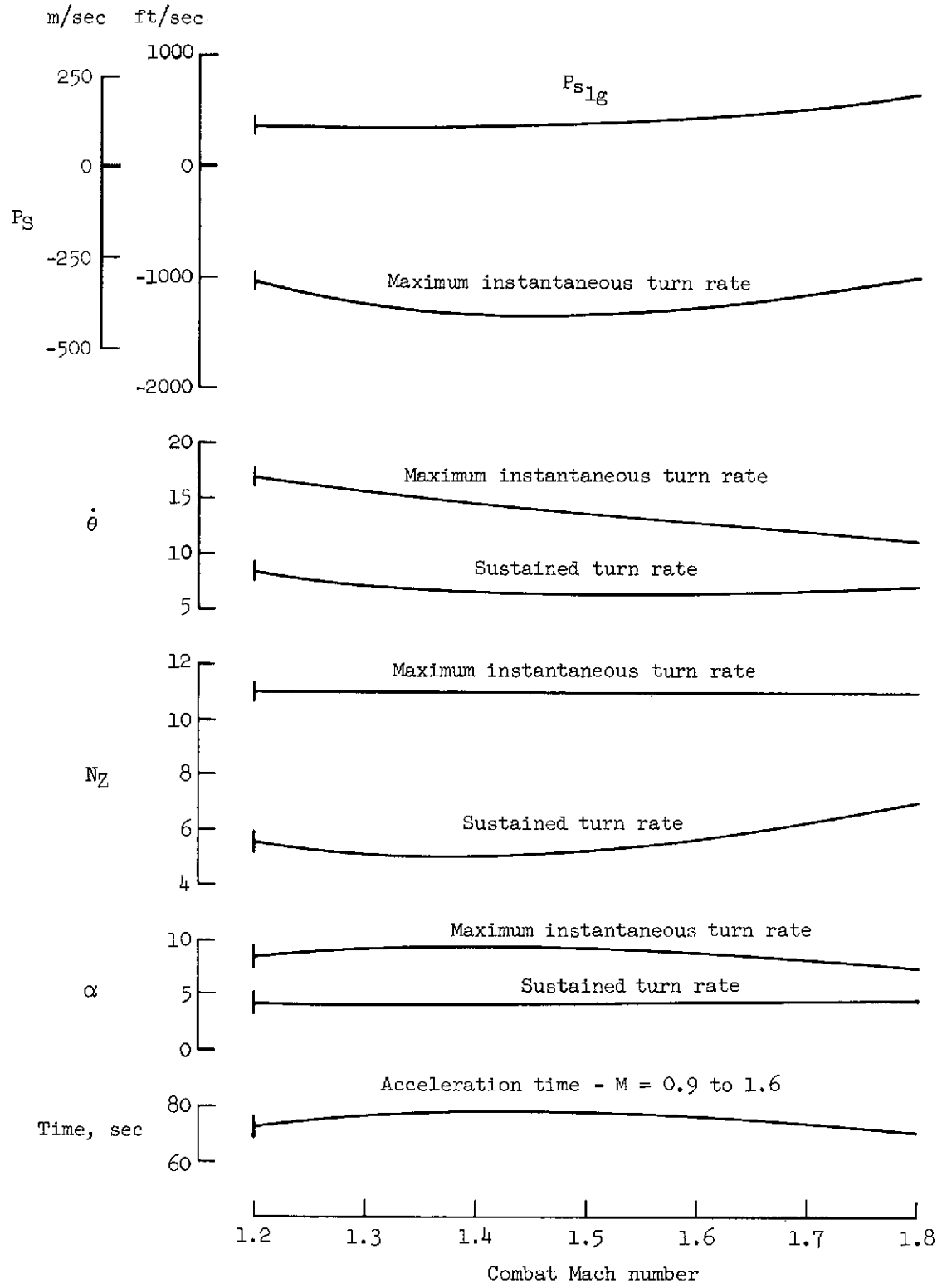

(b) Combat performance (M = supersonic) (concluded).

Figure 29.– Concluded.

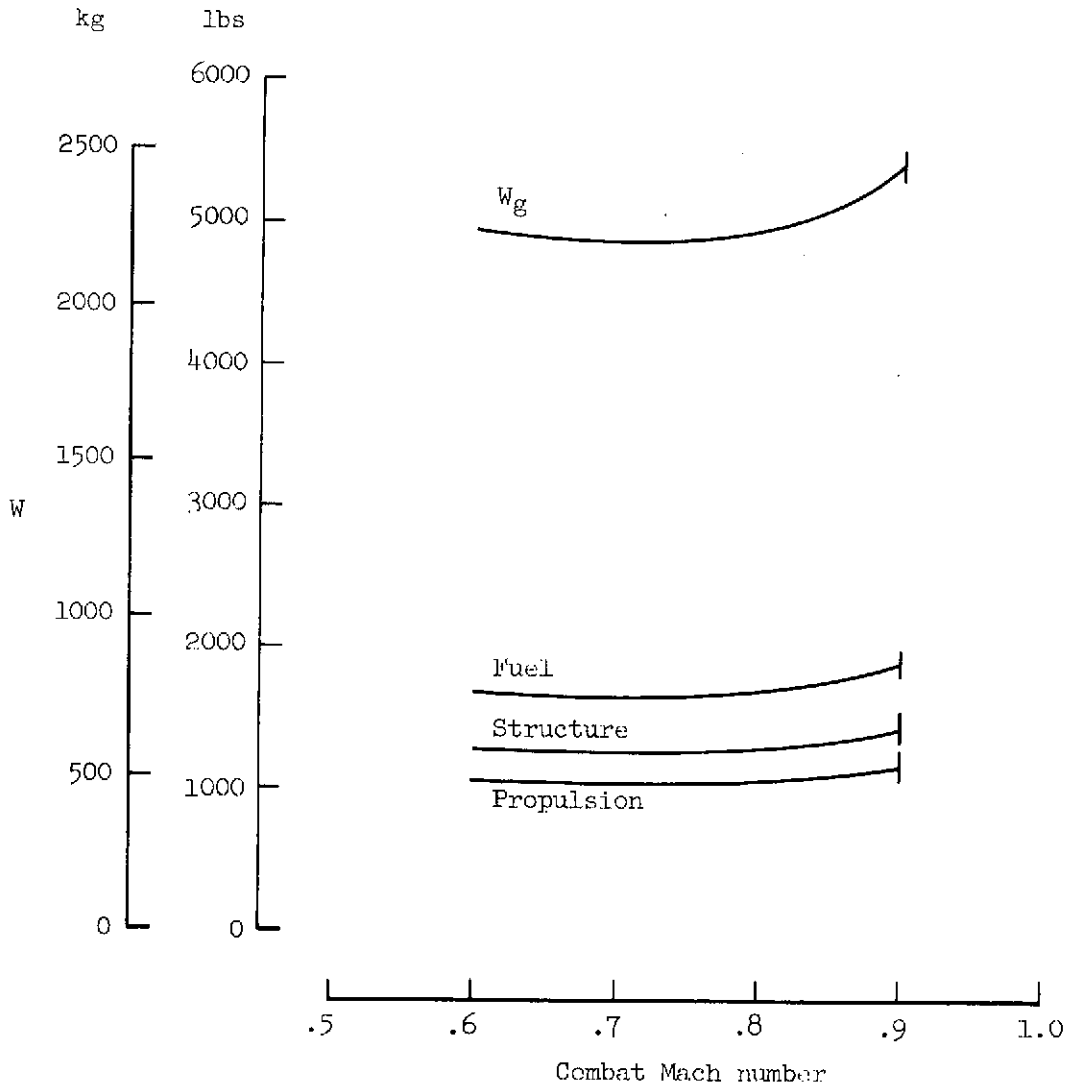

(a) Weights.

Figure 30.– Effect of subsonic combat Mach number.

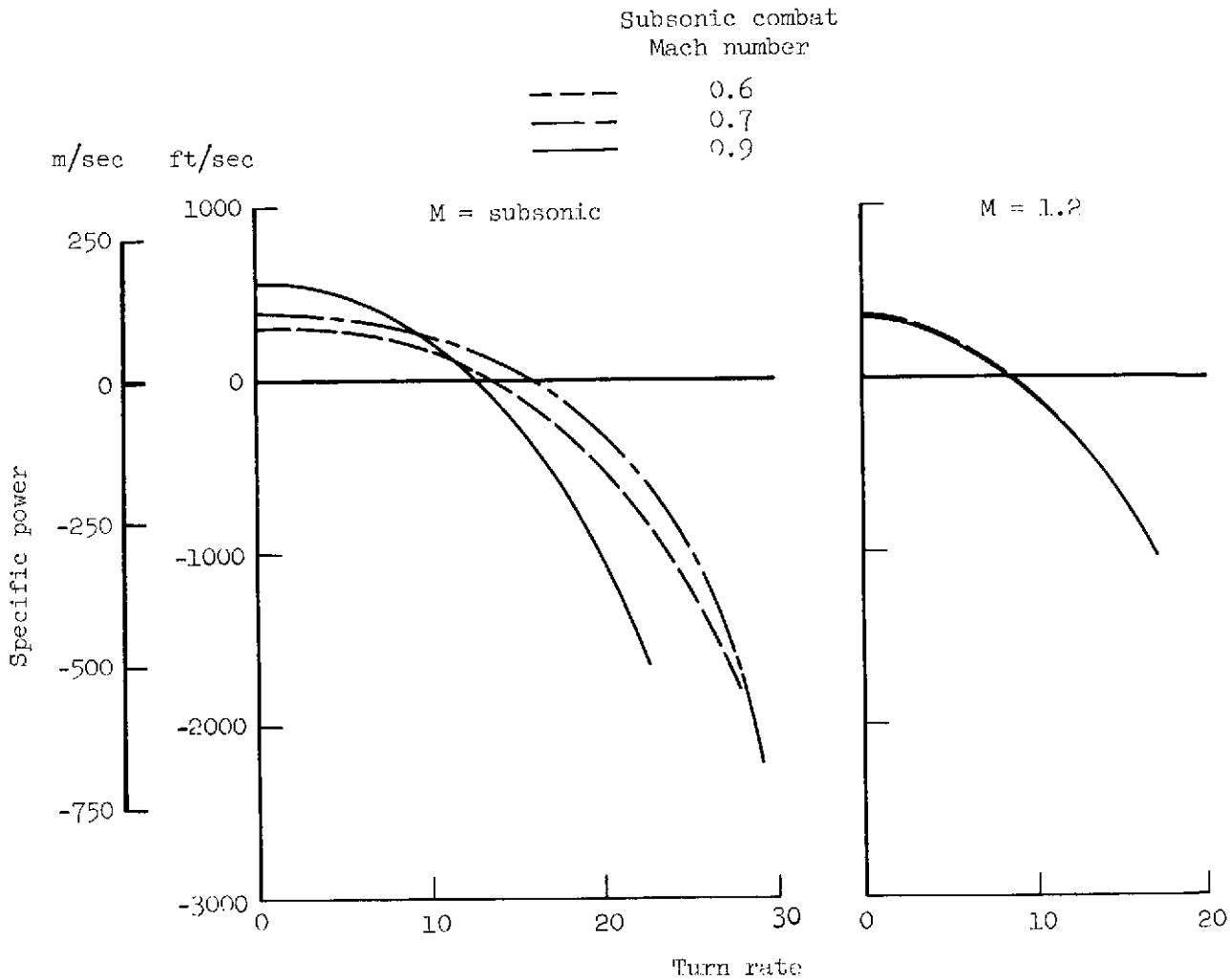

(b) Combat performance.

Figure 30.– Continued.

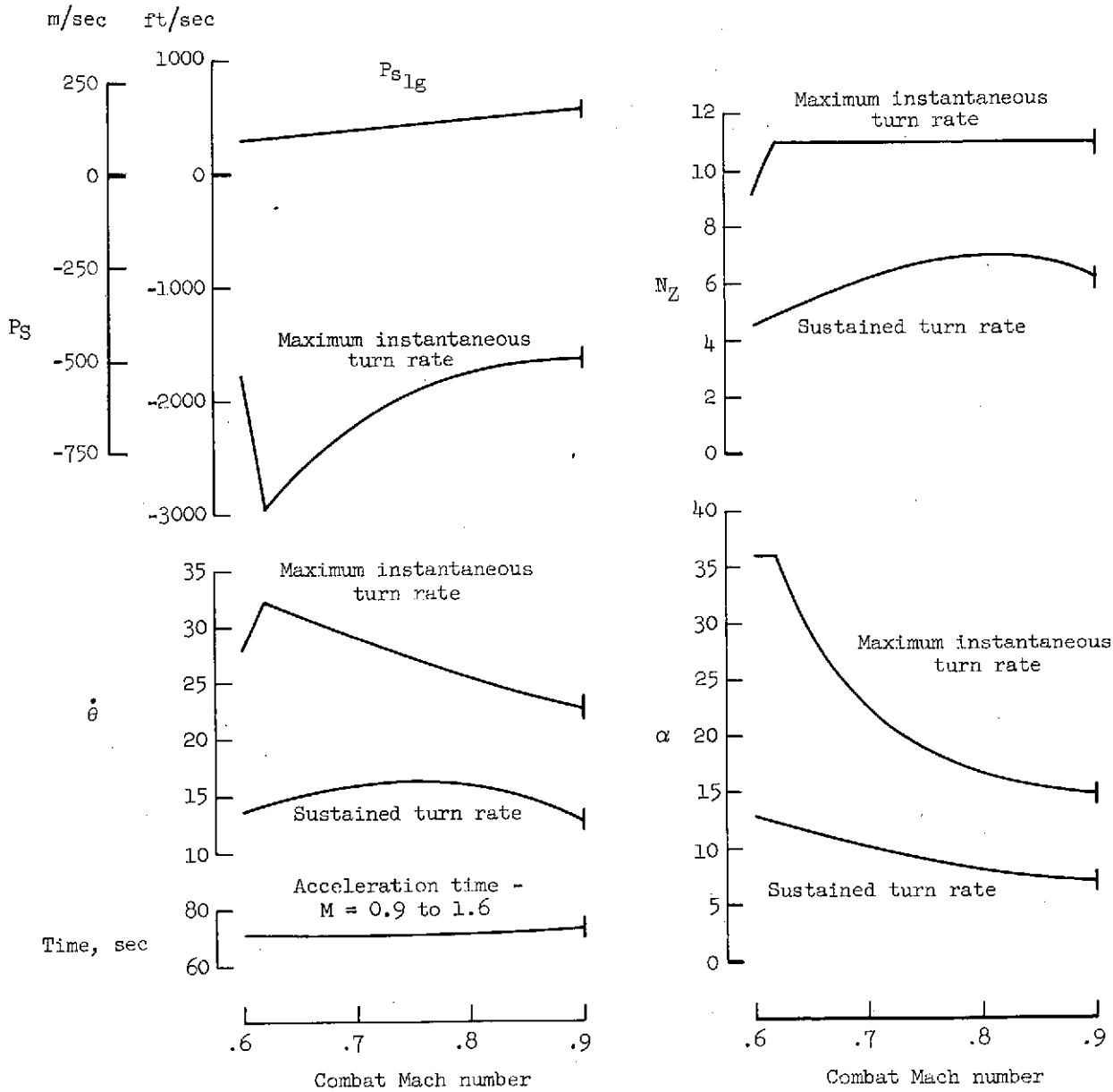

(b) Combat performance (M = subsonic) (concluded).

Figure 30.– Concluded.

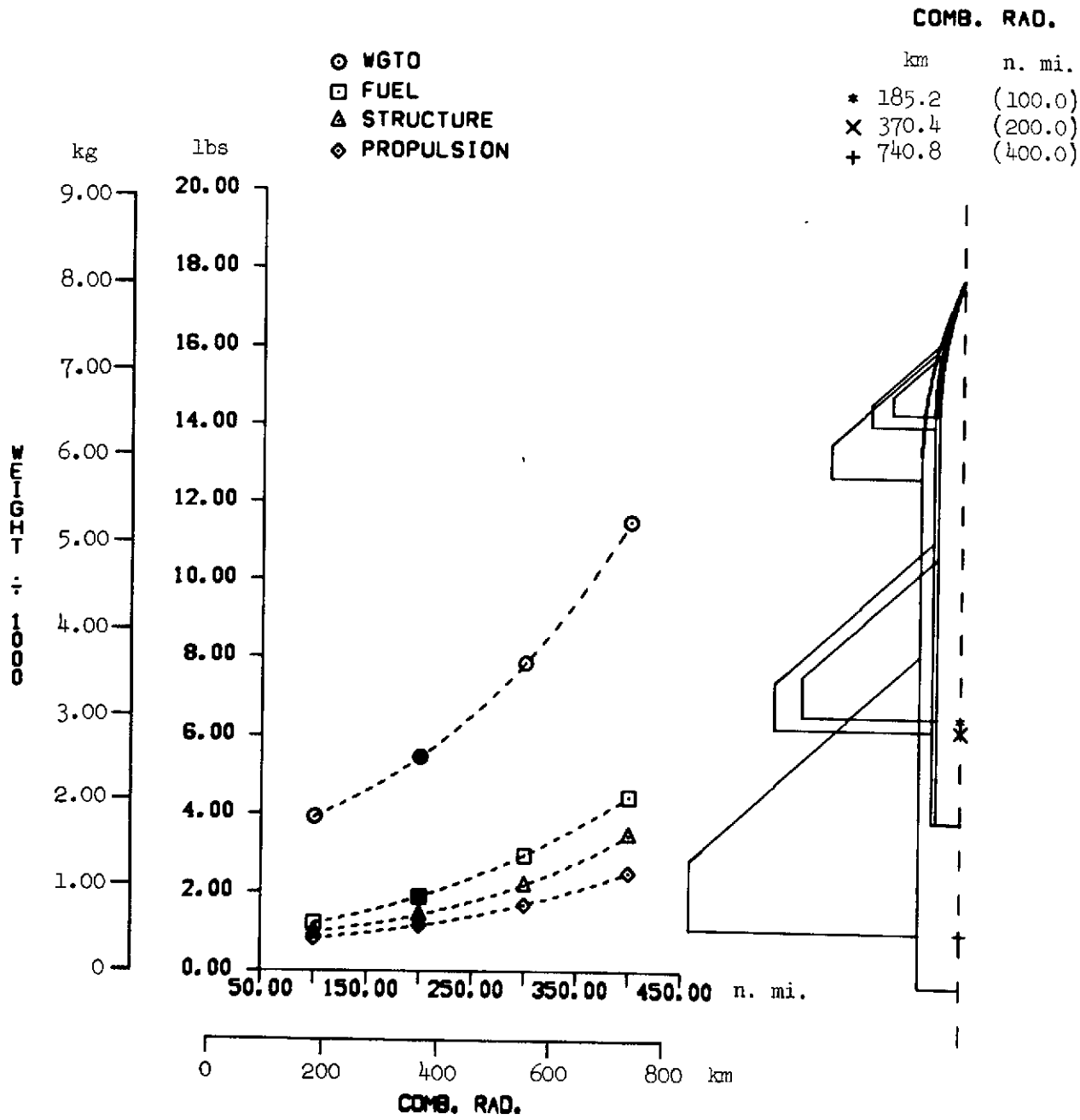

(a) Weights.

Figure 31.— Effect of combat radius.

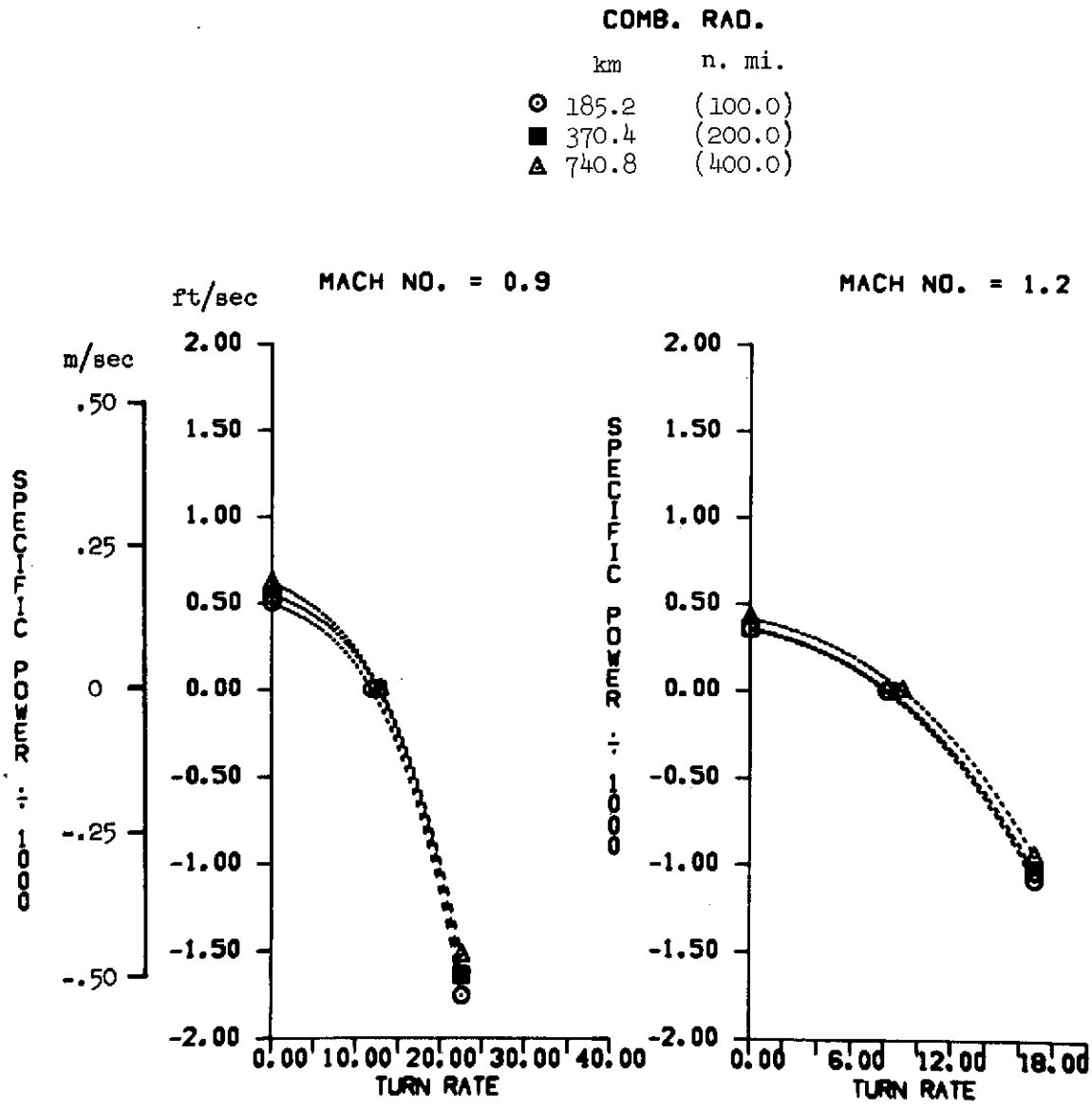

(b) Combat performance.

Figure 31.– Concluded.

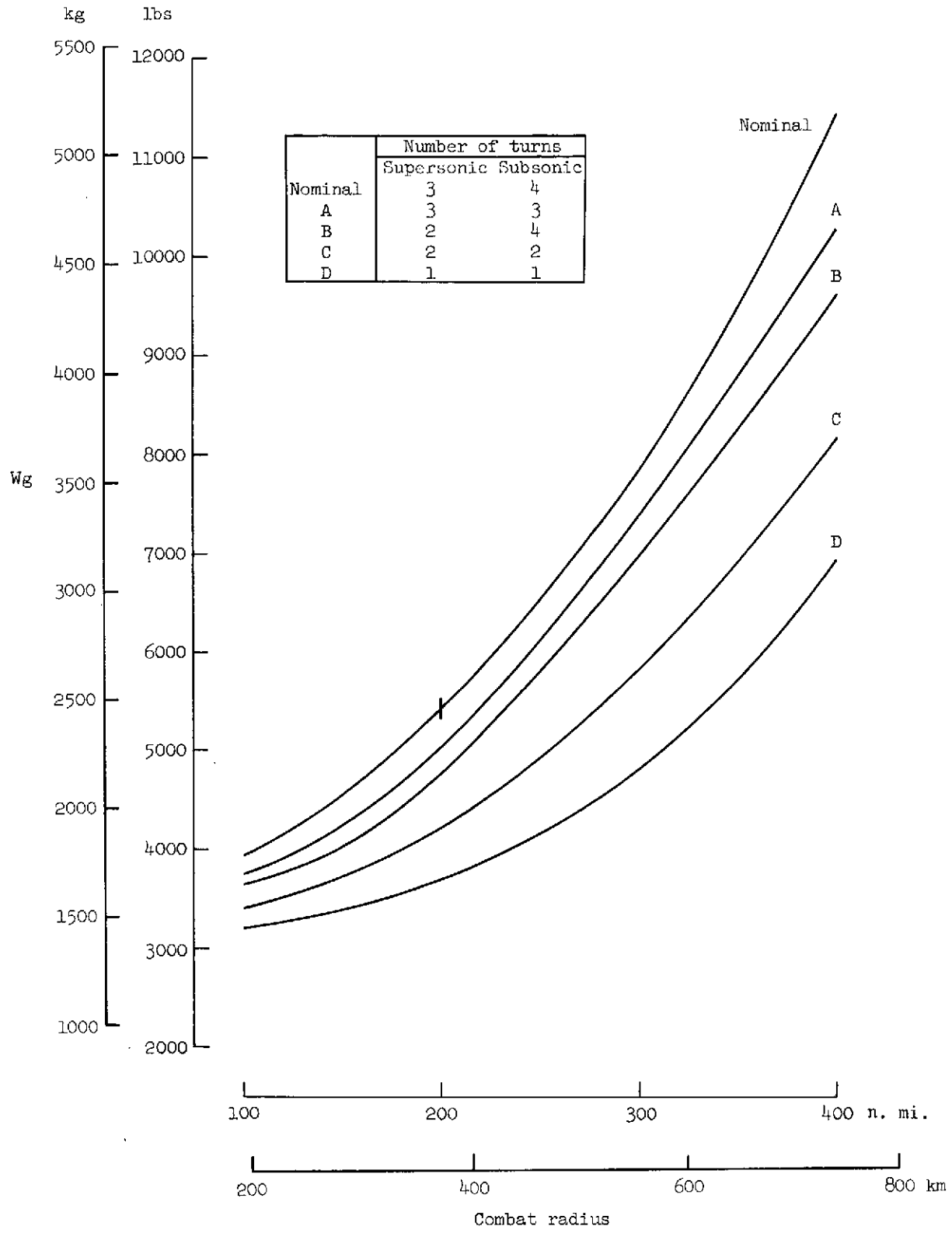

Figure 32.– Effect of number of combat turns and combat radius.

NASA-Langley, 1974 —— 2 A-5157